

# **Tropomyosin Phosphorylation and Oxidative Stress in Hypertrophic Cardiomyopathy**

BY

---

TANGANYIKA WILDER

**B.S., Florida Agricultural & Mechanical University, 2004**

THESIS

Submitted as partial fulfillment of the requirements for the degree of  
Doctor of Philosophy in Physiology and Biophysics  
in the Graduate College of the  
University of Illinois at Chicago, 2014  
Chicago, Illinois

Thesis Committee:

Beata M. Wolska, Chair  
R. John Solaro, Advisor  
Jesus Garcia-Martinez  
E. Douglas Lewandowski  
MaryJo LaDu, Anatomy and Cell Biology

First giving honor to my Lord and God who is the Light of my life and my constant source of peace.

## ACKNOWLEDGMENTS

My heart is filled with gratitude for all of the people who have played a role in my life throughout my studies. I would first like to thank my thesis advisor, Dr. R. John Solaro who has been very gracious, patient, and understanding of me. I will cherish your wisdom and enthusiasm for the life sciences. I am very grateful for my thesis committee members, Dr. Beata Wolska (Chair), Dr. Jesus Garcia-Martinez, Dr. Mary Jo LaDu, and Dr. E. Douglas Lewandowski all of which have guided me, encouraged me, asked me the hard questions and forced me to be better. There are those of you who remind me that there are jobs to do, expectations to fulfill, and hopes for my future that I needed to focus on. So, thank you for being those integral pieces to the perfect plan for my life. I have learned and am taking a piece of goodness from each one of you. Special thanks goes to an unofficial mentor, Dr. Primal de Lanerolle who has been an unsolicited mentor that has inspired, advised and generally cared about my success, shared resources, and advised me throughout. I hold you in high esteem. To the Wieczorek lab with special thanks to Dr. Emily Schulz for generating the mice and for their generosity of collaboration.

I am thankful for the Solaro lab and departmental members that have supported me in the past and present, who are too many to mention. I want to thank especially Chad Warren for his unwavering mentorship, technical expertise, and friendship. To my colleague and friend Jillian Simon, for her scientific and spiritual conversation, her strength, and her generosity. To Tammy Tamayo for being an amazing scientist, mother and friend. I would not have made it through baby number three if it were not for you. Thank you for sharing you and encouraging me. I wish you both so much joy and success. I would like to thank a true Godsend: David Ryba, you have given me much more than you could ever know. You have given so freely of your time, your heart, your scientific enthusiasm, your impatience to get things to turn out ☺ I would not have made it without your assistance, thank you for being by my side throughout the last few years at UIC. It has been a pleasure!

To my parents, Martin and Rosa Vasquez for your relentless and abounding amount of love support, and encouragement in everything I have ever accomplished in my life! To my dad, Johnny Saddler for your joy and enthusiasm for life. To my sister, Rose Monique Saddler, for teaching me to be strong, for your unconditional love, and for giving us two beautifully smart nieces (Ivianna and T'Anna) to share! To my aunts, especially Tut and Irene for always sharing spiritual and motherly advice and for your generosity towards us and our children. To my Godsisiter, Christina Pleas, I am eternally grateful to have you in my life, for your kind heart and love spills over onto our children and I can only say from the bottom of my heart, thank you for everything! I love you to pieces. To my dearest friends, Rebecca Salter, Atiya Goodins, and Brittini Jones; I am so fortunate to have all of you as my lifelong sisters, friends, and confidants. You all hold a very special place in my heart and I will treasure you forever.

Finally, to my husband, Carlos Wilder, because of your love, faith, discipline, perseverance and wisdom I am able to be who I am today. I am so proud to be your wife. To my dear children, Jalen, Kylie, Gabriel, and Alexandra you make my life happy, full, and complete. Thank you all for walking this journey with me. I love you all.

TW

## TABLE OF CONTENTS

<u>CHAPTER</u>	<u>PAGE</u>
I. Introduction .....	1
A. Switching sarcomeres on and off .....	1
1. The Sarcomere acts as a force generating signaling hub .....	1
B. The thin, titin, and thick myofilament proteins.....	3
1. The Troponins.....	3
2. Tropomyosin.....	5
3. Titin.....	6
4. Thick filament proteins.....	7
5. The myofilaments are relaxed in their off position.....	8
6. Switching on the heart .....	10
C. A Genetic disease of the sarcomere: Hypertrophic Cardiomyopathy.....	10
1. Changing the sarcomere.....	10
2. Structural consequences of $\alpha$ -TmE180G mutation. ....	12
3. To phosphorylate or not to phosphorylate Tm .....	13
4. Functional consequences of the $\alpha$ -TmE180G mutation.....	14
D. Oxidative stress in hypertrophy.....	15
1. Major Intracellular antioxidant – Glutathione .....	15
2. Protein S-Glutathionylation.....	16
3. Oxidative Signals.....	16
II. Tm dephosphorylation and implication of oxidative stress .....	20
A. Introduction .....	20
B. Methods.....	21
1. Generation of $\alpha$ -cMyBP-C, $\alpha$ -cMyBP-C/S283A Transgenic Mice:.....	21
2. Echocardiography .....	22
3. Measurements of $\text{Ca}^{2+}$ Dependent Activation of Tension.....	23
4. <i>Transgenic Protein Quantification and Western Blot Analyses</i> .....	23
5. Carbonylation Assessement .....	25
6. <i>Quantitative Real-Time PCR Analyses</i> .....	25



## TABLE OF CONTENTS (CONTINUED)

<u>CHAPTER</u>	<u>PAGE</u>
7. Statistics.....	26
C. Results.....	26
1. <i>Phosphorylation Status of <math>\alpha</math>-TmE180G and <math>\alpha</math>-TmE180G/S283A Mice</i> .....	26
2. Dephosphorylation of cardiac $\alpha$ -Tm reduces heart failure markers .....	30
3. Dephosphorylation of cardiac $\alpha$ -Tm prevents hypertrophy.....	30
5. Dephosphorylation of cardiac $\alpha$ -Tm improves $\text{Ca}^{2+}$ sensitivity .....	36
6. Dephosphorylation of cardiac $\alpha$ -Tm generates a reduced myocyte .....	39
D. Discussion .....	42
III. Novel control of cardiac myofilament response .....	47
A. Introduction .....	47
B. Methods.....	50
1. Isolation of Cardiac Myofibrils and Measurements of ATPase Activity.....	50
2. Force Measurement of Skinned Fiber Bundles .....	51
3. Immunoblotting.....	52
4. Mass Spectrometry.....	52
5. Statistical Analysis .....	53
C. Results.....	54
1. Myofibrillar ATPase Activity .....	54
2. Glutathionylation of Myofibrillar Preparations .....	56
3. The effect of GSSG and DTT on skinned fiber force generation.....	58
4. Mass Spectrometry.....	60
D. Discussion .....	63
IV. Treatment with N-Acetylcysteine (NAC) improves cardiac function and myofilament disorders in Hypertrophic Cardiomyopathy .....	67
A. Introduction .....	67
B. Materials and Methods .....	71
1. <i><math>\alpha</math> -Tm-E180G Transgenic Mice</i> .....	71
2. <i>Placebo-controlled study and administration of NAC</i> .....	71
3. <i>Echocardiography</i> .....	72
4. <i>Glutathione Assay</i> .....	73
5. <i>Immunoblotting</i> .....	73

## TABLE OF CONTENTS (CONTINUED)

<b><u>CHAPTER</u></b>	<b><u>PAGE</u></b>
6. Measurement of isometric tension, ATPase and $k_{tr}$ .....	73
7. Statistical Analysis .....	74
C. RESULTS .....	74
1. TG- $\alpha$ -Tm-E180G mice display an increase in oxidative stress markers that is reversed by administration of N-Acetylcysteine (NAC) .....	74
2. NAC administration improves cardiac morphology and function in HCM.....	77
3. NAC affects SERCA2a expression and phosphorylation of phospholamban.....	77
4. NAC decreases isometric tension and improves cross-bridge dynamic measurements in .....	82
skinned fiber bundles, facilitating relaxation.....	82
D. Discussion .....	91
V. GENERAL CONCLUSIONS AND SPECULATIONS.....	98
VI. CITED LITERATURE .....	102
VII. APPENDICES.....	111
VIII. CURRICULUM VITAE .....	114

## LIST OF FIGURES

<u>FIGURE</u>	<u>PAGE</u>
Schematic of the sarcomere with multiplex functions. ....	2
Schematic illustration of integral sarcomeric components.....	4
Illustration of a sarcomere in diastolic and systolic states. ....	9
Schematic diagram of current $\alpha$ -TmE180G phenotype.....	19
Generation and morphology of $\alpha$ -TmE180G/S283A (DMTG) mice. ....	28
Phosphorylation status of $\alpha$ -TmE180G and DMTG hearts. ....	29
Expression of heart failure markers in HCM.....	31
Morphology measurements of $\alpha$ -TmE180G compared to DMTG. ....	32
Diastolic function of $\alpha$ -TmE180G compared to DMTG.....	34
Measurement of $\text{Ca}^{2+}$ dependent activation of tension. ....	37
Post-translational status of cTnI and $\text{Ca}^{2+}$ handling proteins. ....	38
Glutathione status among groups.....	40
Glutathionylation and carbonylation of myofibril proteins.....	41
Schematic of dephosphorylation findings. ....	46
Structure of cMyBP-C schematic diagram showing C0-C10 domains. ....	49
Myofibril pCa_ATPase activity of control and GSSG treated samples.....	55
Western blot analysis of proteins subject to glutathionylation during ATPase assay. ....	57
The effects of GSSG and DTT on force generation of skinned fibers. ....	59
SDS-PAGE gel for in gel digestion. ....	61
Schematic of redox hypothesis. ....	70
Graph of intracellular glutathione from 10mg of LV tissue.....	76
NAC's effect on morphology in HCM.....	79
NAC effect on hypertrophic signal. ....	81
Skinned papillary fiber function from mice treated with or without NAC. ....	83
Tension cost in $\alpha$ -TmE180G treated with NAC. ....	84
Immunoblot analysis of SERCA2a and PLN protein expression. ....	85
Kinetics of tension redevelopment ( $k_{tr}$ ).....	86
Phosphorylation status of myofilament proteins after NAC treatment.....	88
GSH blot of myofibrillar cMyBP-C protein.....	90
Schematic of the NAC treatment in HCM findings.....	97
Schematic diagram explaining the findings of collective data. ....	101

## LIST OF TABLES

<u>TABLE</u>	<u>PAGE</u>
Morphology and contractile function assessed in NTG, $\alpha$ -TmE180G, and DMTG .....	35
Glutathionylated peptides discovered by mass spectrometry. ....	62
Echocardiographic phenotype following NAC treatment for one month.....	80

## LIST OF ABBREVIATIONS

ANOVA	Analysis of Variance
ANP	Atrial naturetic peptide
ATP	Adenosine Tri-phosphate
BNP	Bovine naturetic peptide
CaMKII	Ca <sup>2+</sup> calmodulin kinase II
DMTG	Double mutant transgenic ( $\alpha$ -TmE180G/S283A)
DOCA	Deoxycorticosterone acetate
DTT	Dithiothreitol
EF	Ejection fraction
ERK	p42/42 MAPK kinase
FS	Fractional shortening
FVBN	Friend virus B-type strain of mouse
GSH	Glutathione
GSSG	Oxidized glutathione
HCM	Hypertrophic cardiomyopathy
HR	Heart rate
HW	Heart weight
LVIDd	Left ventricular internal diameter during diastole
MLC	Myosin light chain
MS	Mass spectra

### **LIST OF ABBREVIATIONS (CONTINUED)**

MyBP	Cardiac myosin binding protein C
MyHC	Myosin heavy chain
NAC	N-acetylcysteine
NAPDH	Nicotinamide Adenine Dinucleotide Hydrogenase
NO	Nitric oxide
OH	Hydroxyl
PCR	Polymerase chain reaction
PKA	Protein kinase A
PKC	Protein kinase C
PLN	Phospholamban
RNA	Ribonucleic Acid
RCS	Reactive carbonyl species
RNS	Reactive nitrogen species
ROS	Reactive oxygen species
RSK3	Ribosome S6 Kinase
RT-PCR	Real time RT-PCR
SEM	Standard error of the mean
SERCA2a	Sarcoendoplasmic reticulum ATPase 2a
SR	Sarcoplasmic Reticulum
TG	Transgenic
Tm	Tropomyosin

## **LIST OF ABBREVIATIONS (CONTINUED)**

$\alpha$ -TmE180G	$\alpha$ -Tropomyosin E180G
cMyBP	Cardiac myosin binding protein C
cTnC	Cardiac troponin C
cTnI	Cardiac troponin I
cTnT	Cardiac troponin T

## SUMMARY

The work described within this dissertation investigates the general hypothesis that post-translational modifications of  $\alpha$ -Tm elicit a progression of a pathophysiological phenotype through a mechanism involving altered redox signals. Hypertrophic cardiomyopathy (HCM) is a genetic disease of the sarcomere that ultimately results in left ventricular hypertrophy and diastolic dysfunction. This disease affects 1 in 500 and is the leading cause of sudden cardiac death in young, especially athletes. The exact mechanism by which these mutations elicit hypertrophy is unknown. In order to gain a better understanding of this disorder and how to devise effective treatments, a mouse model has been generated that mimics human HCM where cardiac specific  $\alpha$ -tropomyosin ( $\alpha$ -Tm) glutamic acid (E) at position 180 was exchanged with uncharged glycine (G) ( $\alpha$ -cMyBP-C). This well characterized model displays severely enlarged left atria, fibrosis, myocyte disarray, hypertrophy, and diastolic dysfunction associated with an increased  $\text{Ca}^{2+}$ -sensitivity of myofilaments. Human HCM hearts have been shown to exhibit increases in oxidation that inappropriately activate kinases and phosphatases. When we examined the HCM myofibrils, we detected an increase in oxidative markers that target myofilament proteins. Moreover, in the adult stages of this model, the 30-60% reduction in the phosphorylation status of  $\alpha$ -Tm was not evident compared to non-transgenic (NTG) littermates. Collectively these data led us to hypothesize that decreasing phosphorylation of  $\alpha$ -Tm at S283 would facilitate the rescue of the phenotype, including preventing the oxidative modifications associated with cMyBP-C. We further hypothesized that antioxidant treatment using N-acetylcysteine (NAC) would reverse the HCM phenotype.



## SUMMARY (CONTINUED)

Experiments reported in chapter one uses a double mutant transgenic (DMTG) mouse model incorporating  $\alpha$ -cMyBP-C with dephosphorylated  $\alpha$ -Tm (S283A) to understand the role phosphorylation plays in disease progression. Dephosphorylation prevented the hypertrophic remodeling, decreased the  $\text{Ca}^{2+}$  sensitivity, improved relaxation, and reduced oxidative glutathionylation of myosin binding protein C (cMyBP-C) and carbonylation of myofibrillar proteins. These data suggest that altered charge status and post-translational modification of  $\alpha$ -Tm causes a strain on the heart that elicits oxidative modifications.

Chapter two examines the direct functional effect and specific sites of glutathionylation of myofilament proteins. Employing Western blotting and mass spectrometry, we induced glutathionylation in vitro by treatment of isolated myofibrils and detergent extracted fiber bundles (skinned fibers) with oxidized glutathione (GSSG). Results indicate that there are at least three cysteines on cMyBP-C that are susceptible to oxidative modification. Force generating skinned fiber bundles showed an increase in  $\text{Ca}^{2+}$ -sensitivity when treated with oxidized glutathione, which was reversed with the reducing agent, dithiothreitol. These results indicated that antioxidants would be beneficial to reduce  $\text{Ca}^{2+}$ -sensitivity in HCM.

The object of experiments reported in chapter three aimed to determine whether antioxidant treatment could reverse HCM. In our approach, we treated NTG and cMyBP-C mice with N-Acetylcysteine (NAC) for one month. NAC is a precursor to the major intracellular antioxidant glutathione. Glutathione is found in every mammalian cell at a concentration between 1-10 mM.

## SUMMARY (CONTINUED)

Oxidative stress has been demonstrated to decrease the cellular antioxidant capacity and alter the redox potential. We found that oral administration of NAC reverses redox mediated hypertrophic signaling, remodeling, and improves the relaxation kinetics by a mechanism that involves modifying key sarcomeric and  $\text{Ca}^{2+}$  handling proteins that mediate contraction and relaxation.

Our findings provide a new appreciation of the role of tropomyosin phosphorylation in control of hypertrophic and oxidative signaling. Results of this thesis work show the complexity of the relation between myofilament modifications, oxidative stress, and the hypertrophic phenotype in HCM. HCM mutations inducing oxidative myofilament modifications could be resolved by treatment with antioxidants that relieve the constraint placed on the molecular motors that drive the cardiac cycle.

## I. Introduction

### A. Switching sarcomeres on and off

#### 1. The Sarcomere acts as a force generating signaling hub

The sarcomere is the basic contractile unit of a cardiac cell. Electron microscope images show that each sarcomere is delineated by two dark lines termed the Z-disc that spans a range of about 1.6 to 2.4  $\mu\text{m}$  in length. Fig. 1 depicts half of a sarcomere and illustrates the cytoskeletal filamentous arrangement of a cardiomyocyte and the cellular elements that control mechano-electro-chemical coupling, energetics, and transcriptional processes. One main function of the Z-disc is to sense the mechanical strain that is induced by alteration in hemodynamic stimuli such as elevation in end diastolic volume and cellular stretch. Reaction to the mechanical cues occurs due to a complex set of signaling molecules that are interspersed within the Z-discs. These signaling kinases and phosphatases diverge on different cellular elements within the cell to mediate a network of communication between the integral components that maintain muscle homeostasis. These signaling molecules can traverse the nuclear membrane to elicit transcriptional regulation of key regulatory proteins that mediate the myofilaments response to  $\text{Ca}^{2+}$ . For example, under adrenergic stimulation the protein expression of sarco-endoplasmic reticulum calcium ATPase (SERCA2a), the main ATPase responsible for Ca re-uptake, is enhanced through the transcriptional regulation of NFAT (Anwar, Schlüter et al. 2008). Overexpression of SERCA2a protein enhances cardiac relaxation (Baker, Hashimoto et al. 1998), but reduction in SERCA2a expression results in the progression of heart failure in mice (Schultz Jel, Glascock et al. 2004). Since SERCA2a is an ATPase, the process of  $\text{Ca}^{2+}$  re-uptake, thus relaxation, uses a considerable amount of energy. The energy required for the contractile and relaxant processes within the cardiomyocyte is generated from the mitochondria.

Figure 1

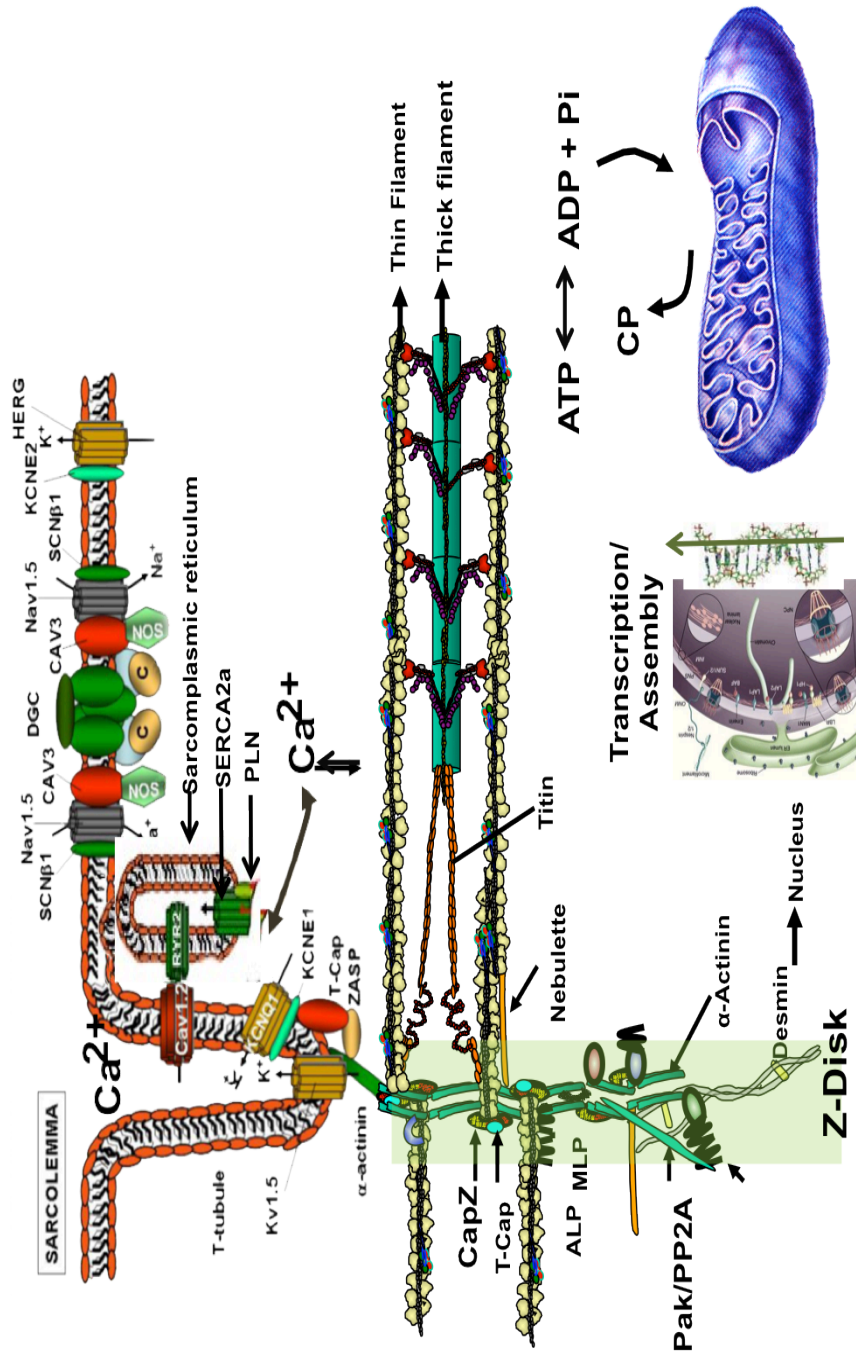


**Fig 1. Schematic of the sarcomere with multiplex functions.**

This illustration depicts the sarcolemma in association with half of a sarcomere (including the Z-disc with several signaling molecules), the nucleus, the mitochondria and the calcium flux proteins. The image represents the network of events that occur between the thin and thick filaments to the elements that involve transcription, energetics, and signaling. The See text for more detail. Figure modified from Vatta and Solaro . 2013 In Biophysics of Heart Failure, (Solaro and Tardiff eds.)

The mitochondria comprises approximately 30-40% of a cardiomyocyte and serve not only as the major source of adenosine triphosphate (ATP) production, but also produce the largest amount of reactive oxygen species (ROS) (Rutledge and Dudley 2013). The produced energy is required for proper ion pump function as well as for regulation of the actin-myosin interaction during the on and off states of the contractile apparatus (to be discussed below). Thus, contraction and relaxation are energetically costly events. Our current investigations focus on a general hypothesis suggesting that a disruption in the cross-talk between the physiological signals, transcription, and energy production or usage could potentially elicit a cyclic cascade of events that result in maladaptive myocardial remodeling and alterations in the myofilaments response to  $\text{Ca}^{2+}$ .

## **B. The thin, titin, and thick myofilament proteins**

### **1. The Troponins**

The troponin (Tn) complex is made up of three regulatory subunits that are all required for  $\text{Ca}^{2+}$  activation of muscle contraction (see schematic Fig. 2). The three subunits are troponin C ( $\text{Ca}^{2+}$  binding subunit), I (inhibitory subunit), and T (tropomyosin binding subunit). The structure of cTnC has been elucidated to be in the form of a dumb-bell shaped protein with two globular domains connected by a central helix. The two structural  $\text{Ca}^{2+}$  binding sites are located at the C-terminal globular region. The N-terminal domain contains one regulatory  $\text{Ca}^{2+}$  binding site, and in low  $\text{Ca}^{2+}$  concentrations ( $\sim 0.01\text{-}0.5\ \mu\text{M}$ ), TnC weakly interacts with TnI.

Cardiac TnI is a rod-like flexible protein that contains five distinct regions that facilitate the switching of the myofilaments to an activated state. The regions include a cardiac specific N-terminal region, and IT-arm region, an inhibitory region, the switch region, and the C-terminal mobile region (Solaro, Rosevear et al. 2008). The mobile and inhibitory regions interact and bind



strongly to actin to facilitate the blocking of the actin-myosin interaction during relaxation (discussed below).

Troponin T is a 280 amino acid protein that contains a globular domain that associates with TnC, TnI, and Tm (Solaro and Van Eyk 1996, Solaro and Rarick 1998). Cardiac TnT has two tropomyosin binding sites, one located in the carboxyl region at positions 175 - 190 and the other located in the overlap region (discussed below) over positions 258 – 284 (Li, Gagne et al. 1997, Jin and Chong 2010). These regions are functionally important because they influence the cooperativity, possibly the flexibility, and the positioning of tropomyosin on the actin filament.

## **2. Tropomyosin**

The alpha-helical structure of tropomyosin (Tm) is essential to the regulation of contraction and relaxation. Tm is made up of 284 amino acids that are arranged such that a seven amino acid (heptad) sequence (a-b-c-d-e-f-g)<sub>n</sub> is repeated throughout. Positions a and d are generally hydrophobic in nature where the branching of the tertiary and quaternary structure positions facilitate the interlocking of these residues around each other helps to create and stabilize the  $\alpha$ -helical chains (Conway and Parry 1990). Positions e and g, on the other hand mediate the ionic interactions that govern the packing of the  $\alpha$ -helix between adjacent  $\alpha$ -helices (Conway and Parry 1990).

High-resolution x-ray crystallography reveals that the  $\alpha$ -helices positioned at the C-terminal 22 residues, 263-284, splay apart and are stabilized by dimerization with an adjacent Tm molecule (Li, Mui et al. 2002). Each end of the Tm molecule extends 8-11 residues and overlaps with another neighboring Tm molecule to establish a continuous strand that lies along the thin filament. This  $\alpha$ -helical structure delineates function because Tm spans actin in a 1:7 ratio preventing myosin from

binding during relaxation. Tropomyosin has conserved regions (1-7) that have important actin binding sites. Disruption in certain regions, specifically region 5 inhibits the myosin cross-bridge from binding, thus impedes the inhibitory function of Tm. Phosphorylation at the penultimate amino acid at position S283 modulates the inhibitory effect of Tm. However, the specific role of Tm-phosphorylation is still unclear (further discussion can be found in Introduction Section C-3 below).

### **3. Titin.**

Titin is the largest protein in the human body (Labeit and Kolmerer 1995) and in the heart it is independently considered as another type of filament protein. As mentioned previously, it spans half of the sarcomere where the N-terminus extends from the Z-line to the M-line of the sarcomere. Through its structure, titin becomes the main factor responsible for passive tension, stiffness, and elasticity of the diastolic heart (Linke and Krüger 2010). Titin is composed of unstructured polypeptides flanked within approximately 100- folded immunoglobulin (Ig) domains linked in series (Alegre-Cebollada, Kosuri et al. 2014). In a healthy heart during diastole, titin is known to serve as the determinant factor for the Frank-Starling law of contraction. This mechanism states that the stroke volume of the heart increases as the blood volume increases during diastole, when other factors remain constant. Titin uses two mechanisms to respond to the alterations in mechanical stretch that is induced by blood filling: recoil of the unstructured regions and unfolding and refolding of the Ig domains. Thus, the stiffness of this extensible protein is regulated based on the state of the heart. Movement of titin transduces a signal to the Z-disc that elicits a molecular response from kinases and phosphatases that feedback onto the myofilament proteins to alter the response to  $\text{Ca}^{2+}$ . Furthermore, it has been determined that unfolding of the unstructured domains under stressful conditions, decreases titins stiffness and exposes oxidizable cysteines (Alegre-Cebollada, Kosuri et al. 2014).



#### 4. Thick filament proteins

The thick filament is composed mainly of myosin heavy chain. This molecule is made of two N-terminal globular head structures called S1 and S2 that wind around one another and terminate as  $\alpha$ -helical tails. The myosin S1 head domain (synonymous with cross-bridge) is responsible for binding to actin to generate force in an ATP dependent manner. The chemical energy released is converted to mechanical energy to cause the myocyte to shorten. Associated with the myosin heavy chains are the myosin light chains and myosin binding protein – C (MyBP-C), that help to stabilize myosin and regulate its interaction with actin.

Attached to the base of myosin heavy chain is a cardiac specific MyBP-C. This 150 kDa protein is made of 8 Ig-like and 3 fibronectin type 3 repeating domains that associate with titin. Cardiac MyBP-C has a special alanine-proline rich region that serves as a hub for phosphorylation (Sadayappan and de Tombe 2014). Phosphorylation of MyBP-C decreases the distance between myosin S1 and actin filaments and promotes the acto-myosin interaction. Several regulatory kinases are activated under varying conditions. Protein kinase A (PKA), CaMKII, and RSK3 and others have been shown to phosphorylate one of the highly conserved M-domain serines at either 273, 282, 302, and/or 307 (Sadayappan, Osinska et al. 2006). These sites are alternatively modified depending on the physiological demand to fine-tune the cross-bridge cycling dynamics. For example, under beta-adrenergic stimulation, PKA can phosphorylate all three sites. However, under oxidative strain, RSK3 is activated to phosphorylate only S282 (Gupta and Robbins 2014). Concomitantly, in a  $\text{Ca}^{2+}$  dependent and independent manner, CaMKII can modify either of the four aforementioned sites (Gupta and Robbins 2014). No matter the kinase involved, the levels of MyBP-C phosphorylation in heart failure are relatively low. In addition to the regulatory phosphorylation sites , we have

recently reported that MyBP-C contains sequences that are susceptible to oxidative modification that regulates contractile function (Patel, Wilder et al. 2013).

#### **5. The myofilaments are relaxed in their off position.**

The sarcomere is made of long fibrous, helical, and intertwined proteins that slide past one another during a contraction (Fig. 3). After each shortening event, the sarcomere relaxes as the heart fills with blood. This means that in the absence of  $\text{Ca}^{2+}$  the isometric tension is low, not zero. During this state, regulatory cTnC is devoid of bound  $\text{Ca}^{2+}$ . TnI is bound to actin; TnT is tethered to Tm, holding Tm in a position that blocks the actin binding sites. On the thick filament, the ATP products ADP and  $\text{P}_i$  are bound to myosin, which decreases the affinity of myosin to actin. The reason the isometric tension is low at this stage is perhaps due to a minimal amount of cross-bridge binding to actin (Stein, Schwarz et al. 1979, Chalovich, Chock et al. 1981). Thus, the inhibition by Tm plays a critical role in mediating the relaxed state of myofilaments. Changes in the flexibility or stability of this protein would prematurely activate the myofilament during relaxation. (Fig. 3).

Figure 3

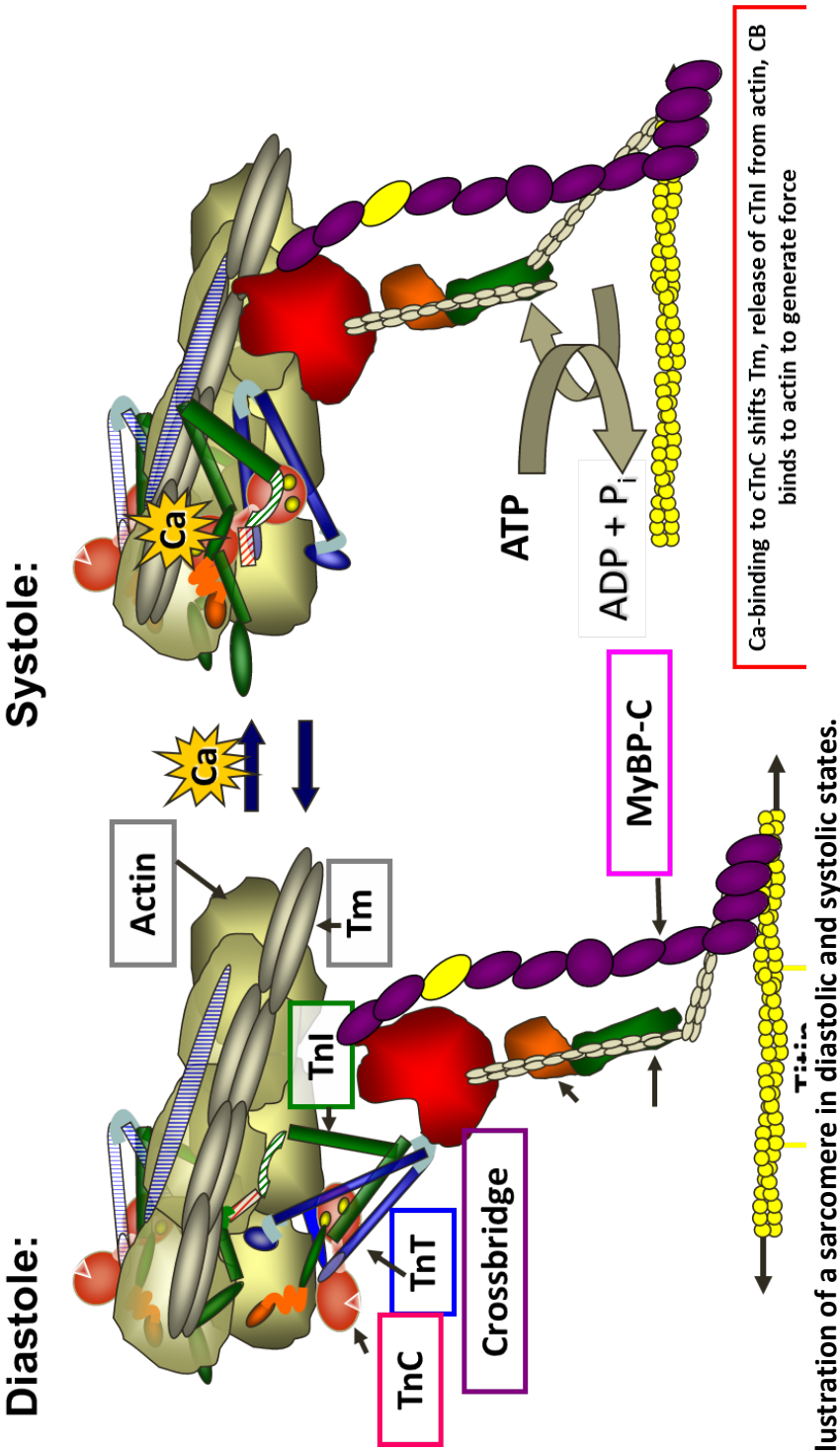


Figure 3 Illustration of a sarcomere in diastolic and systolic states.

Diastole is the state of relaxation where the red globular cross-bridge is prevented from attaching to the actin filaments by Tm-Tn structural impedance. Systole is the state of contraction and is depicted on the right showing the cross-bridge engaged with the actin filaments. (Figure is courtesy of Dr. R. John Solaro, Department of Physiology and Biophysics, University of Illinois at Chicago)

## 6. Switching on the heart

Depolarization of the myocardium allows a small influx of  $\text{Ca}^{2+}$  that induces a larger release of  $\text{Ca}^{2+}$  from the sarcoplasmic reticulum (SR) calcium stores. This  $\text{Ca}^{2+}$  binds to cTnC and elicits a series of highly ordered cooperative interactions among the thin filament proteins (Spyracopoulos, Li et al. 1997, Farah and Reinach 1999).  $\text{Ca}^{2+}$  binds to cTnC, which induces TnC to interact with higher affinity with the switch region of TnI (Razumova, Bukatina et al. 2000, Hinken and Solaro 2007). Simultaneously, the inhibitory region of cTnI detaches from actin (Solaro and Van Eyk 1996). This leads to Tm shifting its azimuthal position to a closed position on the actin filament, such that the actin binding sites are exposed and weak molecular acto-myosin interaction exist. Once Tm shifts to a fully opened position, myosin S1 strongly binds, releases ADP and  $\text{P}_i$  and generates force such that the thin filaments move inward toward the M-line shortening the entire length of the sarcomere. Strongly bound cross-bridges are thought to spread activation along the thin filament in a Tm dependent manner. This accounts for the steep dependence of force on  $\text{Ca}^{2+}$  despite TnC having a single regulatory site.

### C. A Genetic disease of the sarcomere: Hypertrophic Cardiomyopathy

#### 1. Changing the sarcomere

Mutations in approximately ten genes, usually autosomal dominant and associated with the cardiac sarcomere, lead to a condition known as hypertrophic cardiomyopathy (HCM) (Jagatheesan, Rajan et al. 2003). Single point mutation(s) (Seidman and Seidman 2001, Maron 2002) in every sarcomeric protein including but not limited to MyHC, cMyBP-C, cTnI, T, titin, and tropomyosin, can contribute to a form of HCM. Symptoms of the disease range from asymptomatic to dyspnea, syncope, angina, palpitations, and the most devastating presentation of sudden cardiac death. Hearts display increased  $\text{Ca}^{2+}$  sensitivity of the myofilaments, myocyte disarray, fibrosis, left ventricular

hypertrophy, left atrial enlargement, arrhythmia, and diastolic dysfunction. The first cases and the predominate cases of sarcomere mutations leading to HCM are found in myosin heavy chain (Geisterfer-Lowrance, Kass et al. 1990). However, mutations of  $\alpha$ -Tm lead to mild to severe cases of HCM depending on the location of the aberration. For the purpose of these studies, we will focus on one Tm mutation. Alpha-Tm mutations affect only 5% of the American population and contribute to mild cardiac hypertrophy that has an onset beyond the third decade (Wieczorek, Jagatheesan et al. 2008).

Eleven single point mutations have been identified in  $\alpha$ -Tm. Six of these mutations are located between residues 172 - 192 and lead to HCM (Nakajima-Taniguchi, Matsui et al. 1995, Coviello, Maron et al. 1997, Bottinelli, Coviello et al. 1998, Maron 2002). These mutations are located in the TnT binding region and are thought to interrupt the Tm-TnT and Tm-Tm interactions to negatively affect cooperativity of force transmission (Wieczorek, Jagatheesan et al. 2008). The heart appears to adapt to this defect by remodeling as hypertrophy in an effort to maintain functional performance. Chronic disruption elicits a pathological signaling cascade that alternatively targets myofilaments and depresses function. Research has aimed to understand the underlying etiology of HCM, and animal models are used to gain insight into the pathological progression that occurs because of these mutations.

Our collaborators (Prabhakar, Boivin et al. 2001) have generated a FVBN mouse model using the cardiac specific  $\alpha$ -myosin heavy chain promoter to drive expression of Tm with a single point mutation at amino acid position 180 on  $\alpha$ -Tm where glutamic acid (E) has been exchanged with glycine (G), thus  $\alpha$ -TmE180G was characterized in 2001 (Prabhakar, Boivin et al. 2001). This model will be used throughout these experiments. The mutant gene expression replaces the endogenous protein such that the total protein level is unaltered. Phenotypically, this model mimics human HCM

as it displays the myocyte disarray, fibrosis, left ventricular hypertrophy, severe left atrial enlargement, increased  $\text{Ca}^{2+}$  responsiveness of myofilaments, and diastolic dysfunction with preserved systolic function. How this mutation progresses to the disease state and ultimately result in sudden cardiac arrest is still unclear. It is well documented that the  $\alpha$ -Tm mutation alters cardiac function and results in the development of cardiac hypertrophy (Evans, Pena et al. 2000, Prabhakar, Boivin et al. 2001, Jagatheesan, Rajan et al. 2003, Prabhakar, Petrashevskaya et al. 2003, Wieczorek, Jagatheesan et al. 2008).

## **2. Structural consequences of $\alpha$ -TmE180G mutation.**

The position of Tm lying on the thin filament is integral in controlling actin activation. The cMyBP-C mutation located in the cTnT calcium sensitive binding region could disrupt the ionic interactions between the helices that decrease the affinity of Tm to actin (Wolska and Wieczorek 2003). This adjustment should have a direct effect in the cooperative activation of the myofilaments. However, in vitro measurements showed that in N-terminal  $\alpha$ -Tm mutants, myosin-S1 bound cooperatively to F-actin and maintained the same stability as wild-type, however the local flexibility increased near position Cys190, leading to altered response when S1 switched on the thin filaments (Golitsina, An et al. 1997). Additionally, human cardiac  $\alpha$ -cMyBP-C cDNA was used to generate single molecules of mutant  $\alpha$ -Tm that were exposed to atomic force microscopy. The mutation rendered the Tm 35% more flexible compared to wild-type, suggesting a local spatial gradient of activation during systole (Loong, Zhou et al. 2012). *In vivo* mutations of  $\alpha$ -Tm, such as  $\alpha$ -TmE180G, have been suggested to increase flexibility of Tm that would weaken the interaction between actin and result in fewer blocked states that would induce an increase in the  $\text{Ca}^{2+}$  sensitivity as well the demand for ATP and altered ATPase rate.

### 3. To phosphorylate or not to phosphorylate Tm

There appears to be a Tm specific kinase that phosphorylates Tm at position S283 (Mak, Smillie et al. 1978), however regulation of this kinase remains elusive, possibly due to developmentally related low levels of expression. At birth, 70% of  $\alpha$ -Tm is basally phosphorylated in mice (Heeley, Moir et al. 1982). In adults, the percent of phosphorylation decreases to 10-30% (Heeley, Moir et al. 1982). Perhaps these changes are responding to cardiomyocyte requirement to contract at a faster rate during development. In vitro studies show that phosphorylation of  $\alpha$ -Tm increases the myosin ATPase rate without altering the  $\text{Ca}^{2+}$  affinity to cTnC (Heeley, Watson et al. 1989). This would speed relaxation. Recent studies using single myofibril preparations have demonstrated that increased levels of phospho-Tm depresses relaxation and  $\text{Ca}^{2+}$  release from TnC (Nixon, Liu et al. 2012). Genetically mutated mouse models of  $\alpha$ -Tm display altered phosphorylation status depending on the phenotype and age at the time of evaluation.

Dilated cardiomyopathic hearts have a diminished level of Tm phosphorylation (Warren, Arteaga et al. 2008) while HCM hearts characteristically display increased levels of phosphorylation as adults (Prabhakar, Boivin et al. 2001, Schulz, Correll et al. 2012). In HCM, if phosphorylation increases the ATPase rate and decreases the maximum developed tension (Vahebi, Ota et al. 2007), it is expected that this combination would support dysfunctional relaxation kinetics associated with energy impairment. The functional role of  $\alpha$ -Tm phosphorylation was tested when a mouse model incorporating a non-phosphorylatable S283A mutation revealed an increase in cardiomyocyte cross-sectional area resulting in compensated hypertrophy, with no changes in sensitivity of myofilaments or in the cooperativity of activation (Schulz, Correll et al. 2012). Neither the autophagic nor apoptotic cell death processes were ruled out, however the increases in wall dimensions, coupled with the lack of cardiac dysfunction indicated an adaptive state of hypertrophy. Nonetheless, S283

is located in a critical Tm regulatory region that interacts with TnT (Wieczorek, Jagatheesan et al. 2008). Phosphorylation of  $\alpha$ -Tm also increases the head to tail interactions of adjacent molecules without affecting the ability to bind actin (Heeley, Watson et al. 1989). Given the collective data, we hypothesize that Tm phosphorylation may play a role in the progression HCM.

#### **4. Functional consequences of the $\alpha$ -TmE180G mutation**

The diminished functional dynamics of the  $\alpha$ -TmE180G mouse heart are attributable to:

- (1) Increased Tm flexibility that predisposes the cross-bridge to actin in low calcium
- (2) Loss of the calcium handling machinery responsible for  $\text{Ca}^{2+}$  re-uptake
- (3) Increases in oxidant strain.

In the  $\alpha$ -TmE180G model, the increased flexibility exposes myosin heads to actin even in low intracellular  $[\text{Ca}^{2+}]$ . When myosin binds to actin this causes an increase in the affinity of  $\text{Ca}^{2+}$  to cTnC (Baker, Hashimoto et al. 1998, Lehrer and Geeves 2014) which increases the affinity of cTnI binding to cTnC during the end stages of systole. It is expected that these hearts would display increased  $\text{Ca}^{2+}$  sensitivity.

The rate of sequestration of intracellular  $\text{Ca}^{2+}$  into the sarcoplasmic reticulum during relaxation is diminished in  $\alpha$ -TmE180G due to a reduced level of SERCA2 protein expression as well as its regulation. Collectively, this leads to depression in the rates of relaxation. Recent studies reveal that restoring/altering  $\text{Ca}^{2+}$  fluxes and desensitizing myofilaments prevents the pathophysiological development of HCM in  $\alpha$ -TmE180G hearts (Alves, Gaffin et al. 2010, Peña, Szkudlarek et al. 2010, Gaffin, Peña et al. 2011, Alves, Dias et al. 2014).

We believe that intrinsic stressors, like mutations of sarcomeric proteins, have the ability to elicit stress response signals that place neuro-humoral, mechanical, metabolic, chemical, and redox



strains on the heart. In HCM, reactive oxygen species can stimulate aberrant signaling cascades that affect not only the phosphorylation and protein expression in heart, but can also mediate a redox signal that supports remodeling. One goal of this thesis work is to gain a better understanding of the role oxidant stress plays in disease progression.

#### **D. Oxidative stress in hypertrophy**

Oxidative stress is defined by H. Sies and D.P. Jones as, “an imbalance between oxidants and antioxidants in favor of the oxidants, leading to a disruption of redox signaling and control and/or molecular damage” (D 2007, Dalle-Donne, Milzani et al. 2008). Cells generally operate in a reduced environment where low levels of reactive oxygen, nitrogen, or carbonyl species (ROS, RNS, or RCS, collectively termed ROS) are produced and quickly neutralized. ROS appear in the form of superoxide ( $O\bullet^-$ ), nitroxyls ( $\bullet NO$ ) or hydroxyls ( $\bullet OH$ ). The buffering capacity of these species depends on the defense system that includes superoxide dismutase, vitamins, and the major intracellular antioxidant, glutathione, to name a few. The beneficial effect of ischemic preconditioning and cardioprotection has been associated with small acute and intermittent exposure to ROS (Maddika, Elimban et al. 2009). The excess production of ROS is expected to contribute to the pathology of disease through redox signaling in various human disorders including cardiovascular disease (Dalle-Donne, Giustarini et al. 2003).

##### **1. Major Intracellular antioxidant – Glutathione**

One signaling protein that mediates the redox status of the cell is glutathione. Glutathione is a tripeptide (glycine–cysteine–glutamic acid) that is ubiquitously expressed in millimolar concentrations in every mammalian cell (Asensi, Sastre et al.). The tri-complex of glutathione is less oxidative than cysteine because the reactive thiol region is contained within the molecule, and it serves well as a compound that can maintain the intracellular redox potential by reacting with

oxidized molecules. Glutathione scavenges free radicals in the presence of glutathione peroxidase and is converted to GSSG. GSSG can interact with cellular proteins. Despite evidence that antioxidant treatment including vitamin E supplementation in humans to date have been disappointing, perhaps increasing the concentration of the major intracellular antioxidant may prove more beneficial.

## **2. Protein S-Glutathionylation**

The reversible binding of oxidized glutathione to protein thiols is now termed S-Glutathionylation of proteins and serves as another post-translational modification mediated through altered redox status. Many diseases are now associated with S-glutathionylation (cite). The process of this post-translational modification occurs when the cellular levels of reduced glutathione, are oxidized, to produce glutathione disulfide (GS-SG). This oxidized form of glutathione becomes reactive with exposed protein thiols to either alter function or mark the protein for degradation (Dalle-Donne, Milzani et al. 2008). Glutathione reductase can re-establish the GSH/GSSG ratio by reducing the oxidized GSSG and converting it back into glutathione (Dalle-Donne, Milzani et al. 2008).

## **3. Oxidative Signals**

Excess ROS can damage cardiac tissue through varying types of modifications including covalent and non-covalent protein interactions. Increasing amounts of data suggest that these modifications could be a primary or secondary mechanism that link to the progression of hypertrophy (Maulik and Kumar 2012, Steinberg 2013, Qin, Siwik et al. 2014). ROS induced modifications of proteins alter signaling cascades that affect myocardial remodeling through kinases and phosphatases. For example, ERK 1/2 phosphorylation, a protein involved in hypertrophic growth, has been shown to be mediated through oxidative modifications (Lombardi, Rodriguez et al. 2009). Angiotensin II activation of  $\text{Ca}^{2+}$ /calmodulin kinase II (CaMKII) in heart disease is mediated

through methionine oxidation in a  $\text{Ca}^{2+}$  independent manner (for review see (Luczak and Anderson 2014) and (Erickson, Joiner et al. 2008). As mentioned previously, CaMKII plays an important role in modulating cardiomyocyte  $\text{Ca}^{2+}$  release and re-uptake. Furthermore, ROS have potent effects on SERCA and ryanodine receptor expression (Beyar, Shapiro et al. 1990). Microarray analysis of cMyBP-C hearts demonstrated a number of genes that are transcriptionally altered that may play a role in hypertrophic signaling that are potentially ROS related (Rajan, Pena et al. 2013).

Finally, since the mitochondria makes up approximately 30-40% of the cardiomyocyte, the ROS produced from electron transport is expected to come largely from this source (Rutledge and Dudley 2013). Incorporation of MitoTempo, a specific inhibitor of mitochondrial ROS, blunted excess ROS production and restored disrupted mitochondria in cardiomyocytes susceptible to arrhythmia and sudden death (Rutledge and Dudley 2013). Since mitochondria are the main source of energy and ROS, it is likely that mitochondrial defects can contribute to energetic mismatches that drive disease progression through oxidation. However, other sources of ROS are produced from membrane bound NADPH oxidases, and xanthine oxidase. The focus of our studies was not on the source of ROS, rather we aimed to determine how ROS affects the sarcomere and how this translates into altered pump function.

This background information has led us to test two hypotheses:

**Hypothesis 1:** Decreasing  $\alpha$ -Tm phosphorylation is beneficial and prevents the development of HCM and oxidative stress.

**Specific Aim 1:** Generate a double mutant mouse model that will contain both TmE180G and a non-phosphorylatable S283A mutation:  $\alpha$ -TmE180G/S283A (DMTG).

**Specific Aim 2:** Determine the function associated with the TmE180G hearts compared to NTG and  $\alpha$ -TmE180G/S283A hearts

**Specific Aim 3:** Determine whether dephosphorylation decreases the post-translational modifications associated with oxidant damage.

**Hypothesis 2:** Antioxidant treatment using N-Acetylcysteine reverses the pathology of HCM.

**Specific Aim 1:** Determine the effect of NAC on the morphology of TmE180G.

**Specific Aim 2:** Determine whether NAC reverses the diastolic and cross-bridge cycling impairments in TmE180G.

**Specific Aim 3:** Determine whether NAC can prevent the oxidative modifications of myofilament proteins.

Figure 4

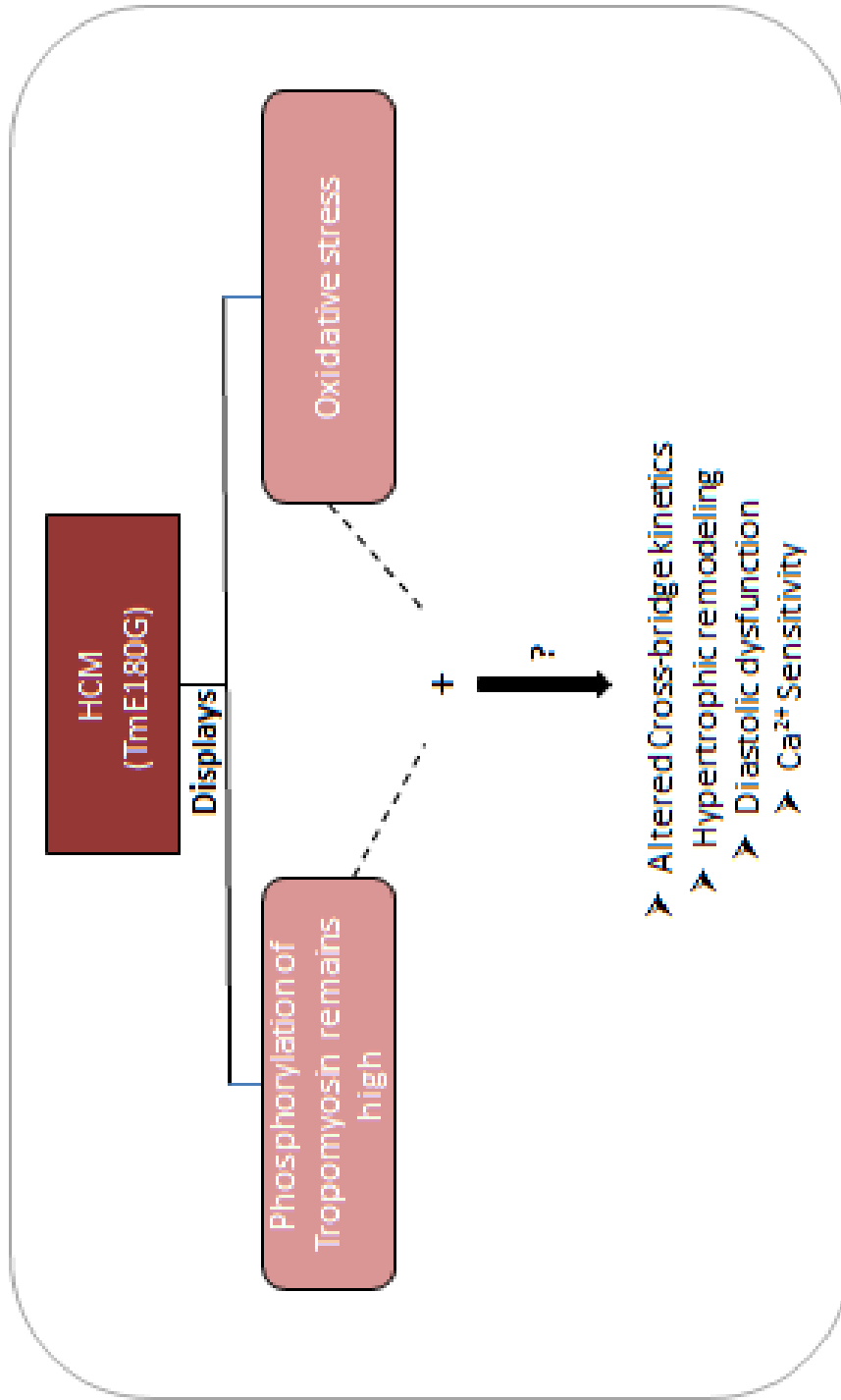


**Figure 4 Schematic diagram of current α-TmE180G phenotype.**

This schematic illustrates what we have observed and what we expect to gain understanding in through this work. In the α-TmE180G hearts there is an increase in the phosphorylation status of α-Tm with age. We expect oxidative stress. We aim to determine how these two factors contribute to pathology of HCM in our model.

## CHAPTER II

### II. Tm dephosphorylation and implications of oxidative stress

#### A. Introduction

Previous studies from David Wieczorek's lab demonstrate that compared to controls, the  $\alpha$ -TmE180G mouse hearts display an increase in the phosphorylation status of  $\alpha$ -Tm at S283 in adulthood, where the pathological phenotype is most severe (Schulz, Wilder et al. 2013). How this mutation leads to altered basal phosphorylation status is unknown. However, our lab and others have shown that phosphorylation of sarcomeric proteins is a mechanism by which the heart regulates cardiac dynamics in health and disease (Solaro, Moir et al. 1976, Solaro and Van Eyk 1996, Kentish, McCloskey et al. 2001, Solaro 2011). Recently, studies using myofibrils demonstrated that increased phosphorylation of  $\alpha$ -Tm decreases the  $\text{Ca}^{2+}$  release from cTnC and depresses relaxation kinetics (Nixon, Liu et al. 2012). These data suggest that Tm phosphorylation is detrimental.

An emerging stream of evidence implicates oxidative stress either in causation, disease progression, or as a secondary consequence of the strains placed on the heart by mechanical impedance (Lang 2002, Sawyer, Siwik et al. 2002, Takimoto and Kass 2007, Maulik and Kumar 2012). When we evaluated cMyBP-C myofibril proteins as targets of oxidative stress, we found increased levels of glutathionylation and carbonylation, both of which are oxidative stress markers found in hypertensive models (Lovelock, Monasky et al. 2012, Jeong, Monasky et al. 2013, Patel, Wilder et al. 2013). We hypothesized that decreasing the phosphorylation status of  $\alpha$ -Tm would reverse the deleterious functional effects of the E180G mutation and prevent the associated oxidant damage. To test our hypothesis, a double mutant transgenic mouse model encoding both the  $\alpha$ -TmE180G

mutation as well as a constitutively non-phosphorylatable  $\alpha$ -Tm, S283A was generated by the Wieczorek lab to mimic dephosphorylation (Schulz, Wilder et al. 2013). We aimed to determine the role of phosphorylation in HCM and its effect on inhibiting oxidative stress. In our approach, we assessed morphology, whole heart and myofibrillar function, and myofilament post-translational modifications including those incurred by oxidative damage among  $\alpha$ -TmE180G and  $\alpha$ -TmE180G/S283A, the double mutant transgenic (DMTG) mice compared to NTG littermates.

## **B. Methods**

All protocols and procedures involving animals were approved by the Animal Care Policies and Procedures Committee at the University of Illinois in Chicago (Institutional Animal Care and Use Committee accredited), and animals were maintained in accordance with the Guide for the Care and Use of Laboratory Animals published by the United States National Institutes of Health (*National Institutes of Health Publication No. 85-23*, revised 1996).

### **1. Generation of $\alpha$ -TmE180G, $\alpha$ -TmE180G/S283A transgenic mice:**

Mouse striated muscle  $\alpha$ -Tm cDNA was subjected to QuikChange II site directed mutagenesis (Agilent Technologies) using the primer 5'-CAC GCT CTC AAC GAT ATG ACT GCC ATA TAA GTT TCT TTG CTT CAC- 3' mutating the penultimate serine to an alanine, and primer 5'-ACG TGC AGA GGG GCG GGC TGA -3' mutating glutamic acid 180 to a glycine (Schulz, Wilder et al. 2013). The mutation was verified through sequencing of the construct by Genewiz. The  $\alpha$ -TmE180G-S283A double mutant transgenic (DMTG) construct was then cloned into a vector containing the cardiac specific  $\alpha$ -myosin heavy chain ( $\alpha$ -MHC) promoter and a human growth hormone (HGH) poly-A tail sequence (Fig. 4A) (Subramaniam, Jones et al. 1991). DMTG mice were generated using the FVB/N strain and founder mice were identified using PCR (Muthuchamy, Grupp et al. 1995). Nucleotide sequencing

of DMTG mouse tail DNA verified the sequence of the  $\alpha$ -TmE180G-S283A transgene. The  $\alpha$ -TmE180G TG mice were previously generated and extensively characterized with respect to their cardiac phenotype and function (Prabhakar, Boivin et al. 2001, Prabhakar, Petrashevskaya et al. 2003, Schulz, Correll et al. 2012). Protein expression of both S283A and DMTG animals are published (Schulz, Correll et al. 2012, Schulz, Correll et al. 2012)

## **2. Echocardiography.**

Echocardiographic measurements were performed using a high-resolution transducer (Vevo 770 High Resolution Imaging System with a center frequency of 30 MHz) after anesthetization of two month old mice as previously described (Rajan, Jagatheesan et al. 2010). M-Mode images of the left ventricle (OV), outflow tract (LVOT), and left atrium (LA) were taken from the left parasternal long axis view. The parasternal short axis view at the level of the papillary muscles was used to measure the LV internal dimension (LVID), anterior wall thickness (AW), and posterior wall thickness (PW). NTG and TG 8-12 week old mice were examined. Pulse Doppler was performed with the apical four-chamber view. The mitral inflow was recorded with the Doppler sample volume at the tip of the mitral valve leaflets. In order to measure time intervals, the Doppler sample volume was moved toward the LVOT and both the mitral inflow and LV outflow were obtained in the same recording. Three parameters of the LV diastolic function were evaluated: 1) E/A ratio = maximal velocity of blood flow in the early diastole (E) / maximal velocity of blood flow in the late diastole (A); 2) E wave deceleration time (DT), which was the time from E to the end of the early diastole; and 3) LV isovolumic relaxation time (IVRT), which was the time measured from the aortic valve closure to the mitral valve opening. Additional information about the diastolic function was obtained with tissue Doppler imaging (TDI). Peak myocardial velocities in the early ( $E_m$ ) diastole were obtained with the sample volume at the septal side of the mitral annulus in the four chamber



view. All measurements and calculations were averaged from 3 consecutive cycles and performed according to the American Society of Echocardiography guideline (Lang, Bierig et al. 2005, Nagueh, Appleton et al. 2009). Data analysis was performed with the Vevo 770 Analytic Software.

### **3. Measurements of $\text{Ca}^{2+}$ dependent activation of tension**

Left ventricular papillary muscles were isolated, cut into fiber bundles approximately 200  $\mu\text{m}$  in width and 3-4 mm in length and 'skinned' in a high relaxing solution (HR: 10mM EGTA, 41.89mM K-Prop, 100mM BES, 6.75mM  $\text{MgCl}_2$ , 6.22mM  $\text{Na}_2\text{ATP}$ , 10mM  $\text{Na}_2\text{CrP}$ , 5mM  $\text{NaN}_3$ ) with 1% Triton X-100 for 3-4 hours at 4°C. Fibers were then mounted between a micromanipulator and a force transducer and bathed in HR solution according to methodology by de Tombe (De Tombe and Ter Keurs 1990). Fibers were then subjected to sequential increases in calcium concentration and their developed force was recorded on a chart recorder. Isometric tension measurements were plotted as a function of calcium and fit by a nonlinear least-squares regression analysis to the Hill equation. All experiments were carried out at 22°C.

### **4. Glutathione Assay**

Freshly isolated hearts were washed in ice-cold PBS + 2 mM EDTA with 25mM NEM (n-ethylamide) and snap-frozen in liquid  $\text{N}_2$ , and subsequently stored at -80°C. Heart samples were used within one week of isolation. Ten mg of ventricular tissue were homogenized in 1 mL of PBS containing 2 mM EDTA and NEM. Glutathione assays were performed using 12.5  $\mu\text{L}$  of the centrifuged extract to detect and quantify the cellular content of glutathione using the GSH-Glo assay kit (Promega) as described by the manufacturer. TCEP at 1 mM final concentration was added to another set of test wells with protein sample to determine the total glutathione (GSH + GSSG) content. Luminescence was read using a luminometer set to read all visible light.

## 5. *Transgenic protein quantification and Western blot Analyses*

Myofibrillar proteins were extracted from NTG,  $\alpha$ -TmE180G, S283A and DMTG mouse ventricles as previously described (Muthuchamy, Grupp et al. 1995). Myofibrillar protein preparations using 20  $\mu$ g protein were separated on a 12% SDS-PAGE gel, which was stained with Coomassie Blue. The presence of the  $\alpha$ -TmE180G mutation results in differential mobility on an SDS-PAGE gel (Muthuchamy, Grupp et al. 1995, Muthuchamy, Pieples et al. 1999), allowing quantification of endogenous and DMTG proteins in the sample. Measurements were performed using ImageQuant 5.1. To confirm the double mutant Tm was properly assembled into the sarcomere, cytoplasmic protein fractions (25  $\mu$ g), isolated from 3 month NTG and DMTG male mice, were run on 12% SDS-PAGE gels and visualized with Coomassie Blue stain.

Western blot analyses on myofibrillar protein preparations (4  $\mu$ g) from 3 month male NTG,  $\alpha$ -TmE180G, and  $\alpha$ -TmE180G/S283A hearts were conducted using the Tm specific antibody CH1 (Sigma Aldrich), Tm S283 phosphorylation specific antibody generated for this lab (YenZyme), and sarcomeric  $\alpha$ -actin antibody 5C5 (Sigma Aldrich) as a loading control.

Whole ventricular homogenates from 3 month old NTG,  $\alpha$ -TmE180G, and DMTG mice were utilized to visualize  $\text{Ca}^{2+}$  handling protein expression levels. Western blots were used to visualize sarcoplasmic reticulum ATPase 2a (SERCA2a) (AbCam), TnI (Cell Signaling), pTnI23/24 (Cell Signaling), phospholamban (PLN) (Thermo Scientific), phosphorylated serine 16 PLN (PLN Ser16) (Badrilla), and phosphorylated PLN threonine 17 (PLN Thr17) (Badrilla). Sarcomeric actin (Sigma) was used as a loading control. Phosphorylated PLN levels are given as a ratio of the phosphorylated form over total PLN expression. Total PLN expression is calculated by adding the monomeric and pentameric species of PLN for each sample and normalizing to actin.

Expression levels and post-translational modifications of proteins implicated in oxidative modifications including ERK 1/2, phospholamban and sarco-endoplasmic reticular  $\text{Ca}^{2+}$  ATPase (SERCA 2A) were assessed. An enriched fraction of sarcomeric proteins was also probed to determine whether there were altered phosphorylation states of cTnI (Ser 23, 24), MyBP-C (Abcam) Tm or S-glutathione (Virogen). Measurements of densities were assessed using ImageQuant 5.1.

## **6. Carbonylation Assessment**

The Millipore OxyBlot Protein Oxidation Detection Kit was used per manufacturer recommendations against an enriched isolated myofibril preparation from animal models.

## **7. Quantitative Real-Time PCR Analyses**

RNA was isolated from 3 month old NTG,  $\alpha$ -TmE180G,  $\alpha$ -Tm S283A, and  $\alpha$ -TmE180G/S283A mouse ventricular tissue using TRIZOL Reagent (Invitrogen). cDNA was generated using the Superscript III kit (Invitrogen). Real time RT-PCR was performed using an Opticon 2 real time RT-PCR machine (MJ Research). Each sample was measured in triplicate and each experiment was repeated twice. Target mRNA was normalized to GAPDH expression as described by Pfaffl's method (Pfaffl 2001). Specific primers include:

### ANP:

Forward 5'-GCTTCCAGGCCATATTGGAG-3';

Reverse 5'-GGGGGCATGACCTCATCTT-3;

### $\beta$ MHC:

Forward 5'-TCATCCGAATCCATTTTGGG-3'

Reverse 5'-CATAATCGTAGGGGTTGTTG-3';

BNP:

Forward 5'-GAGGTCACTCCTATCCTCTGG-3';

Reverse 5'-GCCATTTCTCCGACTTTTCTC-3';

GAPDH:

Forward 5'-TGACCACAGTCCATGCCATC-3'

Reverse 5'-GACGGACACATTGGGGGTAG-3'

## 8. Statistics

All data were expressed as means  $\pm$  SEM and analyzed using a one-way ANOVA with either Bonferroni or Tukey's post-hoc test. Significance was set as  $p < 0.05$ .

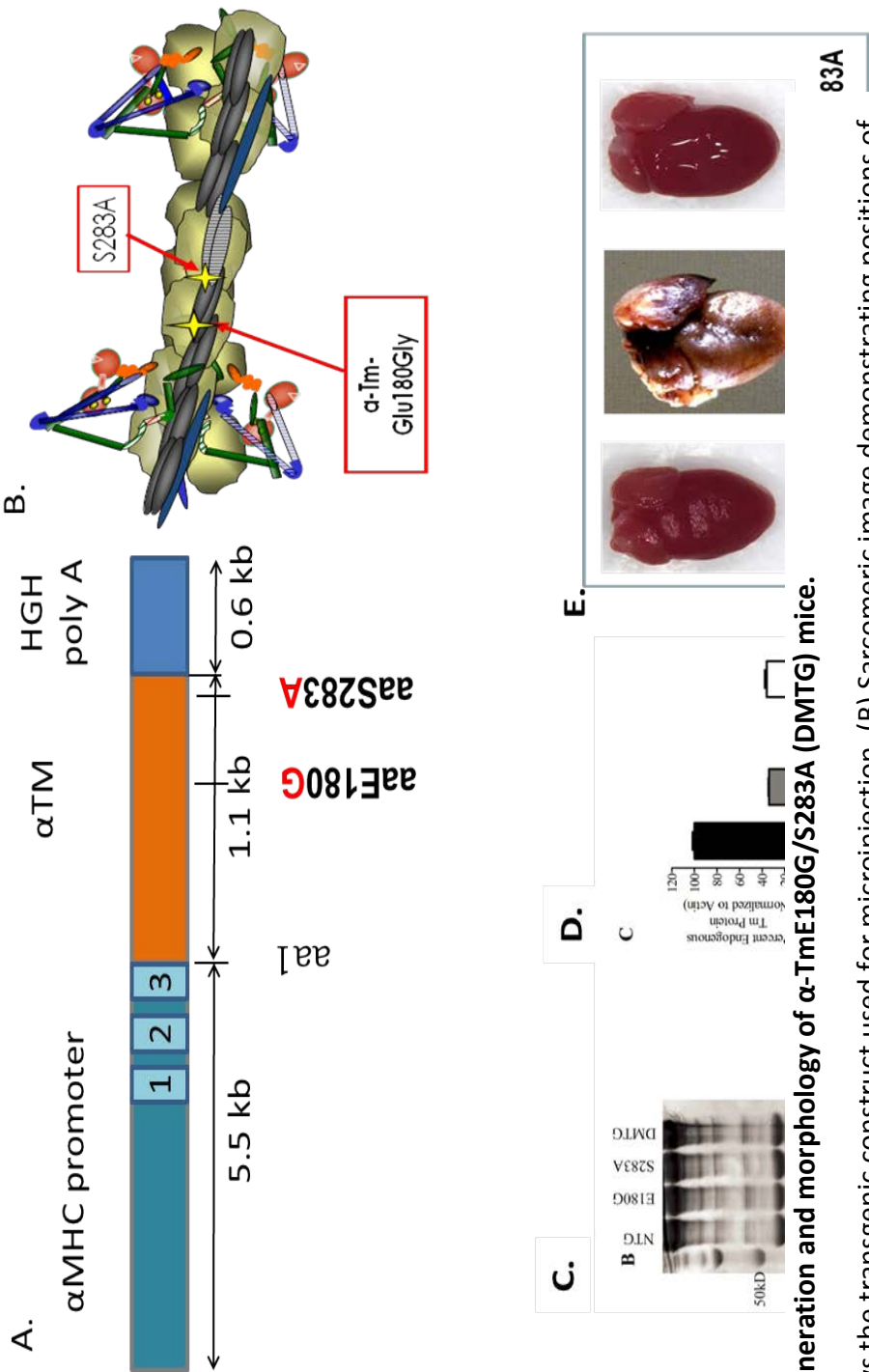
## C. Results

### 1. *Phosphorylation Status of $\alpha$ -Tm in hearts of $\alpha$ -TmE180G and DMTG Mice*

Using a pTm-Ser283 specific antibody (Schulz, Correll et al. 2012), we investigated the phosphorylation status of the  $\alpha$ -TmE180G and DMTG myofibrils. At 3 months of age,  $\alpha$ -TmE180G hearts show a significant increase in Tm phosphorylation that is significantly decreased in DMTG hearts (Fig. 6 A-D). Both the NTG protein and the  $\alpha$ -TmE180G protein are phosphorylated when samples are separated using 2-dimensional isoelectric focusing, indicating that there is no strong bias toward phosphorylating endogenous or TG protein incorporated into the sarcomere (Fig. 5C) (Schulz, Wilder et al. 2013). Additionally, the phosphorylation status of the DMTG hearts resembles

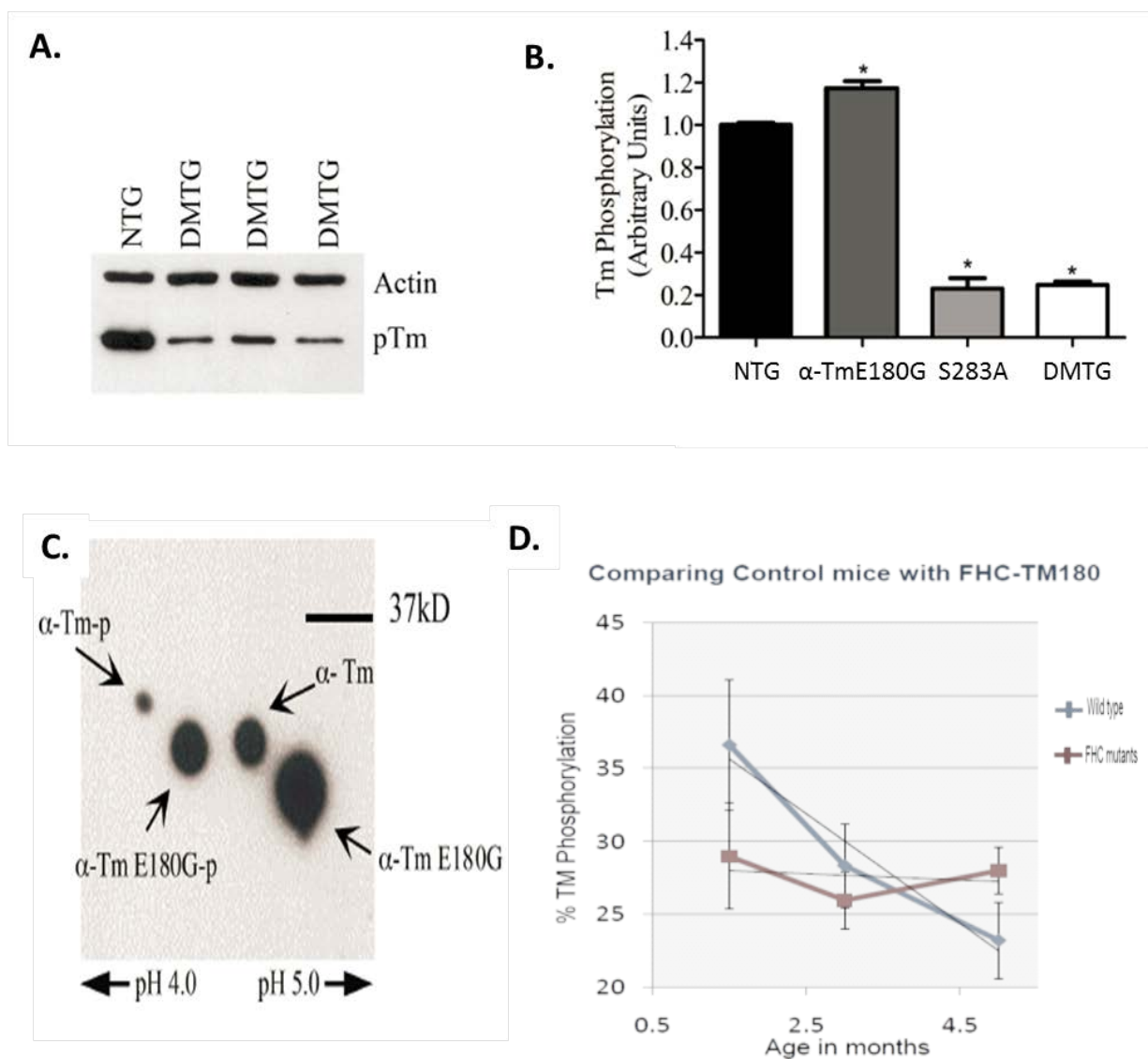
the phosphorylation status of the  $\alpha$ -TmS283A mouse hearts (Fig. 5) (Schulz, Correll et al. 2012, Schulz, Wilder et al. 2013).

Figure 5



**Fig. 5 Generation and morphology of  $\alpha$ -TmE180G/S283A (DMTG) mice.**

(A) Shows the transgenic construct used for microinjection. (B) Sarcomeric image demonstrating positions of mutations along  $\alpha$ -Tm. (C) and (D) Quantified  $\alpha$ -Tm phosphorylation decreased to 23% in the Tm-S283A and DMTG non-phosphorylatable mutants (E) Pathology of HCM hearts compared to NTG and DMTG hearts (Schulz, Wilder et al. 2013).

**Figure 6****Fig. 6 Phosphorylation status of  $\alpha$ -TmE180G and DMTG hearts.**

(A ) Immunoblot of phosphorylation status of  $\alpha$ -Tm DMTG hearts at 3 months of age (B). Histogram showing quantified  $\alpha$ -Tm phosphorylation (C) 2-D SDS-PAGE of  $\alpha$ -Tm from  $\alpha$ -TmE180G myofibers (D) Graphical representation depicting increased phosphorylation in  $\alpha$ -TmE180G hearts compared to NTG. \* vs NTG,  $p < 0.05$ . DMTG is  $\alpha$ -TmE180G/5283A (Schulz, Wilder et al. 2013).

## 2. **Dephosphorylation of cardiac $\alpha$ -Tm reduces heart failure markers**

To assess whether dephosphorylated  $\alpha$ -Tm could prevent the expression of heart failure markers noted in  $\alpha$ -TmE180G, we (Schulz, Wilder et al. 2013) assessed the gene expression of cardiomyopathy markers associated with HCM. Real time RT-PCR analysis of RNA isolated from ventricular tissue shows that DMTG hearts show a significant decrease in atrial natriuretic peptide (ANP), bovine natriuretic peptide (BNP) and  $\beta$ -myosin heavy chain ( $\beta$ -MHC) compared to both NTG and  $\alpha$ -TmE180G hearts (Fig. 7).

## 3. **Dephosphorylation of cardiac $\alpha$ -Tm prevents hypertrophy**

M-mode echocardiography shows that  $\alpha$ -TmE180G hearts demonstrate increased left atrial size and left ventricular mass (Evans, Pena et al. 2000, Prabhakar, Boivin et al. 2001, Prabhakar, Petrashevskaya et al. 2003), confirming the hypertrophic phenotype. In contrast, the DMTG hearts exhibit morphological dimensions and HW:BW ratio as well as myocyte cross-sectional area that resemble NTG controls (Fig. 8) (Schulz, Wilder et al. 2013). Moreover, DMTG cardiomyocytes have normal patterns of sarcomeric arrangement without fibrosis. These findings led us to hypothesize that dephosphorylating  $\alpha$ -Tm prevents the development of hypertrophy in the setting of the E180G mutation.



Figure 7

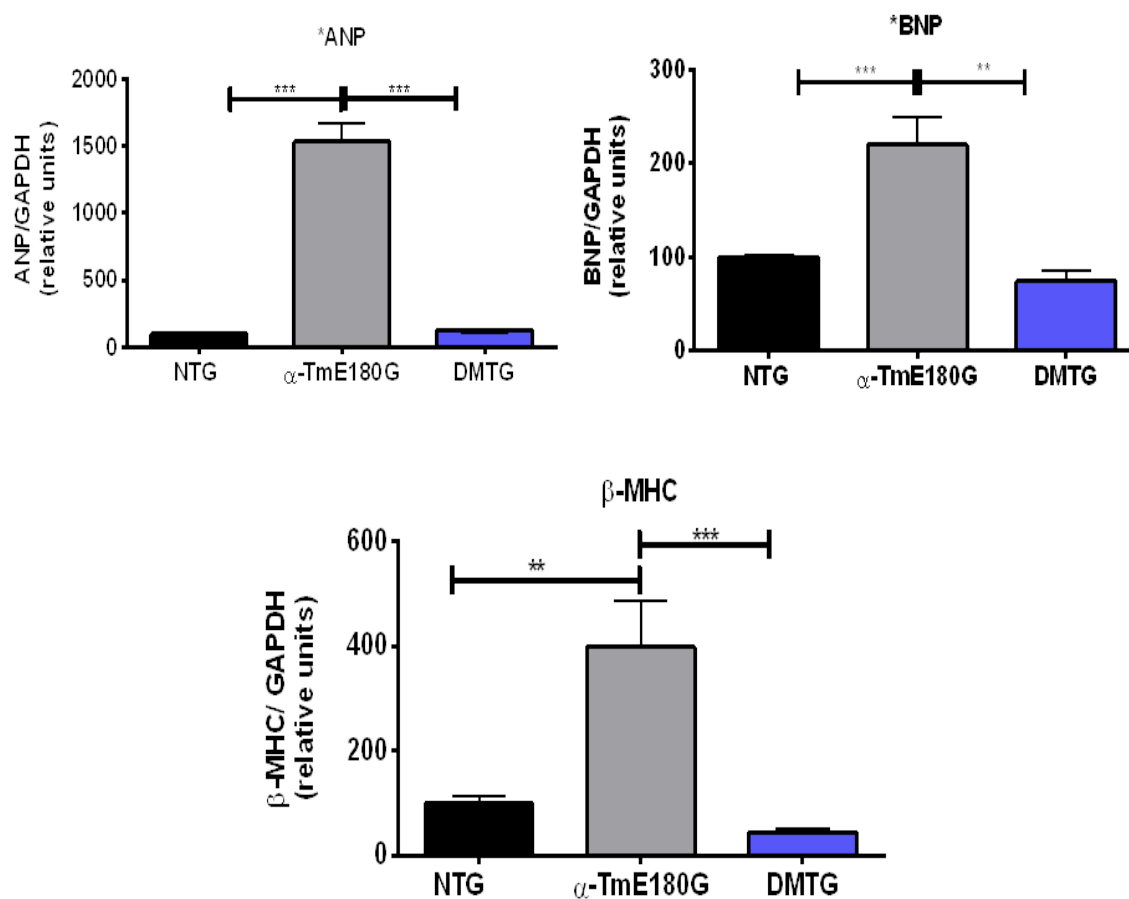


**Figure 7 Expression of heart failure markers in HCM.**

DMTG mice do not express increased heart failure markers. Cardiac heart failure makers atrial natrietic peptide (ANP), brain natrietic peptide (BNP), and  $\beta$ - Myosin Heavy Chain are decreased in the DMTG mice when compared to  $\alpha$ -TmE180G mice. n= 3-7 per group

\*p<0.05; \*\*p<0.01; \*\*\*p<0.001 (Schulz, Wilder et al. 2013)

Figure 8

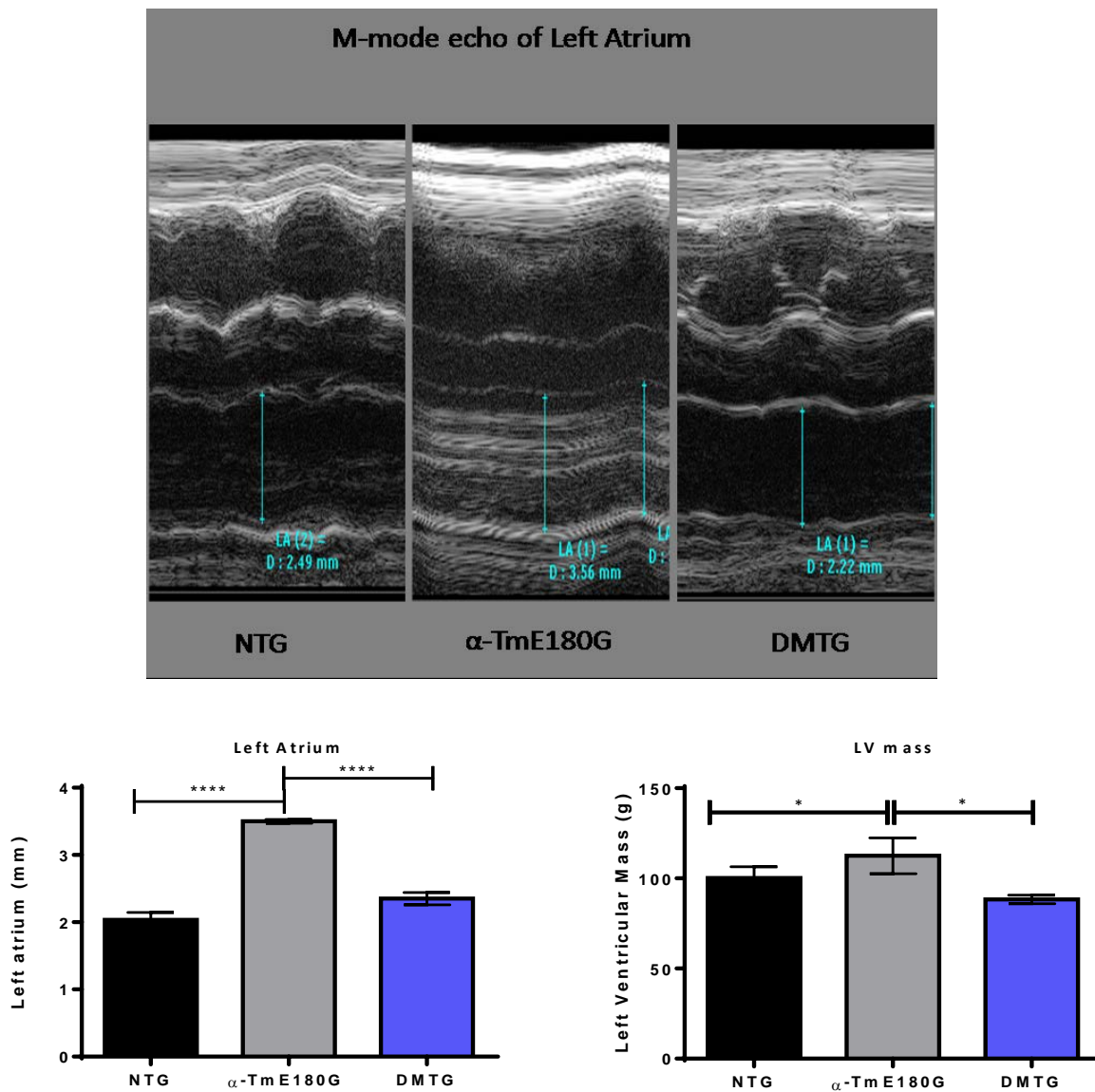


**Figure 8 Morphology measurements of  $\alpha$ -TmE180G compared to DMTG.**

Echocardiography measurements. (A) M-mode echo-cardiography shows that  $\alpha$ TmE180G mice demonstrate increased left atrial size that was reduced in the DMTG hearts. There is also a decrease in  $\alpha$ -TmE180G left ventricular mass with no change in the left ventricular internal diameter during diastole, suggesting  $\alpha$ -TmE180G hearts are hypertrophied compared to DMTG and NTG. (B) Quantitation of echocardiography measurements. n= 6-10 per group. \* $p < 0.05$ , \*\*\*  $p < 0.001$  (Schulz, Wilder et al. 2013)

#### **4. Dephosphorylation of cardiac $\alpha$ -Tm corrects cardiac function**

To assess whether decreasing phosphorylation of  $\alpha$ -Tm in  $\alpha$ -TmE180G improves cardiac function, we performed pulse-wave and doppler echocardiographic analysis on 3 month old NTG,  $\alpha$ -TmE180G and DMTG mice (Table 1). Results reveal that the elevation in the E/A and E/E<sub>m</sub> ratio characteristic of the  $\alpha$ -TmE180G starting at two weeks of age is reversed in the DMTG hearts to control levels (Fig. 9). Doppler images show that the reversal of diastolic dysfunction is a result of normalizing the late atrial filling during diastole (Fig. 9). The evaluated systolic parameters of the DMTG showed significant increases in ejection fraction (EF), fractional shortening (FS), and circumferential fiber shortening (Vcf) when compared to both NTG and  $\alpha$ -TmE180G hearts (Table 1) suggesting hypercontractility.

Figure 9

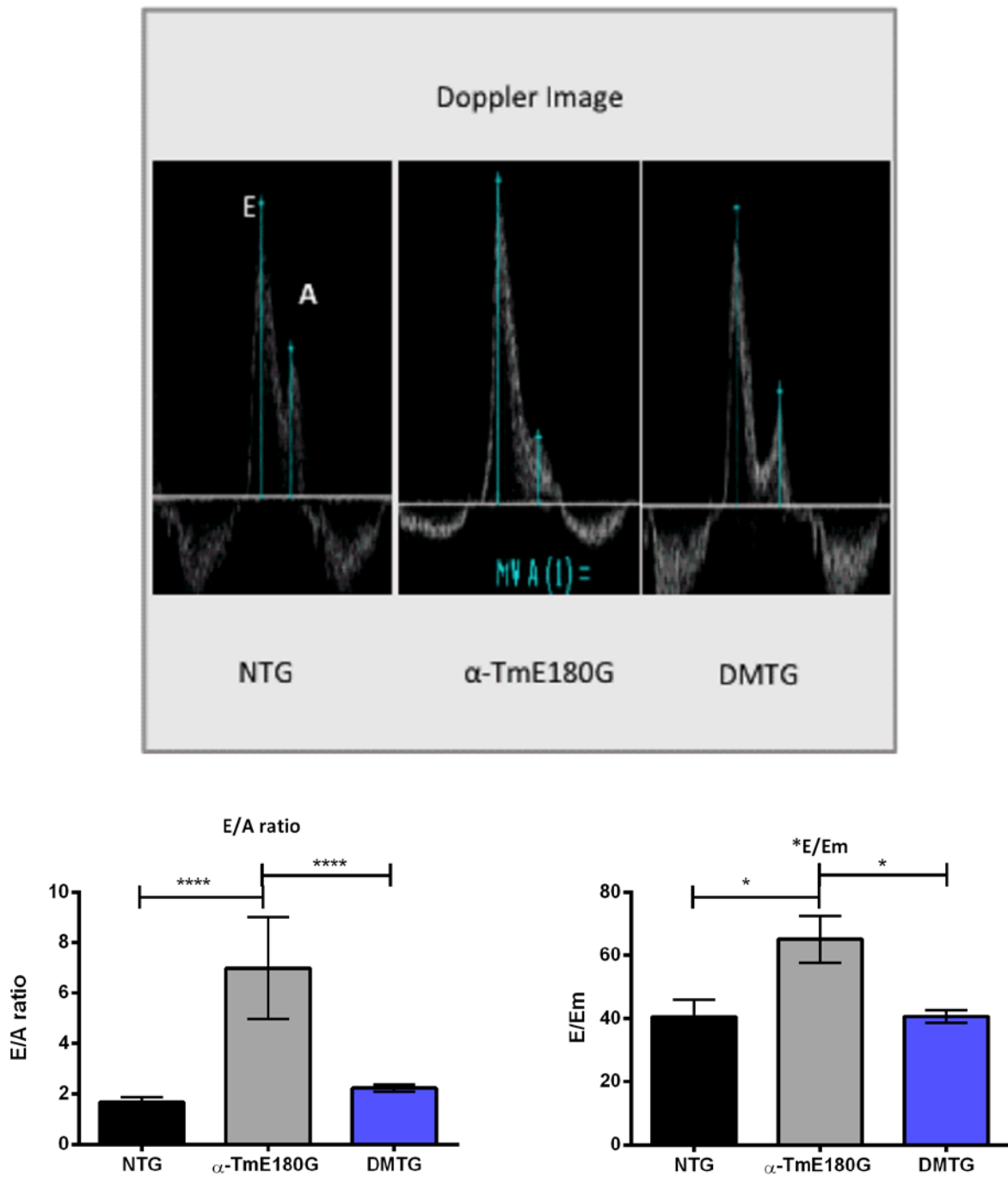


**Figure 9 Diastolic function of  $\alpha$ -TmE180G compared to DTMG.**

Diastolic function is improved in DMTG hearts. (A) Doppler images showing E/A and E/Em ratio's. (B) Quantification of E/A and E/Em ratios of NTG,  $\alpha$ -TME180G and DMTG mice. n= 6-10 per group \*p<0.05, \*\*\* p<0.001 (Schulz, Wilder et al. 2013).

**Table 1****Table 1 Morphology and contractile function assessed in NTG,  $\alpha$ -TmE180G, and DMTG**

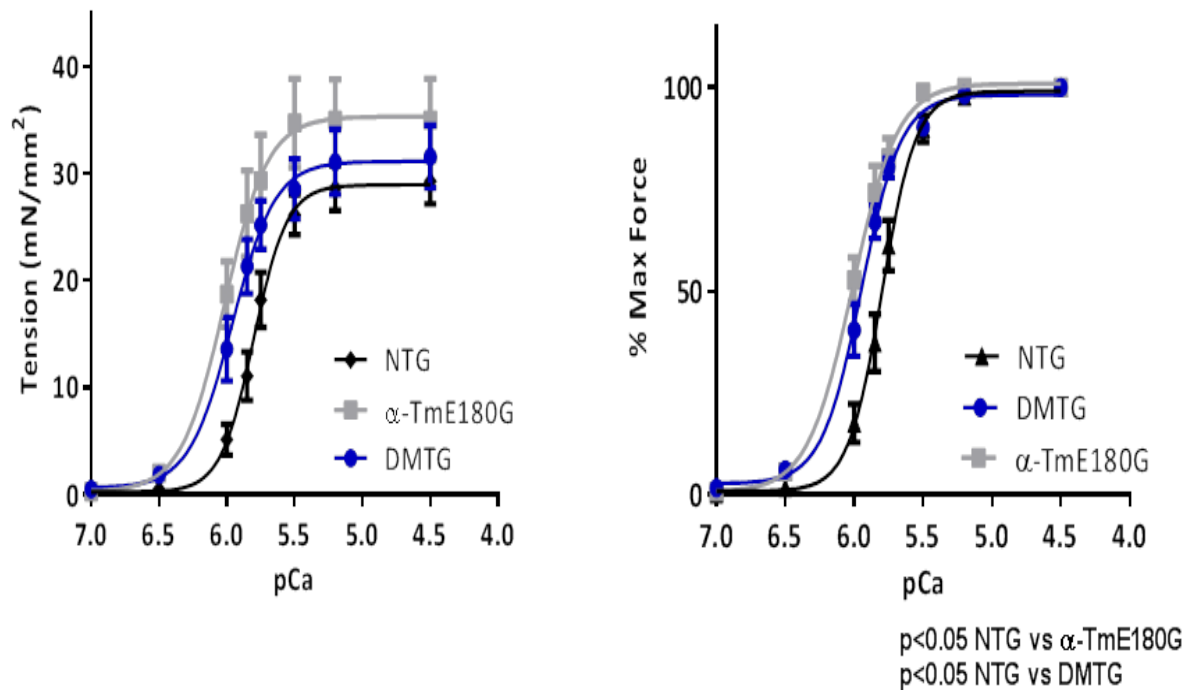
	NTG	TmE180G	DMTG	p < 0.05
(Sample size)	(n=6)	(n=6)	(n=10)	
<b><u>Size Dimensions</u></b>				
LV Mass (mg)	100.1 $\pm$ 6.28	77.2 $\pm$ 2.35*	88.28 $\pm$ 2.40	* vs. NTG
Left Atrium (mm)	2.037 $\pm$ 0.11	3.5 $\pm$ 0.03 * †	2.351 $\pm$ 0.09	* vs. NTG † vs. DMTG
LVIDd (mm)	4.13 $\pm$ 0.17	3.87 $\pm$ 0.10	3.83 $\pm$ 0.06	
RWT	0.39 $\pm$ 0.21	0.37 $\pm$ 0.01	0.42 $\pm$ 0.01	
<b><u>Systole</u></b>				
FS (%)	38.95 $\pm$ 1.47	40.56 $\pm$ 1.23 †	51.49 $\pm$ 2.01*	* vs. NTG † vs. DMTG
EF (%)	69.55 $\pm$ 1.85	71.96 $\pm$ 1.38 †	82.64 $\pm$ 1.85*	* vs. NTG † vs. DMTG
<b><u>Diastole</u></b>				
E/A Ratio	1.69 $\pm$ 0.19	6.99 $\pm$ 2.02* †	2.23 $\pm$ 0.14	* vs. NTG † vs. DMTG
E/Em Ratio	40.52 $\pm$ 5.41	65.1 $\pm$ 7.33 * †	40.62 $\pm$ 1.99	* vs. NTG † vs. DMTG
E wave DT (msec)	22.17 $\pm$ 2.42	26.46 $\pm$ 1.88	22.17 $\pm$ 0.77	
IVRT (msec)	12.66 $\pm$ 0.38	13.75 $\pm$ 2.08	13.71 $\pm$ 0.65	

## 5. Dephosphorylation of cardiac $\alpha$ -Tm improves $\text{Ca}^{2+}$ sensitivity through $\text{Ca}^{2+}$ handling expression

To determine whether phosphorylation of Tm at S283 plays a role in altering the myofilament  $\text{Ca}^{2+}$  sensitivity, we measured force- $\text{Ca}^{2+}$  relations in skinned, detergent extracted fiber bundles from the papillary muscle of 3 month old NTG,  $\alpha$ -TmE180G, and DMTG hearts. Although myofilaments from  $\alpha$ -TmE180G/S283A mice show an increased  $\text{Ca}^{2+}$  sensitivity compared to NTG controls, the  $\text{Ca}^{2+}$  sensitivity of the DMTG were significantly less than  $\alpha$ -Tm E180G myofilaments (Fig. 10). At half-maximum  $\text{Ca}^{2+}$  concentration, the DMTG was  $5.94 \pm 0.01^*$ , NTG  $5.81 \pm 0.02$ , and  $\alpha$ -TmE180G  $6.01 \pm 0.03^*$ , (\* $p < 0.05$  vs NTG) (Fig. 10). The maximum tension and Hill Coefficient ( $n_H$ ) were not significantly different among the groups.

Decreased cTnI phosphorylation at S23/24 (Solaro, Moir et al. 1976, Zhang, Zhao et al. 1995) increases the  $\text{Ca}^{2+}$  sensitivity. However, we did not detect any changes in the phosphorylation status of cTnI (Fig. 11A). However, dephosphorylation of  $\alpha$ -TmE180G increases SERCA2a and phospholamban (PLN) protein expression (Fig. 11). Our results also show that dephosphorylation normalized the phosphorylation status of PLN at both Ser16 and Thr17, the PKA and CaMKII sites respectively.

Figure 10



Group	pCa <sub>50</sub>	n <sub>H</sub>	n
NTG	5.81 ± 0.02	3.58 ± 0.47	12
$\alpha$ -TmE180G	6.01 ± 0.03*	2.65 ± 0.42	5
DMTG	5.94 ± 0.01* <sup>†</sup>	3.44 ± 0.34	10

**Fig. 10 Measurement of Ca<sup>2+</sup> dependent activation of tension.**

Measure of Ca dependent activation is decreased in DMTG. (A) Ca<sup>2+</sup> tension relations in skinned fiber bundles from NTG,  $\alpha$ -TmE180G and DMTG hearts. (B) normalized force relations in skinned fiber bundles from NTG,  $\alpha$ -TmE180G and DMTG hearts. \*  $p < 0.05$  vs. NTG, +  $p < 0.05$  vs  $\alpha$ -TmE180G. (Schulz, Wilder et al. 2013)

Figure 11

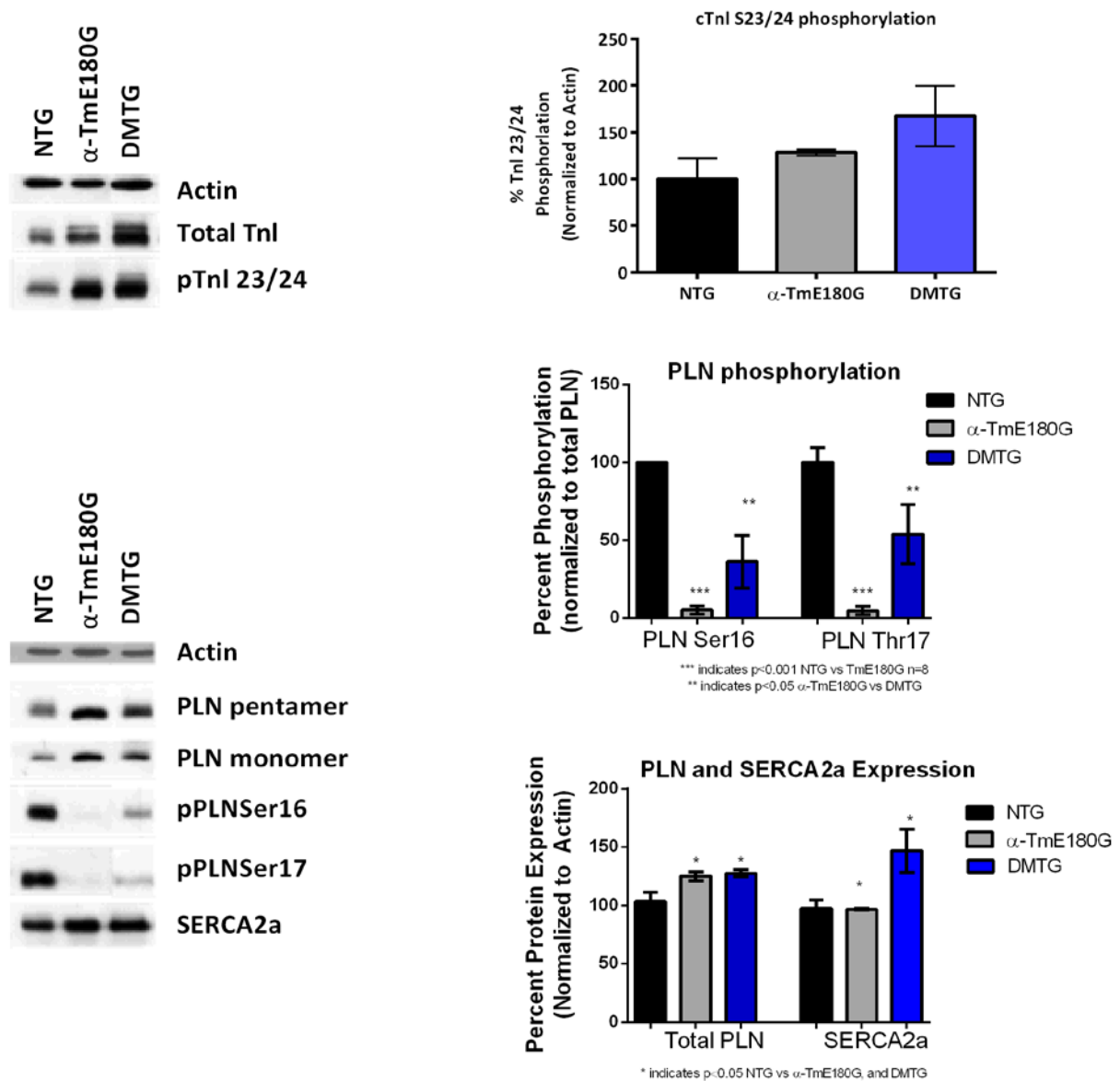


**Fig. 11 Post-translational status of cTnI and  $\text{Ca}^{2+}$  handling proteins.**

Post-translational status of cTnI and  $\text{Ca}^{2+}$  handling proteins. (A and C) Western blots of phosphor-cTnI S23/24 and  $\text{Ca}^{2+}$  handling proteins in NTG, α-TmE180G and DMTG hearts. (B and D) Quantification of images in A. (E) Quantification of expression of PLN and SERCA2a expression. (D) Western blots of cTnI and p-TnI from NTG, α-TmE180G and DMTG hearts. (E) Quantification of data from panel D.  $n = 6-8$  for all groups \*  $p < 0.05$  vs. NTG, +  $p < 0.05$  vs TmE180G. (Schulz, Wilder et al. 2013)



## 6. DMTG cardiomyocytes have normal GSH/GSSG ratio

To assess the intracellular antioxidant capacity among the groups, we employed the GSH-Glo assay, and found reduced levels of GSH in  $\alpha$ -TmE180G mice (Fig. 12A). We report 26% increase in the levels of oxidized glutathione, GSSG, which significantly decreased total (GSH+GSSG) (Fig. 12B and 12C), possibly due to the export or degradation of GSSG, further examination would have be carried out to determine the levels and activity of glutathione peroxidase and reductase to assess the outcome of the total glutathione concentration. Because of the increase in GSSG, the total GSH/GSSG ratio declined 4-fold, indicating an altered redox potential (Fig. 12D). To determine whether the oxidant damage affected sarcomeric proteins, we assessed the levels of protein S-glutathionylation and carbonylation of an enriched fraction of myofilament proteins, both are early indicators of oxidative stress. There is a significant increase in protein glutathionylation of cMyBP-C in  $\alpha$ -TmE180G (Fig. 13A). Compared to NTG controls, there were no changes in either measurement in the DMTG mice and there was only less than a 2-fold change in the GSH/GSSG ratio. We detected an overall increase of carbonylation of myofibril proteins only in  $\alpha$ -TmE180G hearts (Fig. 13B). Taken together, these data show that hypertrophic hearts have increased oxidative stress signals that target sarcomeric proteins and that reduced phosphorylation of  $\alpha$ -Tm in HCM prevents oxidative modification of myofilament proteins.

Figure 12

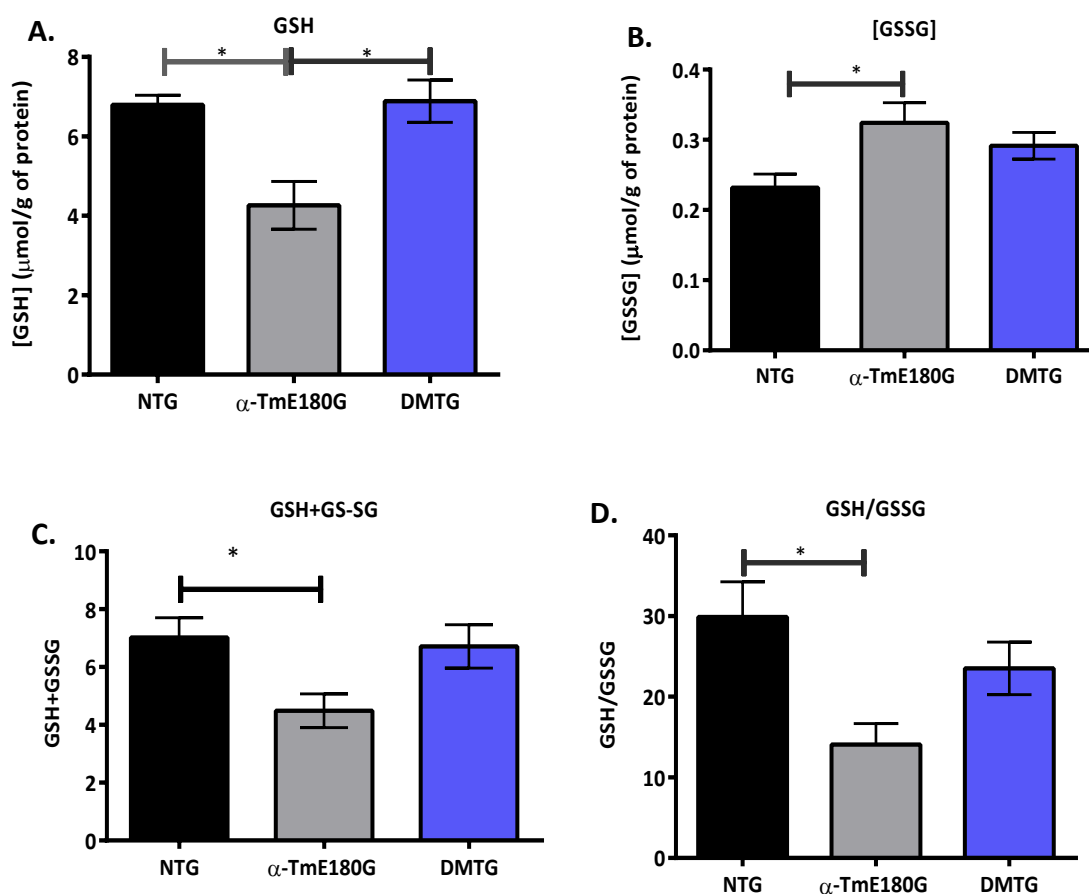
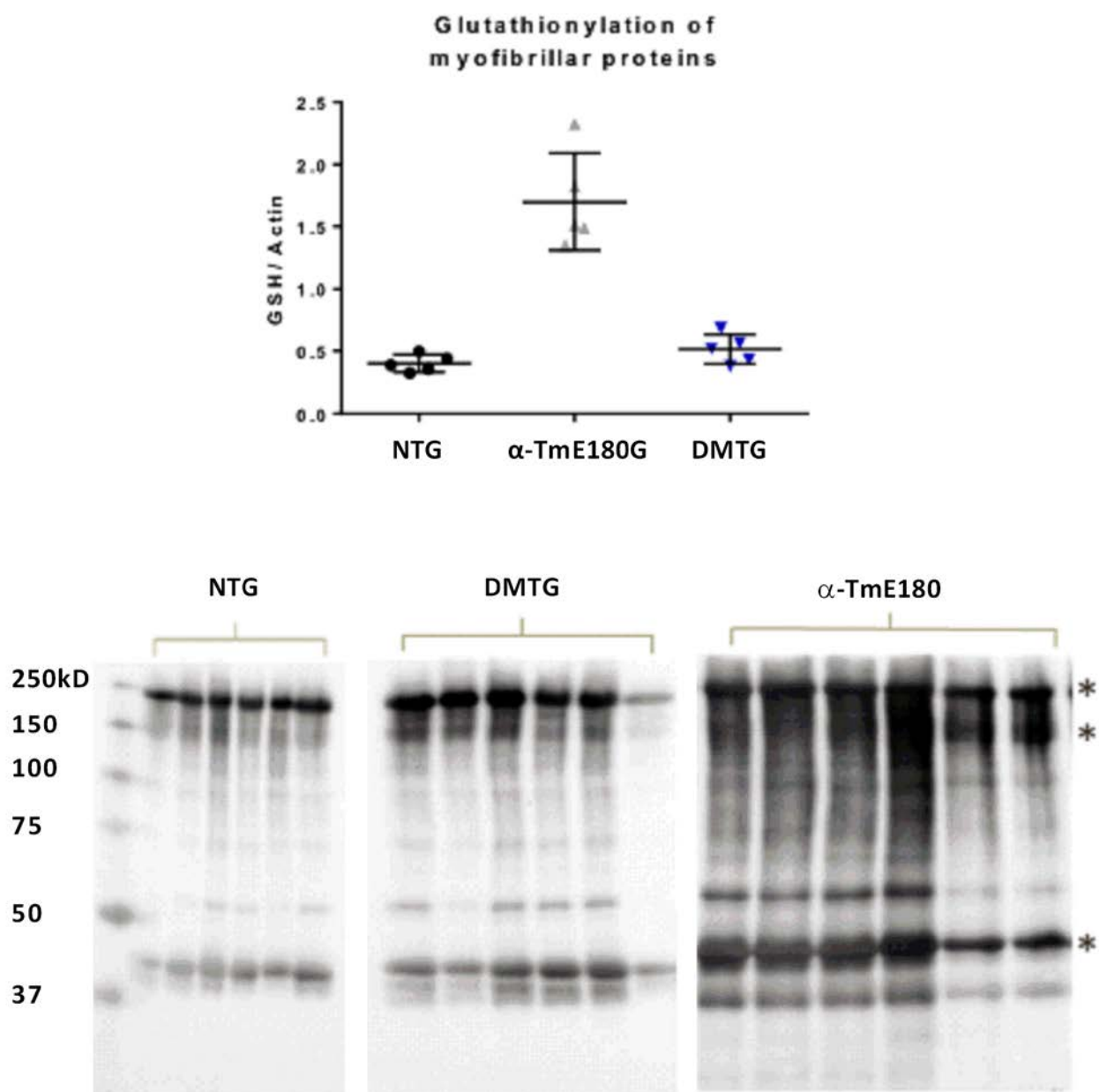


Figure 12 Glutathione status among groups.

Quantified GSH assay(A) Concentration of GSH (all samples were evaluated using 10mg of heart tissue homogenized with 25mM NEM) (B) Concentration of GSSG (C) Concentration of Total glutathione (GSH + GSSG) (D) GSH ratio. n= 5-6 per group

\*p<0.05

Figure 13



**Fig. 13 Glutathionylation and carbonylation of myofibril proteins.**

Glutathionylation and carbonylation of myofibril proteins is reduced in DMTG. (A) Quantitation of a Western Blot probing for anti-GSH or GSSG against an enriched myofibril preparation (B) Immunoblot of carbonylation of an enriched myofibril preparation. n= 6 per group. \*p<0.05

## D. Discussion

The present study revealed that reduction in the phosphorylation status of  $\alpha$ -Tm in a mouse model that mimics HCM,  $\alpha$ -TmE180G, prevented the development of the disorder and reduced oxidative stress. Previous studies using two HCM models showed that the levels of phosphorylation of  $\alpha$ -Tm are increased with age compared with control animals (Sheikh 2009). The role of phosphorylation in modulating the acto-myosin interaction is unknown. Using myofibril preparations, it was recently demonstrated that increased phosphorylation of Tm depresses relaxation kinetics and  $\text{Ca}^{2+}$  release rate from cTnC (Nixon, Liu et al. 2012). Furthermore, the  $\alpha$ -TmE180G mice generally have a shortened life span and die between 6-8 months. Given these observations, we hypothesized that reducing the phosphorylation of  $\alpha$ -Tm would be beneficial by enhancing relaxation. To determine the functional effect of dephosphorylation *in vivo*, a mouse model was generated that incorporated the  $\alpha$ -TmE180G mutation and a mutation exchanging Ser at position 283 to Ala, the sole known phosphorylation site. Thus  $\alpha$ -Tm was dephosphorylated in HCM;  $\alpha$ -TmE180G/S283A (DMTG) (Schulz, Wilder et al. 2013). These alterations prevented hypertrophy, diastolic dysfunction, and normalized the redox potential in the DMTG mice. Further, the life span of these animals is extended to >18 months and have no markers of heart failure (Schulz, Wilder et al. 2013). Together, these data support an integral physiological role of Tm phosphorylation in the regulation of contraction and relaxation, which contributes in part to the pathophysiology of HCM.

Our results indicate that the functional improvements in the contractility of DMTG hearts compared to  $\alpha$ -TmE180G hearts are likely due to a reduction in redox related myofilament protein modifications. Protein S-glutathionylation and carbonylation, both of which were reduced in DMTG ,

have been shown previously to alter the activity of several proteins in mammalian cells (Dalle-Donne, Milzani et al. 2008, Lovelock, Monasky et al. 2012, Jeong, Monasky et al. 2013). Further experiments are required to determine myofilament protein modifications in the heart are implicated in contractile dynamics. Our studies using a glutathione specific antibody revealed three myofilament proteins that run at the same molecular weights as cMyBP-C, titin, and actin are S-glutathionylated. We know that the regulation of these proteins is integral in mediating the acto-myosin interaction and all of the molecular events associated with cardiomyocyte shortening (Alegre-Cebollada, Kosuri et al. 2014). A short-term future goal (Chapter III) would be to identify the sites of MyBP-C that are glutathionylated and determine the effect on function. We suspect that this modification will have an effect on the  $\text{Ca}^{2+}$  responsiveness of the myofilaments due to its regulatory role in preventing acto-myosin interaction.

The DMTG myofilaments display a decreased  $\text{Ca}^{2+}$  sensitivity that is close to that of NTG littermates. The reduction in sensitivity is likely to be a result of the removal of S-glutathionylation and carbonylation of cMyBP-C, because we did not detect any changes in cTnI phosphorylation. Phosphorylated cTnI decreases  $\text{Ca}^{2+}$  sensitivity (Zhang, Zhao et al. 1995, Solaro, Rosevear et al. 2008). We did not assess any other proteins that regulate the sensitivity in these studies. Previous studies show that the C-terminus of  $\alpha$ -Tm plays a role in regulating the  $\text{Ca}^{2+}$  sensitivity (Jagatheesan, Rajan et al. 2003). It has been reported that desensitizing the myofilaments of cMyBP-C rescues HCM (Alves, Gaffin et al. 2010, Alves, Dias et al. 2014). Another way our labs have reversed the disease state is through alterations in  $\text{Ca}^{2+}$  handling proteins. We have reported that overexpressing SERCA2a in neonates as well as deleting PLN in the  $\alpha$ -TmE180G heart, prevents the progression of HCM (Peña, Szkudlarek et al. 2010, Gaffin, Peña et al. 2011). The inclusion of the S283A construct in  $\alpha$ -TmE180G is now a new strategy that recovers the SERCA2 and PLN protein expression and

increases the regulation by PLN phosphorylation. This implies that dephosphorylation relieves strain that alters the transcriptional and translational expression of proteins controlling  $\text{Ca}^{2+}$  fluxes required to facilitate relaxation.

We report the first evidence that in hearts controlled by constitutively low relative levels of  $\alpha$ -Tm phosphorylation there is an increase in glutathione, the major intracellular antioxidant. The relatively low phosphorylation of  $\alpha$ -Tm may normalize the flexibility of the strand and prevents mechanical strain that contributes to altering the redox potential within a cell. Although, the cooperativity of DMTG myofilaments were not significantly different from  $\alpha$ -TmE180G (Table 2), there was no difference in the average Hill slope compared to NTG control animals. The C-terminal end of Tm may be responsible for stabilizing cTnT, actin, and other Tm cooperative interactions (Jagatheesan, Rajan et al. 2003, Wieczorek, Jagatheesan et al. 2008). Furthermore, the lack of strain possibly translates to normalized force development that does not stimulate an altered redox signaling cascade of events. Excess strain causes titin to abnormally unfold and expose cryptic cysteines to S-glutathionylation (Alegre-Cebollada, Kosuri et al. 2014). These data support the hypothesis that these modifications as well as others elicit the Z-disc to alter the activation or deactivation of kinases and phosphatases that feedback onto the myofilaments in the form of post-translational modifications or regulators of transcription. Future studies should be carried out to assess the upregulation of Z-disc associated proteins in HCM.

In conclusion, in the setting of the  $\alpha$ -TmE180G mutation, we have shown that decreasing  $\alpha$ -Tm phosphorylation by 65% appears to block the primary insult of mechanical strain induced by the mutation (see Fig. 14 for schematic). This dephosphorylated blocking effect prevents the  $\alpha$ -Tm C-terminus from destabilization. In effect, the altered redox state is not elicited; kinases function and target the myofilaments and  $\text{Ca}^{2+}$  handling proteins in a manner that resembles wild-type hearts;

and oxidation of intracellular proteins is prevented. The Tm interactions with the other sarcomeric regulatory proteins are thus positioned such that they function properly and cooperative activation of the myofilaments occurs in a manner much like that of healthy cells. Whether we are preventing the alterations in the flexibility of cMyBP-C mutation is unknown and further investigation must be carried out to determine if the strain is relieved or if dephosphorylation of Tm causes an allosteric change that facilitates inhibition of the acto-myosin interaction during relaxation. (see Fig. 14 for schematic of findings).

Figure 14

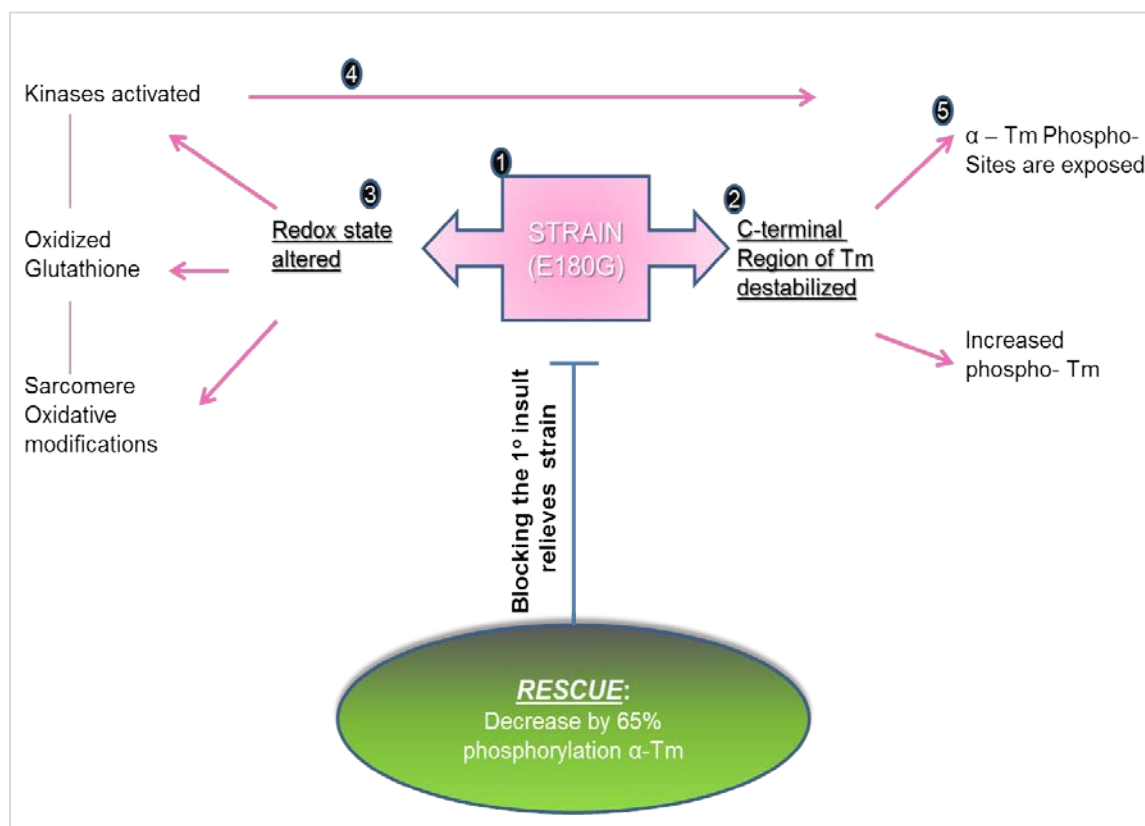


**Fig. 14 Schematic of dephosphorylation findings.**

We demonstrate a rescue of  $\alpha$ -TmE180G HCM mice by dephosphorylating the C-terminus of  $\alpha$ -Tm by 65%.



## Chapter III

### III. Novel control of cardiac myofilament response

#### A. Introduction

In previous studies, we reported data indicating a new role for cMyBP-C in the response of the myocardium to hypertensive stress in a mouse DOCA-salt model stressed by administration of salt, deoxycorticosterone acetate and unilateral nephrectomy (Lovelock, Monasky et al. 2012, Jeong, Monasky et al. 2013). These mice demonstrated oxidative stress and a diastolic abnormality in hearts and isolated myocytes, which occurred with no apparent change in cellular  $\text{Ca}^{2+}$ -fluxes (Lovelock, Monasky et al. 2012). These findings indicate that altered  $\text{Ca}^{2+}$ -responsiveness of the myofilaments might be involved, and indeed our experiments demonstrated enhanced myofilament response to  $\text{Ca}^{2+}$  with slowing of cross-bridge kinetics (Lovelock, Monasky et al. 2012). We also reported a correlation of levels of MyBP-C S-glutathionylation with diastolic dysfunction with reversal of the oxidative stress by treating the DOCA-salt mice with tetrahydro-biopterin (Jeong, Monasky et al. 2013). We identified S-glutathionylation of cMyBP-C as a post-translational modification likely to induce the altered response to  $\text{Ca}^{2+}$  (Lovelock, Monasky et al. 2012, Jeong, Monasky et al. 2013). Yet, we also found that myofilaments from the DOCA-salt model had significantly depressed levels of MyBP-C phosphorylation at Ser 282, which correlated with a depression of cardiac TnI (cTnI) phosphorylation at Ser 23, Ser 24. Thus, questions remained regarding whether the functional effects of MyBP-C could be demonstrated by direct glutathionylation of cMyBP-C at the same levels of phosphorylation of cMyBP-C and cTnI. A question also remained regarding the sites of the glutathionylation on cMyBP-C.

In experiments reported here, we tested the hypothesis that oxidative modification of cardiac myosin binding protein C (cMyBP-C) at specific sites modifies myofilament response to  $\text{Ca}^{2+}$ . We pursued an approach to these questions by developing *in vitro* conditions for direct S-glutathionylation of sarcomeric proteins. This approach provided a direct test of the hypothesis that this post-translational modification is the major mechanism of the altered sarcomeric response to  $\text{Ca}^{2+}$ . Our findings support this hypothesis and show for the first time that S-glutathionylation occurs on Cys residues in domains of cMyBP-C not generally expected to be major players in controlling myofilament function

Figure 15

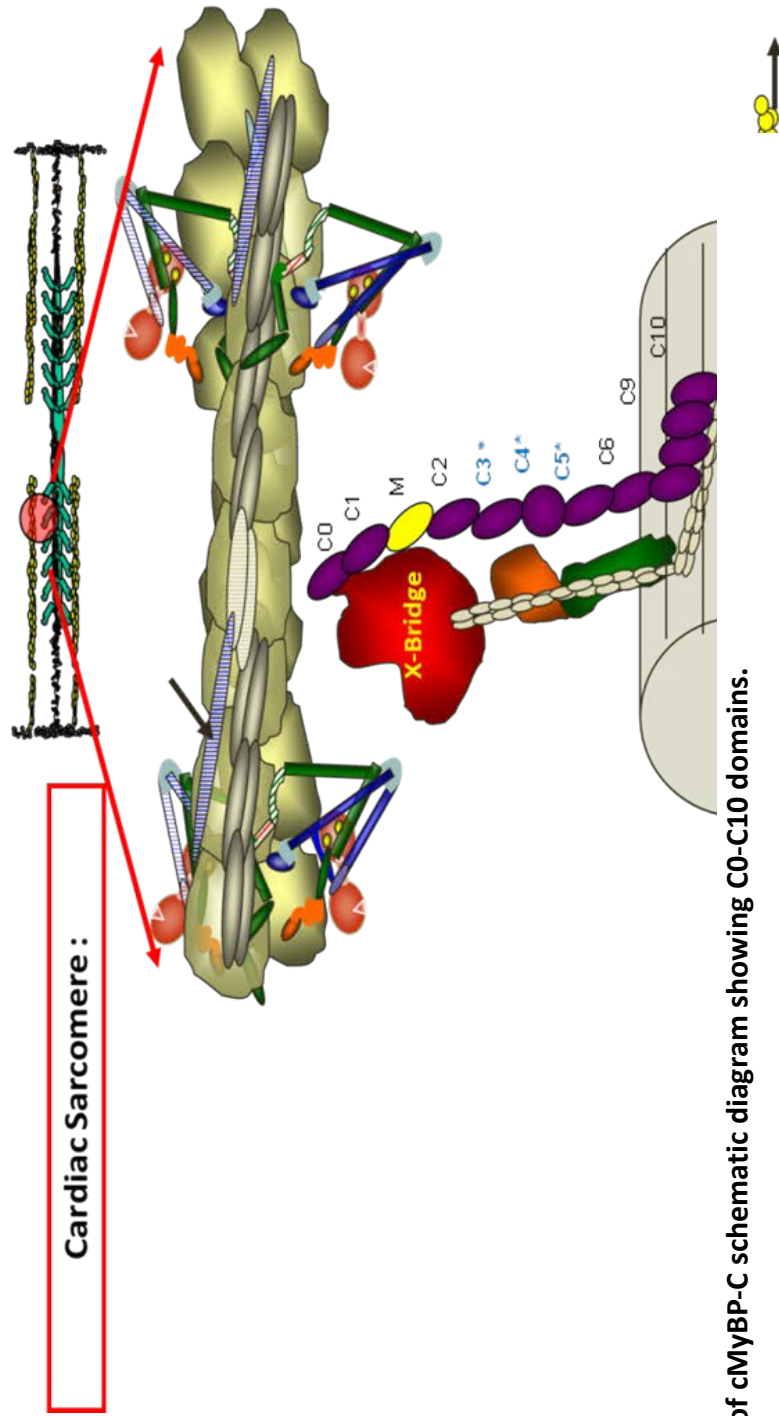


**Fig. 15 Structure of cMyBP-C schematic diagram showing C0-C10 domains.**

Myosin binding protein C (MyBP-C) interactions in the overlap region of the sarcomere. The illustration depicts a relaxed state with troponins (TnC, TnT, TnI) and tropomyosin (TM) blocking the actin-cross-bridge reaction. Myosin light chain 2 (MLC2) and cMyBP-C contribute to radial movements of the myosin heads relative to the thick filament backbone (as indicated by the double headed arrow). cMyBP-C has interaction sites via the M domain with the neck region of myosin (S2) and with titin via C-terminal domains C8, C9 and C10. cMyBP-C may also interact directly with the thin filament. See text and results for details. (Patel, Wilder et al. 2013) Figure courtesy of Dr. R. John Solaro, Department of Physiology and Biophysics, University of Illinois at Chicago

## B. Methods

### 1. Isolation of Cardiac Myofibrils and Measurements of ATPase Activity

Four month old female FVBN mice were deeply anesthetized with 60 mg/kg pentobarbital. The heart was quickly excised and rinsed in cold 0.9% sodium chloride. We isolated myofibrillar fractions from ~50 mg wet weight of left ventricular tissue using a modification of procedures described by Solaro et al (Solaro, Pang et al. 1971) and Layland et al (Layland, Cave et al. 2005). Membranes in the tissue were extracted by two homogenizations in 1 ml of a standard buffer with Triton X-100 (75 mM KCl, 10 mM imidazole, pH 7.2, 2 mM  $\text{MgCl}_2$ , 2 mM EGTA, 1 mM  $\text{NaN}_3$ , and 1% v/v Triton X-100) using a 2 ml Dounce homogenizer. Following centrifugation, pellets were washed twice with 1 ml standard buffer without Triton X-100 and resuspended in the assay buffer (A-70 containing 70 mM NaCl, 10 mM  $\text{MgCl}_2$ , and 40 mM MOPS, pH 7.0) (Kobayashi and Solaro 2006). A DC assay (Bio-Rad) was performed to determine protein concentration of the sample. Modifications of assays of myofibrillar activity were carried out on fresh isolated preparations. For in vitro glutathionylation (Chen, Zhang et al. 2007), myofibrillar protein suspensions (0.2 mg/ml) were incubated for 1 h at room temperature in either A-70 buffer or A-70 containing various concentrations of oxidized glutathione (GSSG). Following the glutathionylation reaction, the myofibrils were suspended in an assay buffer containing 0.1 mg/ml protein, 35 mM NaCl, 5 mM  $\text{MgCl}_2$ , 1 mM EGTA, 20 mM MOPS, pH 7.0 with  $\text{CaCl}_2$  to achieve a range of pCa ( $-\log [\text{Ca}^{2+}]$ ) values from pCa 7.8 to pCa. 4.6. Free  $\text{Ca}^{2+}$  concentration was calculated using WEBMAXC STANDARD. We determined myofibrillar ATPase activity at 30°C by starting the reaction with 1 mM ATP and stopping the progress by addition of trichloroacetic every 3 min for 15 min, during which Pi generation, as determined with a malachite green based assay, was linear (Kodama, Fukui et al. 1986). Data were normalized to maximum activity. Graph Pad Prism 5.00 was used to

analyze ATPase rates and to fit the data to the Hill equation to generate half maximally activating pCa values (pCa<sub>50</sub>) and Hill n values.

## **2. Force Measurement of Skinned Fiber Bundles**

Measurements of the force-  $\text{Ca}^{2+}$  relationship were carried out on fiber bundles from left ventricular papillary muscle of adult mice essentially as previously described (Evans, Pena et al. 2000). Female mice 4 months old were anesthetized as above and hearts were quickly excised and placed in ice cold high relaxing (HR) solution pCa 10.0 of the following composition in mM: K-propionic acid 41.89,  $\text{MgCl}_2$  6.57, BES 100, EGTA 10, ATP 6.25, phosphocreatine 10, Na-azide 5, pH adjusted to 7.0 using KOH. The ionic strength of all solutions was 150 mM. All solutions contained protease inhibitors pepstatin (2.5  $\mu\text{g/ml}$ ), leupeptin (1  $\mu\text{g/ml}$ ) and phenylmethylsulphonyl fluoride (PMSF, 50  $\mu\text{M}$ ). Fiber bundles (150-200  $\mu\text{m}$  in width and approximately 4-5 mm long) were dissected from papillary muscles. Membranes were extracted from the fiber bundles by immersing them for 30 min in HR buffer containing 1% Triton X-100. We mounted the fiber bundles between a force transducer and micromanipulator and set the sarcomere length at 2.2  $\mu\text{m}$  using laser diffraction patterns. The fibers were then exposed to solutions of incrementally increasing  $\text{Ca}^{2+}$  concentrations ranging from  $10^{-7}\text{M}$  to  $10^{-4.5}\text{M}$  and force was recorded to determine the force-pCa relations. Fibers were then incubated in 5 mM GSSG in A-70 as prepared above for 10 min, and then subjected to the varying  $\text{Ca}^{2+}$  concentrations. This process was repeated using 10 mM dithiothreitol (DTT) solubilized in A-70 for 10 min. Tension was calculated by dividing the force by the cross-sectional area, as described previously (Evans, Pena et al. 2000). Assuming a cylindrical shape, we determined radius from measurements of two perpendicular planes at three points on the fiber. The mean radius was used to calculate the cross-sectional area. Data were fit to the Hill equation for non-linear regression using Graphpad Prism 5 software.

### 3. Immunoblotting

Control and GSSG treated myofibrils in A-70 assay buffer were solubilized in a non-reducing 2X Laemmli buffer (Laemmli 1970) (4% SDS, 20% glycerol, 0.004% bromophenol blue, and 0.125 M Tris HCl pH 6.8) with 25 mM N-ethylmaleimide (NEM) in a 1:1 ratio. A negative control was prepared by adding 10 mM DTT to myofibril proteins. 20 µg of total protein was applied to 1D 12% non-reducing resolving SDS-PAGE gel (Fritz, Swartz et al. 1989) and transferred onto a 0.2 µM PVDF membrane (Matsudaira 1987). The blot was blocked in 5% nonfat dry milk with 2.5 mM NEM for 1 hour. Anti-glutathione mouse monoclonal primary antibody (Virogen) was used at 1:1000 dilution along with anti-mouse HRP-conjugated secondary antibody (Sigma) at 1:40,000 dilution to detect for S-glutathionylation (Hill, Ramana et al. 2010). Skinned fibers (4 to 6 fiber bundles) from force measurement studies were solubilized in 30 µl of the 2X Laemmli buffer with 25 mM NEM. Proteins in the samples (4 to 10 µl) were separated on 1D 12% non-reducing resolving SDS-PAGE gel. Transfer and western blot procedure was same as above. Optical density of the bands was measured with ImageQuant TL (GE Healthcare) and exported to Excel for statistical analysis.

### 4. Mass Spectrometry

An 8% non-reducing 1D SDS-PAGE gel was stained with Imperial Protein Stain (Thermo) according to manufacturer's protocol. The band around 140 kDa (MyBP-C) was cut from the gel and subjected to in-gel digest with Trypsin Gold (Promega). Reduction and alkylation steps were omitted to preserve the S-glutathionylation of the proteins. Pooled digestion extracts were concentrated via Speed Vac to less than 20 µl and brought up to 40 µl with mobile phase solution (5% ACN and 0.1% formic acid). Peptides were filtered with 0.22 µm PVDF Millipore Ultrafree-MC spin filter and 35 µl of sample was analyzed with Thermo Finnigan LTQ hybrid linear ion trap – Fourier Transform ICR mass spectrometer coupled to Dionex U3000 nano LC. Dionex acclaim PepMap100 C18 trapping column

(500  $\mu\text{m}$   $\times$  5 mm column packed with 5  $\mu\text{m}$ , 100 Å Symmetry C18 material) was used to concentrate the samples at flow rate of 50  $\mu\text{l}/\text{min}$  and Agilent Zorbax 300SB-C18 Nanoflow column (75  $\mu\text{m}$   $\times$  150 mm column packed with 3.5  $\mu\text{m}$ , C18 material) was used for separation at flow rate of 0.250  $\mu\text{l}/\text{min}$ . Peptides were eluted with a linear gradient of 5-45% solution B (95% ACN, 0.1% formic acid) through New Objective uncoated SilicaTips™ (5 cm long, tubing OD 360/75  $\mu\text{m}$ , tip ID 8  $\mu\text{m}$ ). Peptides were ionized via electrospray ionization with LTQ source voltage set to 1.0 kV and capillary temperature set to 200°C. Mass spectra were obtained in positive ion mode over  $m/z$  range of 400 to 1800 at a resolution of 50,000 and top ten most intense ions were selected for tandem MS. MS/MS were obtained in collision induced dissociation mode with minimum signal required 5000, isolation width 3, and normalized collision energy 35.

Mass spectrometry data were collected with Xcalibur 2.0.7 software as .Raw file, which were converted to mzXML and MGF files using MassMatrix MS Data File Conversion tool (Xu and Freitas 2009). Mascot search engine was used to analyze the MS/MS data (Perkins, Pappin et al. 1999). Searches were performed using NCBI nr Mus musculus and a decoy (automatically generated reversed protein sequences) database with peptide tolerance of  $\pm 15$  ppm. Variable modifications were set to glutathione (C). The results are representative of three similar and separate mass spectrometry runs.

## **5. Statistical Analysis**

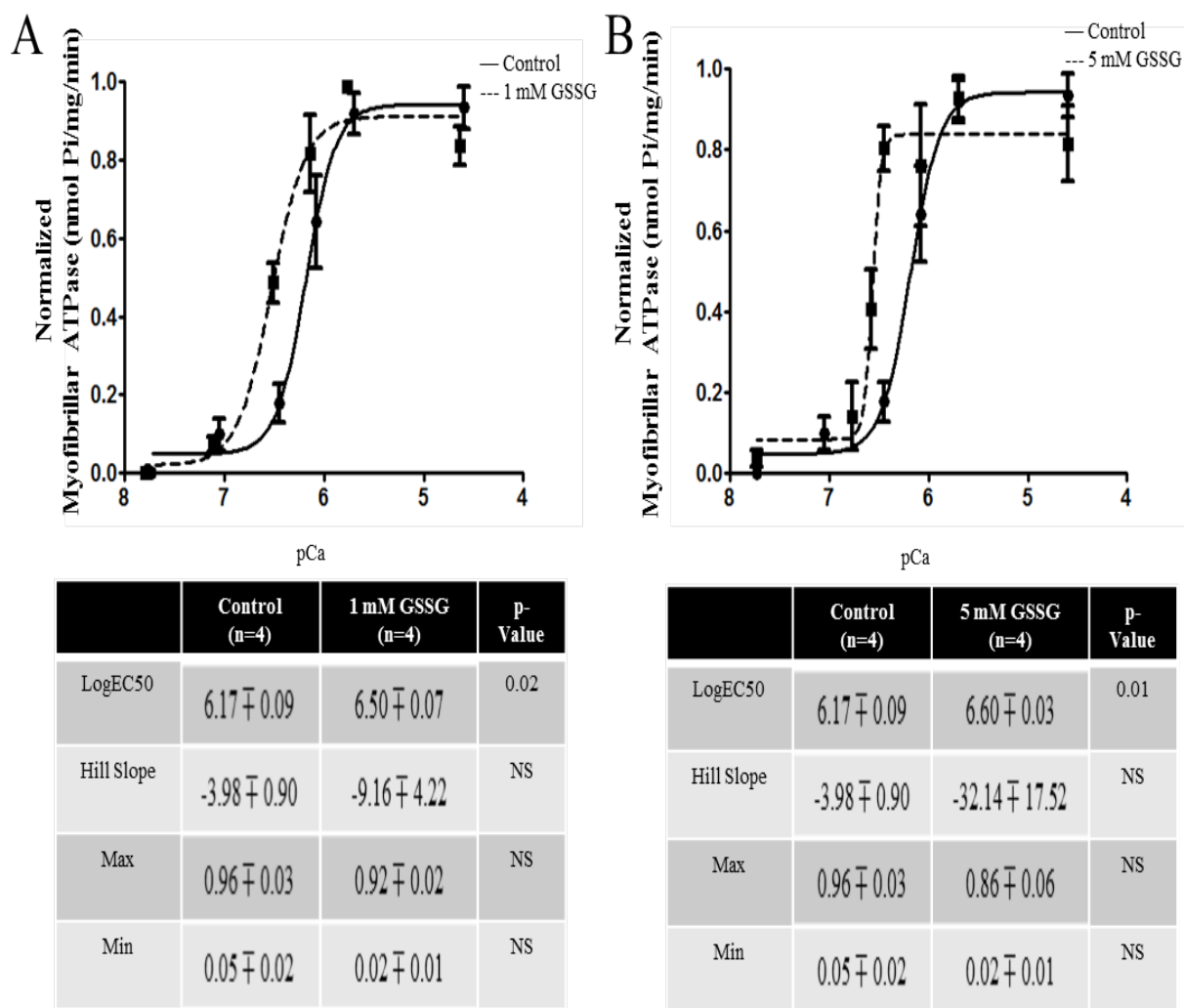
We determined pCa values at half-maximum ATPase activity and force generation from data normalized to maximum activity. The data were fit to a modified Hill equation (Takeda, Kobayashi et al. 1997, Kobayashi and Solaro 2006). Statistical significance was determined using paired Student t-test or one way ANOVA followed by Newman-Keuls test where appropriate. Data are presented as means  $\pm$  SEM with significance set at  $p < 0.05$ .

## c. Results

### 1. Myofibrillar ATPase Activity

In order to determine direct effects of glutathionylation on myofilament response to calcium, we compared ATPase activities of isolated myofibrillar preparations before and after treatment with 1 and 5 mM GSSG (Fig. 16). Compared to controls, myofibrils treated with either 1 mM (Fig. 16A) or 5 mM GSSG (Fig. 16B) demonstrated a significant leftward shift in the relation between pCa and myofibrillar ATPase activity. In the case of modification by 1 mM GSSG, the half-maximally activating pCa value ( $pCa_{50}$ ) was  $6.50 \pm 0.07$  (n=4) compared to a  $pCa_{50}$  of  $6.17 \pm 0.09$  (n=4) for controls. With 5 mM GSSG the  $pCa_{50}$  was  $6.60 \pm 0.03$  (n=4) compared to controls with  $pCa_{50}$  of  $6.02 \pm 0.07$  (n=4). The Hill coefficients, minimum, and maximum ATPase rates did not change significantly between the control myofibrils and myofibrils treated with either 1 or 5 mM GSSG.

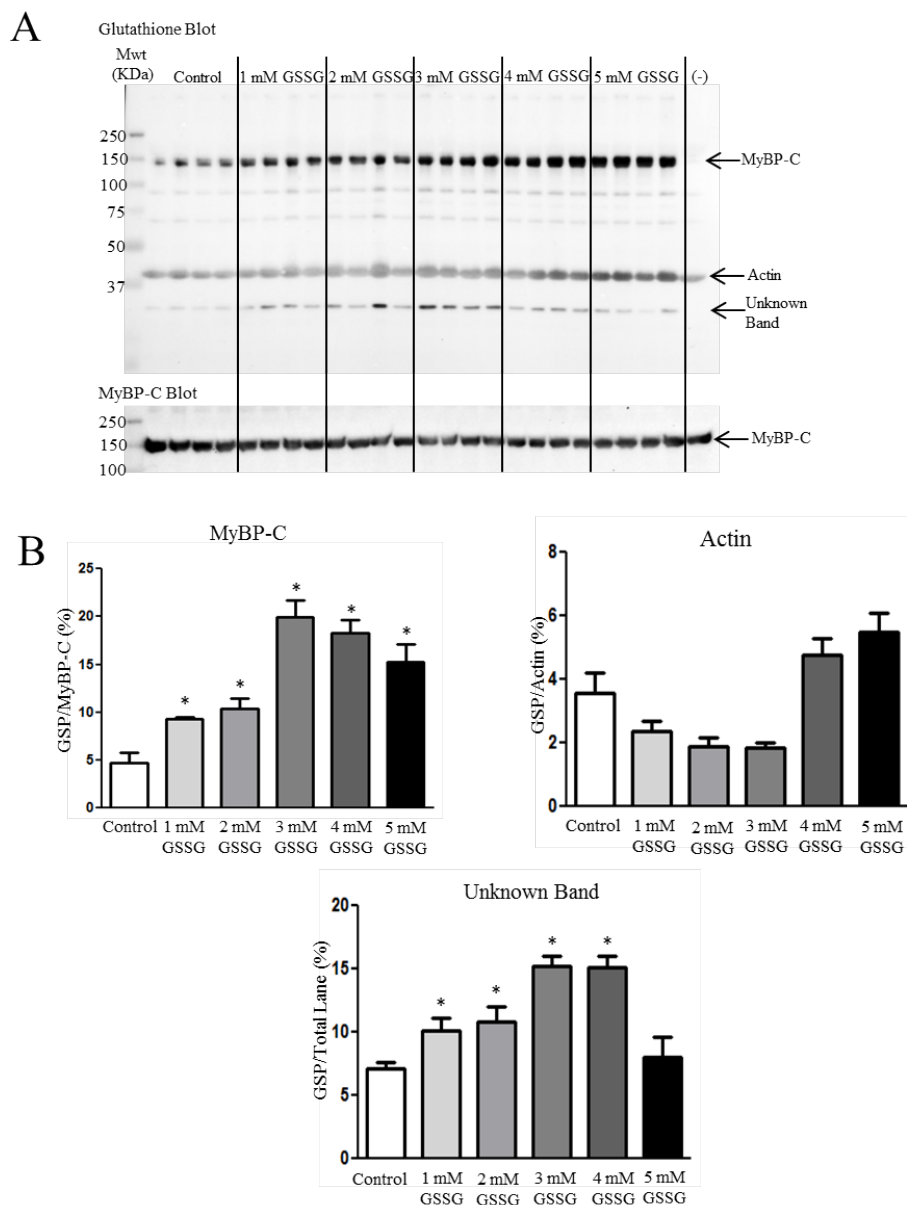


**Figure 16****Figure 16 Myofibril pCa\_ATPase activity of control and GSSG treated samples.**

(A) In vitro ATPase activity of myofibrils prepared from wild type FVBN mouse heart treated with 1 mM GSSG for 1 hour. pCa<sub>50</sub> for control samples is  $6.17 \pm 0.09$  and for 1 mM GSSG treated samples is  $6.50 \pm 0.07$  (B) In vitro ATPase activity of myofibrils prepared from wild type FVBN mouse heart treated with 5 mM GSSG for 1 hour. pCa<sub>50</sub> for control samples is  $6.17 \pm 0.09$  and for 5 mM GSSG treated samples is  $6.60 \pm 0.03$ . Data are expressed as mean  $\pm$  standard error of mean, n=4 from 1 preparation (\*P<0.05). nH, minimum pCa, and maximum pCa values were not significantly different (Patel, Wilder et al. 2013).

## 2. Glutathionylation of Myofibrillar Preparations

To determine the mechanism for the higher  $\text{Ca}^{2+}$  sensitivity of ATPase rate for the GSSG treated myofilaments, we analyzed the samples by Western blot analysis. Fig. 17B shows blots for control samples and samples treated with increasing concentrations of GSSG. The Western blots revealed increased glutathionylation of a band identified as MyBP-C by probing with a specific antibody. As summarized in Fig. 17B, all samples treated with GSSG demonstrated significant increases in glutathionylation compared to controls. Samples treated with 3, 4, and 5 mM GSSG had significantly increased levels of MyBP-C glutathionylation compared with the 1 mM GSSG treated samples, and the samples treated with 3 and 4 mM GSSG had significantly higher levels of glutathionylation than samples treated with 2 mM GSSG. Levels of glutathionylation were not significantly different among the 3, 4, and 5 mM GSSG treated groups. Western blots also detected glutathionylation of actin, but there were no significant differences between the GSSG treated groups and the control although the levels at 4 and 5 mM GSSG treatment were higher than those at 1, 2, and 3 mM GSSG treatment. Another band with mobility faster than that of actin and likely to be tropomyosin showed glutathionylation. However, the glutathionylation detected in this band did not show a dependence on dose of GSSG, and was the same as the control at 5 mM GSSG treatment.

**Figure 17****Figure 17. Western blot analysis of proteins subject to glutathionylation during ATPase assay.**

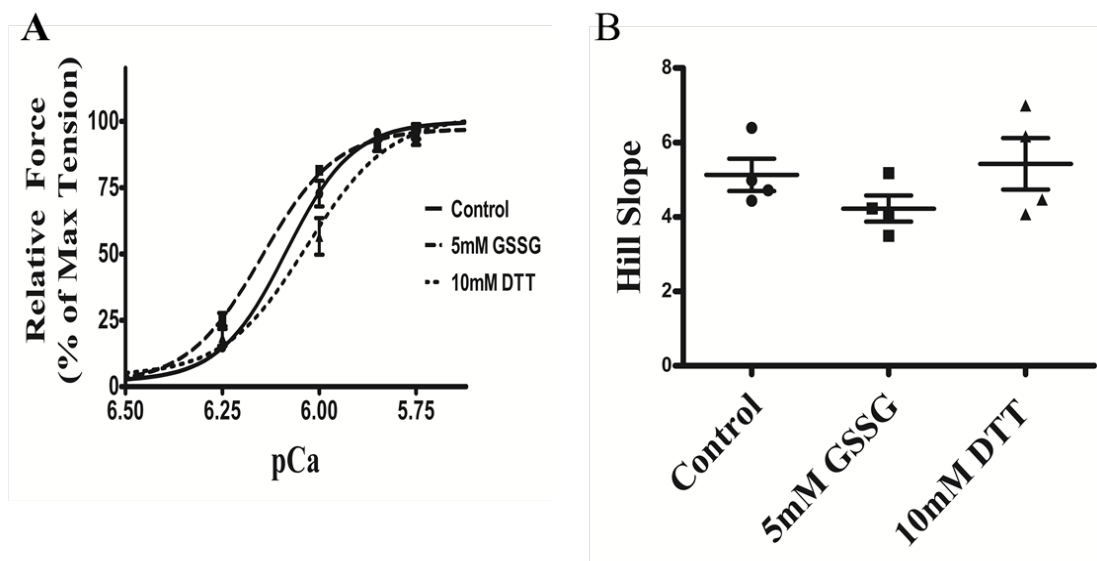
**(A)** Control myofibrils and myofibrils treated with increasing concentrations of GSSG (20  $\mu$ g) were probed with anti-GSH (Virogen) antibody to detect glutathionylated proteins. (-) lane contains myofibrils treated with 10 mM DTT after 5 mM GSSG treatment to serve as a negative control. The blot was also probed with myosin binding protein C antibody for identification of glutathione band. **(B)** Load normalized quantitative results in arbitrary units showing significant difference in glutathionylation (GSP) of cMyBP-C between non-treated and GSSG treated samples. Data are also shown for actin and tropomyosin bands. Data are expressed as mean  $\pm$  standard error of mean,  $n=4$  (\* $P \leq 0.05$ ). (Patel, Wilder et al. 2013)

### 3. The effect of GSSG and DTT on skinned fiber force generation

We also determined the effect of glutathionylation on the force-pCa relation of skinned fiber bundles. The fiber bundles were first incubated for 10 min with A-70 buffer alone or 5 mM GSSG in A-70 buffer and then switched to HR for determination of force at various pCa values. As illustrated in Fig. 18, skinned fiber  $\text{Ca}^{2+}$  sensitivity was significantly higher after GSSG incubation as indicated by  $\text{pCa}_{50}$  of  $6.15 \pm 0.01$  ( $n=4$ ) compared to controls with  $\text{pCa}_{50}$  of  $6.09 \pm 0.01$  ( $n=4$ ). This increase in  $\text{pCa}_{50}$  with direct glutathionylation is similar to the increase in  $\text{pCa}_{50}$  we reported when comparing myofilaments sham mice and DOCA/salt mice (Fig. 4A in Jeong et al. (Jeong, Monasky et al. 2013)). To determine the reversibility of the effect of GSSG, we measured the force-pCa relation in a protocol in which we incubated the fiber bundles in 5 mM GSSG for 10 min followed by 10 mM treatment with dithiothreitol (DTT). As shown in Fig. 18A the increased  $\text{Ca}^{2+}$  sensitivity associated with GSSG treatment was reversed after incubation in DTT as indicated by  $\text{pCa}_{50}$  of  $6.03 \pm 0.02$  ( $n=4$ ). Cooperativity of activation, as measured by the Hill slope tended to decrease after GSSG incubation and return to control levels after DTT incubation, but none of the changes were statistically significant. As with the myofibrillar preparations, Western blots of the skinned fiber preparations revealed glutathionylation of MyBP-C (Fig. 19B). The 5 mM GSSG treated fibers showed higher glutathionylation levels than control fibers, and the level of glutathionylation returned to control levels following 10 mM DTT treatment. Although we detected glutathionylation of myosin heavy chain and actin in the skinned fibers treated with GSSG (data not shown), there were no statistically significant changes in glutathionylation level between the three groups for both proteins.

Figure 18

Figure 17.



	Control (n=4)	5mM GSSG (n=4)	10mM DTT (n=4)	p-Value
LogEC50	6.09 ± 0.011	6.15 ± 0.011*	6.03 ± 0.019	p<0.05 C vs. NTG p<0.002 GSSG vs DTT
Hill Slope	4.98 ± 0.42	4.22 ± 0.35	5.43 ± 0.59	NS

**Fig. 18 The effects of GSSG and DTT on force generation of skinned fibers.**

(A) Data represent the force-pCa relationship in skinned cardiac muscle fibers recorded primarily using only the varying increasing  $\text{Ca}^{2+}$  solutions, then followed by treatment with 5 mM GSSG in A-70 for 10 mins and subsequently bathed in the  $\text{Ca}^{2+}$  solutions. The fibers were then incubated in 10mM DTT in A-70 for 10 mins and were then bathed in increasing  $\text{Ca}^{2+}$  solutions again. The pCa50 values were all statistically significant between treatments. pCa50 values for control fibers, 5 mM GSSG treatment, and 10 mM DTT treatment were  $6.09 \pm 0.01$ ,  $6.15 \pm 0.01$ , and  $6.03 \pm 0.02$ , respectively. Data represented as mean  $\pm$  SEM, n=4 for all groups, significance was set at  $p < 0.05$ . [ $n_H$ , minimum pCa, and maximum pCa values were not significant]. (B) Western blot analysis of skinned fiber showing significant difference in glutathionylation levels between control and GSSG treated fibers ( $p = 0.05$ ). Glutathionylation levels are also significantly decreased when fibers were treated with DTT compared to the GSSG treated fibers ( $p = 0.03$ ). There is no significant difference between control and DTT treatment. Data are expressed as mean  $\pm$  standard error of mean, n=6-7 (\* $P \leq 0.05$ ). (Patel, Wilder et al. 2013)

#### 4. Mass Spectrometry

We employed tandem mass spectrometry to identify glutathionylated proteins and determine the sites of cMyBP-C glutathionylation. Mass spectra resulting from the LC/MS/MS of the ~140 kDa band identified myosin-binding protein C, cardiac-type (gi|134031947), with 43-50% sequence coverage as the number one hit. Tryptic peptides of cMyBP-C were analyzed for a mass shift of 305 Da, indicating covalent attachment of GSH to one of the peptide residues. Three separate peptides,  $^{651}\text{IHLDCPGSTPDTIVVAGN}^{670}$ ,  $^{475}\text{VEFECEVSEEGAQVK}^{489}$ , and  $^{605}\text{LTIDDVTPADEADYSFVPEGFA\text{C}NLSAK}^{632}$ , were found to be glutathionylated (Table 2). When the myofibrils were treated with 1 mM GSSG, only peptide  $^{651}\text{IHLDCPGSTPDTIVVAGN}^{670}$  was found to be glutathionylated at cys655. The precursor ion for the triply charged glutathionylated peptide was observed at  $m/z$  781.04<sup>3+</sup> compared to the unmodified precursor peptide observed at  $m/z$  679.35<sup>3+</sup>. Comparison between select b and y product ions of the glutathionylated and unmodified peptide (Table 2) show mass shift of 305 Da (singly charged ions) or 152.5 Da (doubly charged ions). With treatment of 5 mM GSSG, we identified all three of the above peptides to be glutathionylated at cys655, cys479, and cys627. The triply charged glutathionylated peptide  $^{475}\text{VEFECEVSEEGAQVK}^{489}$  was observed at  $m/z$  663.28<sup>3+</sup> and  $^{605}\text{LTIDDVTPADEADYSFVPEGFA\text{C}NLSAK}^{632}$  glutathionylated precursor peptide was observed at  $m/z$  1098.49<sup>3+</sup>. Expect value of less than 0.1 was considered significant identification of each individual peptide. Significant identification of glutathionylated cMyBP-C peptides was not made in the control non-treated myofibril samples.

Figure 19

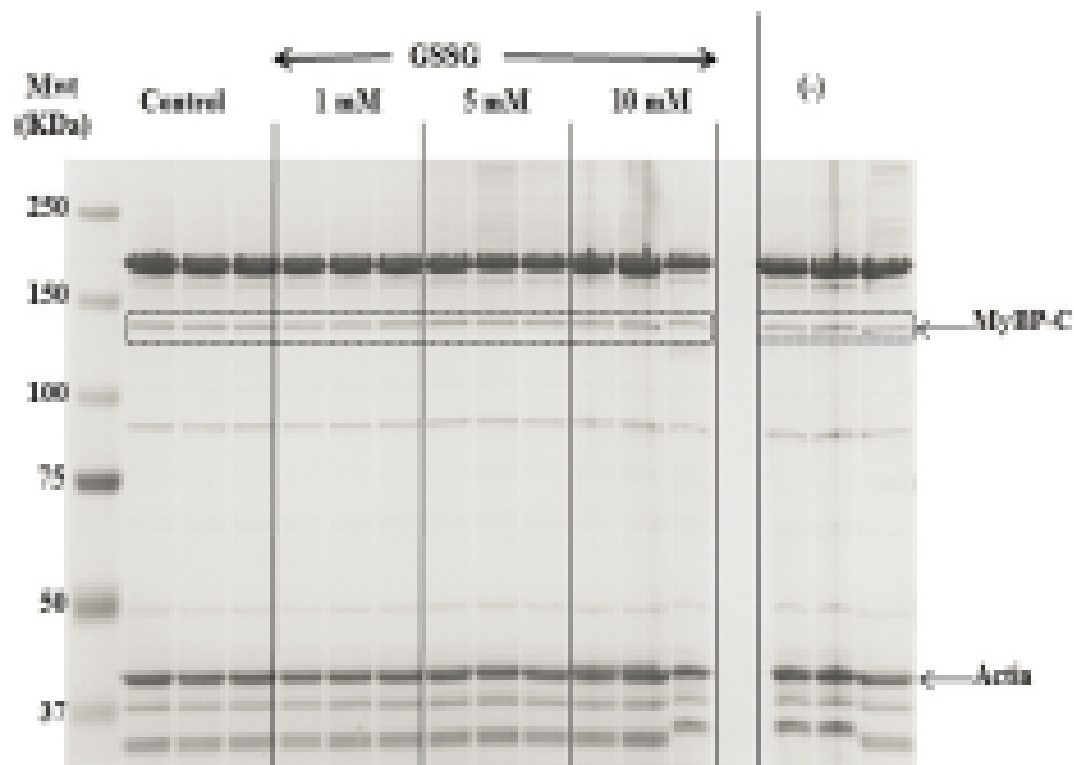


**Fig. 19 SDS-PAGE gel for in gel digestion.**

8% SDS-PAGE gel stained with mass spectrometry compatible Imperial Protein Stain (Thermo): bands at ~140 kDa (dotted boxes) were cut for mass spec analysis. (Patel, Wilder et al. 2013)

Table 2 Glutathionylated peptides discovered by mass spectrometry.

GSSG (mM)	Accession number	Description	Score	Percent coverage	Glutathionylated peptide	Charge	Observed mass	Peptide mass tolerance (ppm)	Miss cleavages	Ions score	Expect
1	gi134031947	myosin-binding protein C, cardiac-type [Mus musculus]	7820	42.9	K.IHLDC*PGST PDTIVWAGNK.L	3+	781.04	-5	0	41	0.0033
5	gi134031947	myosin-binding protein C, cardiac-type [Mus musculus]	8033	49.7	K.IHLDC*PGST PDTIVWAGNK.L	3+	781.04	-5	0	51	0.00033
					K.IHLDC*PGST PDTIVWAGNK.L	3+	781.04	-5	0	48	0.00071
					K.IHLDC*PGST PDTIVWAGNK.L	3+	781.04	-2	0	51	0.00041
					K.IHLDC*PGST PDTIVWAGNK.L	3+	781.04	-2	0	50	0.00049
					R.VEFEC*EV SEEGAQVK.W	3+	663.28	0	0	45	0.00066
					R.VEFEC*EV SEEGAQVK.W	3+	663.28	0	0	36	0.0051
					R.VEFEC*EV SEEGAQVK.W	3+	663.28	1	0	30	0.018
					K.LTIDDVTPADE ADYSFVPEGFAC *NLSAK.L	3+	1098.49	5	0	40	0.0034
					K.LTIDDVTPADE ADYSFVPEGFAC *NLSAK.L	3+	1098.49	3	0	40	0.0031

Myofibrils treated with 1 mM and 5 mM GSSG. Mass spectrometry identified three separate sites as targets for S-glutathionylation. Note the increase in amount of peptides discovered to be glutathionylated and new sites for glutathionylation when myofibrils are treated with increased amount of GSSG.



## D. Discussion

Our data provide support for the hypothesis that S-glutathionylation of MyBP-C is functionally significant in controlling myofilament response to  $\text{Ca}^{2+}$ . Moreover, our data indicate that the sites modified by S-glutathionylation occur at Cys<sup>479</sup>, Cys<sup>627</sup>, and Cys<sup>655</sup>, and are in the poorly understood C3, C4, and C5 domains of MyBP-C. These domains, which are indicated in Fig. 15, have not been previously considered important in the structure and assembly of MyBP-C, but not with major importance in the mechanism of action of MyBP-C. Focus has been on the CO, L, C1, and especially the cardiac specific phosphorylation sites in the M domain. Thus, in addition to phosphorylation, which has well documented effects on cardiac MyBP-C function (Cazorla, Szilagyi et al. 2006, Tong, Stelzer et al. 2008, Sadayappan, Gulick et al. 2009, Hill, Ramana et al. 2010) redox related post translational modifications need to be considered.

With the discovery that many proteins are targets for glutathionylation, the search for functional implications of this post-translational modification has taken on new significance (Brennan, Miller et al. 2006, Pastore and Piemonte 2012). Brennan et al. (Brennan, Miller et al. 2006) reported the presences of S-gluthionylation of MyBP-C in rat hearts, but functional implications were not assessed. Glutathionylation is a form of oxidation involving formation of a mixed disulfide between the tri-peptide glutathione (GSH) and a protein cysteine residue. The tri-peptide glutathione is the most abundant non-protein thiol present in cells, with concentrations varying from 1-10 mM depending on the cell type. For example, the amount of glutathione that is present in the heart is 5 fold lower than that found in the liver (Ishikawa and Sies 1984). Glutathione has many functions including its role as an antioxidant, indicator of oxidative stress, and ROS scavenger (Pastore and Piemonte 2012). Under physiological conditions, much of the cell's GSH pool is present in the reduced form and less than 1% is present in oxidized GSSG. Under oxidative

stress, the ratio of GSH/GSSG decreases and promotes protein glutathionylation. GSSG reacts with protein thiols through a disulfide exchange mechanism to form a protein mixed disulfide. Cardiac myocytes provide an excellent cell type for investigating the potential effects of protein S-glutathionylation in both physiological and pathological redox signaling. Results presented here provide further support that specificity for a particular protein and regulatory process forms an important aspect of signaling via S-glutathionylation. In the case of the DOCA-salt mouse model of hypertension, we could find no change in the levels and dynamics of intracellular  $\text{Ca}^{2+}$  transients, even though it has been reported that glutathionylation of L-type  $\text{Ca}^{2+}$  channel results in an increase in  $\text{Ca}^{2+}$  influx and an increase in diastolic  $\text{Ca}^{2+}$  in cardiac myocytes (Tang, Viola et al. 2011). However, there is a reported glutathionylation of cardiac L-type  $\text{Ca}^{2+}$  channels associated with ischemic heart disease (Tang, Viola et al. 2011). Thus, it appears important to evaluate the role of post-translational modifications by glutathionylation in the context of the particular physiological or pathophysiological condition.

Although it is likely that other proteins in cardiac sarcomeres are S-glutathionylated, based on the present results and our previous data, the impact of S-glutathionylation of MyBP-C appears to be of relatively high significance in controlling cardiac relaxation and as an important mechanism for the diastolic dysfunction associated with hypertension induced oxidative stress. There have been reports that reversible glutathionylation of actin at Cys<sup>374</sup> has functional impact on actin polymerization (Wang, Boja et al. 2001, Dalle-Donne, Giustarini et al. 2003) and actomyosin-S1 ATPase activity (Pizarro and Ogut 2009). However, in the present study, we did not observe actin glutathionylation at Cys<sup>374</sup>. Moreover we could detect no actin glutathionylation in cardiac myofilaments from the DOCA-salt model, although there was an increase in  $\text{Ca}^{2+}$  sensitivity compared to controls (Lovelock, Monasky et al. 2012). Western blots (Fig. 17B ) showed a variable

level of glutathionylation of actin and a protein migrating with the mobility of tropomyosin. However, unlike the case with MyBP-C, the level of glutathionylation of actin and tropomyosin was not correlated with the effects of GSSG on myofibrillar ATPase activity. We also did not detect glutathionylation of the reactive Cys<sup>707</sup> of myosin sub-fragment 1 (S1) (Prochniewicz, Lowe et al. 2008). These data support our conclusion that in some conditions glutathionylation of cMyBP-C is a dominant oxidative stress related post-translational mechanism for control of myofilament Ca<sup>2+</sup> sensitivity.

Our data indicate high susceptibility of cMyBP-C for modification by glutathionylation at specific cysteine residues, which may be exposed in the three dimensional structure for ease of access by GSSG. Glutathionylation has also been correlated with relatively low pKa values for susceptible Cys residues (Pastore and Piemonte 2012). It would be interesting, therefore, to examine the position and comparative pKa values of the Cys<sup>479</sup>, Cys<sup>627</sup>, and Cys<sup>655</sup>. The modification in the C5 domain may be of particular interest inasmuch as this domain contains a cardiac specific region. Some evidence points to a functional significance of these C-terminal domains of cMyBP-C in the heart. Interactions of this region with titin and light meromyosin have been documented but not extensively analyzed in terms of functional significance (Yang, Sanbe et al. 1998, Sadayappan and de Tombe 2012). Surprisingly the C-terminal regions outside C0-C4 bind to actin equally as well as the full length MyBP-C, and the speculation was made by Rybakova et al. (Rybakova, Greaser et al. 2011) that this actin-MyBP-C interaction may be relatively more specific than the relatively non-specific electrostatic interactions of the N-terminal regions. Missense mutations inducing hypertrophic cardiomyopathy occur in all of the MyBP-C domains (Flashman, Redwood et al. 2004, Harris, Lyons et al. 2011) indicating that each domain has a special significance in cardiac homeostasis or that effects of modifications are transmitted to others in the domain

network. Studies by Palmer et al. (Palmer, Sadayappan et al. 2011) have provided some indirect insights into a potential functional role of MyBP-C outside the N-terminal domains and phosphorylation sites. Their studies indicated that phosphorylation and the presence of the N-terminal domains of MyBP-C provide structural support and radial rigidity to the myofilament lattice. However, the presence of cMyBP-C also provided a longitudinal rigidity in the myofilament lattice that did not rely on phosphorylation of the N-terminus. We hypothesize regions of glutathionylation of those regions may be significantly involved in maintenance of longitudinal rigidity as well as potential interactions with as well as dwell time of cross-bridges in their reaction with thin filaments.

In conclusion, our data emphasize and support our earlier data indicating the potential for redox related post-translational modification of MyBP-C as a significant factor controlling cardiac function. Our results also emphasize the need for better understanding of the role of the C-terminal regions of MyBP-C that contain thiols highly reactive with GSSG. The specificity of the correlation of S-glutathionylation with myofilament function also indicates that effects of oxidative stress need to be considered in the context of the particular circumstances generating ROS. It will be important in further studies to determine interactions among these redox related post-translational modifications and phosphorylation. Whether the existence of a S-glutathionylated form has any relevance in a variety of cardiac disorders needs to be further explored.

## Chapter IV

### IV. Treatment with N-Acetylcysteine (NAC) improves cardiac function and myofilament disorders in Hypertrophic Cardiomyopathy

#### A. Introduction

In experiments reported here, we have tested whether anti-oxidant therapy in the form of N-acetylcysteine (NAC) treatment is able to improve the disorders associated with familial hypertrophic cardiomyopathy (HCM). We employed a murine model of HCM expressing cardiac restricted  $\alpha$ -tropomyosin ( $\alpha$ -Tm) with an E to G mutation at position 180 (TG- $\alpha$ Tm-E180G). Our previous studies reported that, compared to controls, this model demonstrates a significant increase in myofilament response to  $\text{Ca}^{2+}$ , and a diastolic abnormality, likely to trigger maladaptive remodeling (Prabhakar, Boivin et al. 2001, Sheehan, Arteaga et al. 2011). Recent studies show that the HCM phenotype can be prevented from developing by genetic induction of constitutive increases in  $\text{Ca}^{2+}$ -fluxes into the sarcoplasmic reticulum (SR) (Alves, Gaffin et al. 2010, Peña, Szkudlarek et al. 2010, Gaffin, Peña et al. 2011), or decreases in myofilament response to  $\text{Ca}^{2+}$  (Alves, Dias et al. 2014). These findings led us to explore translatable therapeutic approaches toward modifying  $\text{Ca}^{2+}$ -fluxes or myofilament response to  $\text{Ca}^{2+}$  in HCM.

Several lines of evidence indicate that anti-oxidant therapy may be effective in preventing and/or reversing the progression of disorders associated with familial HCM. One of the disorders apparent in HCM is a persistent increase in myofilament response to  $\text{Ca}^{2+}$  and increase in actomyosin ATPase rate. A consequence is a mismatch in energy supply for tension and in transport. This inefficient use of ATP has been theorized to decrease the free energy,  $\Delta G$ , for ATP hydrolysis

leading to increased mitochondrial energy demand and excessive production of reactive oxygen species (ROS) (Ashrafian, Redwood et al. 2003). Mitochondrial ROS has been implicated in cardiac arrhythmias and sudden death related to diastolic heart failure with preserved ejection fraction [reviewed in (Rutledge and Dudley 2013)]. In the case of HCM, the loss of energy supply to the sarcomplasmic reticulum (SR) is also likely to alter  $\text{Ca}^{2+}$  fluxes leading to activation of hypertrophic signaling and arrhythmias. In general support of this hypothesis is the report by Crilley et al. of human patients with mutations linked to HCM exhibit a 30% reduction in phospho-creatine/ATP ratio compared to controls (Crilley, Boehm et al. 2003).

Direct actions of ROS at the level of sarcomeres may also contribute to the increased  $\text{Ca}^{2+}$ -sensitivity. We have reported, that ROS associated with a hypertensive model of heart failure with preserved ejection fraction induced S-glutathionylation of myosin binding protein C (MyBP-C), which slowed cross-bridge kinetics and increased  $\text{Ca}^{2+}$ -sensitivity. Ventricular myocytes from the model demonstrated diastolic abnormalities with no change in the  $\text{Ca}^{2+}$ -transients. Relief of the altered redox state in this model also restored diastolic function to control levels in correlation with return of MyBP-C S-glutathionylation to basal levels (Lovelock, Monasky et al. 2012).

Despite these strong indications for a role of redox related modifications in HCM linked to sarcomeric protein mutations, there have been no studies investigating the potential role and mechanisms of ROS induced exacerbation of the HCM phenotype by redox related modifications of the myofilaments.. In experiments reported here, we assessed the redox state and function of TG- $\alpha\text{Tm-E180G}$  hearts. Our data demonstrate that the TG- $\alpha\text{Tm-E180G}$  hearts display early signs of oxidative stress in the form of an altered ratio of reduced to oxidized glutathione as well redox related modifications of the myofilaments. Treatment of the TG- $\alpha\text{Tm-E180G}$  mice with NAC reversed the established cardiac hypertrophy and diastolic dysfunction. Our data support the

hypothesis that altered redox state is a significant contributor to the familial HCM phenotype, and that interventions restoring redox state may be an important therapeutic approach.

Figure 20

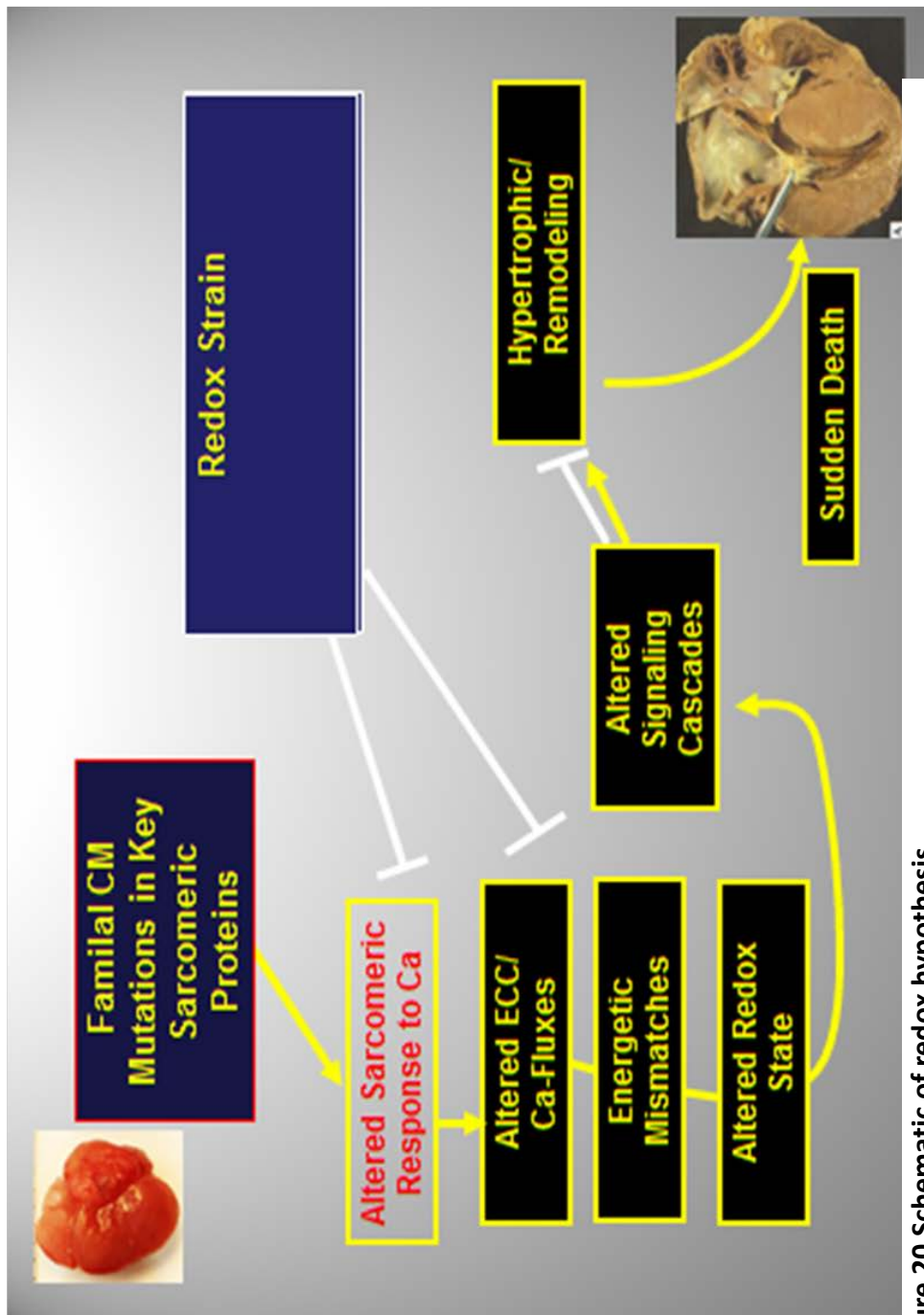


**Figure 20 Schematic of redox hypothesis.**

We hypothesize that oxidant strain plays a role in HCM disease progression.



## **B. Materials and Methods**

All protocols and procedures involving animals were approved by the Animal Care Policies and Procedures Committee at the University of Illinois in Chicago (Institutional Animal Care and Use Committee accredited). Animals were maintained in accordance with the Guide for the Care and Use of Laboratory Animals published by the United States National Institutes of Health (*National Institutes of Health Publication No. 85-23*, revised 1996).

### **1. $\alpha$ -Tm-E180G Transgenic Mice**

We have employed a transgenic FVBN strain mouse model of HCM in which 65% of wild-type  $\alpha$ -Tm is replaced with  $\alpha$ -Tm-E180G (Prabhakar, Boivin et al. 2001). Previous studies have reported that from one week of age transgenic animals begin to exhibit cardiac hypertrophy, myocyte disarray, interstitial fibrosis, and diastolic dysfunction with preserved systolic function (Muthuchamy, Pieples et al. 1999, Evans, Pena et al. 2000, Peña, Szkudlarek et al. 2010, Gaffin, Peña et al. 2011). Controls were non-transgenic FVBN littermates.

### **2. Placebo-controlled study and administration of NAC**

We randomly selected and treated one month old, sex-, and body weight matched  $\alpha$ -Tm-E180G transgenic mice with either placebo (regular drinking water) or with NAC administered at 250mg/kg/day based on prior data (Marian, Senthil et al. 2006) (SIGMA) for four weeks. Non-transgenic mice were included as controls. All mice were subjected to two-dimensional, pulse-wave, and doppler echocardiography before and after the one month treatment. At the completion of the therapy and the final echocardiographic study, animals were euthanized and hearts were extracted for functional and biochemical assessment.

### 3. *Echocardiography*

Echocardiographic measurements were performed using a high-resolution transducer (Vevo 770 High Resolution Imaging System with a center frequency of 30 MHz) after anesthetization of two month old mice as previously described (Rajan, Jagatheesan et al. 2010).

M-Mode images of the left ventricle (OV), outflow tract (LVOT), and left atrium (LA) were taken from the left parasternal long-axis view. The parasternal short-axis view at the level of the papillary muscles was used to measure the LV internal dimension (LVID). NTG and TG 4 and 8 week old mice were examined. Pulse doppler was performed with the apical four-chamber view. The mitral inflow was recorded with the doppler sample volume at the tip of the mitral valve leaflets. In order to measure time intervals, the doppler sample volume was moved toward the LVOT and both the mitral inflow and LV outflow were obtained in the same recording. Three parameters of the LV diastolic function were evaluated: 1) E/A ratio = maximal velocity of blood flow in the early diastole (E) / maximal velocity of blood flow in the late diastole (A); 2) E wave deceleration time (DT), which was the time from E to the end of the early diastole; and 3) LV isovolumic relaxation time (IVRT), which was the time measured from the aortic valve closure to the mitral valve opening. Additional information about the diastolic function was obtained with tissue doppler imaging (TDI). Peak myocardial velocities in the early ( $E_m$ ) diastole were obtained with the sample volume at the septal side of the mitral annulus in the four chamber view. All measurements and calculations were averaged from 3 consecutive cycles and performed according to the American Society of Echocardiography guideline (Lang, Bierig et al. 2005, Nagueh, Appleton et al. 2009). Data analysis was performed offline with the Vevo 770 Analytic Software.

#### **4. *Glutathione Assay***

Freshly isolated hearts were washed in ice-cold PBS + 2 mM EDTA with 25mM NEM (n-ethylamide) and snap-frozen in liquid N<sub>2</sub>, and subsequently stored at -80°C. Heart samples were used within one week of isolation. Ten mg of ventricular tissue were homogenized in 1 mL of PBS containing 2 mM EDTA and NEM. Glutathione assays were performed using 12.5 µl of the centrifuged extract to detect and quantify the cellular content of glutathione using the GSH-Glo assay kit (Promega) as described by the manufacturer. TCEP at 1 mM final concentration was added to another set of test wells with protein sample to determine the total glutathione (GSH + GSSG) content. Luminescence was read using a luminometer set to read all visible light

#### **5. *Immunoblotting***

Hearts and enriched myofibrillar proteins were extracted from ventricles of NTG and TG- $\alpha$ -Tm-E180G hearts from animals treated both with and without NAC as previously described (Muthuchamy, Grupp et al. 1995). Protein expression levels and post-translational modifications implicated in oxidative modifications including ERK 1/2, phospholamban, and sarco-endoplasmic reticular Ca<sup>2+</sup> ATPase (SERCA 2A) were assessed as described (Schulz, Wilder et al. 2013). An enriched fraction of sarcomeric proteins separated by SDS-PAGE and transferred to PVDF, was also probed to determine whether there were altered phosphorylation states of cTnI (Ser 23 and 24), MyBP-C (Ser 273, 282, and 302) (Abcam), Tm (S283) or S-protein glutathione (Virogen). Measurements of densities were assessed using ImageLab3.0.

#### **6. *Measurement of isometric tension, ATPase and $k_{tr}$***

Isometric tension and ATPase activity were measured simultaneously according to deTombe and Steinen as described in detail previously (Henze, Patrick et al. 2013). The sarcomere length throughout the experiment was set at 2.2 µm using laser diffraction following procedures and

methodology of de Tombe and ter Keurs (De Tombe and Ter Keurs 1990). Cross-bridge kinetics were determined from the tension/ATPase ratio (tension cost) or by using a quick release and re-stretch maneuver originally described by Brenner and Eisenberg (Brenner and Eisenberg 1986). The release/restretch provides a measure of the rate at which cross-bridges engage the force generating state. All experiments were carried out at 20°C. In all experiments, only fiber bundles retaining more than 80% of their initial maximum tension were included in the analysis.

## 7. Statistical Analysis

We determined pCa values at half-maximum ATPase activity and force generation from mean data normalized to maximum activity. The data were fit to a modified Hill equation (Takeda, Kobayashi et al. 1997, Kobayashi and Solaro 2006). Statistical significance was determined using one-way ANOVA followed by Tukey's post-hoc test. Data are presented as means  $\pm$  SEM with significance set at  $p < 0.05$ .

## C. RESULTS

### 1. *TG- $\alpha$ Tm-E180G mice display an increase in oxidative stress markers that is reversed by administration of N-Acetylcysteine (NAC)*

To determine whether oxidative stress is increased in the hearts of TG- $\alpha$ Tm-E180G model, we assessed the level of the major intracellular antioxidant, glutathione (GSH) and compared it to the oxidized form, GSSG using the GSH-Glo assay. Fig. 21 A-D shows that the intracellular GSH levels are reduced by 25% in TG- $\alpha$ Tm-E180G hearts with a subsequent increase in GSSG by 50% compared to NTG placebo controls.. These results indicate a reduction in the GSH/GS-SG ratio in the Tm-E180G hearts indicating an intracellular redox imbalance. In NTG or TG mice treated with NAC, there was no effect on the levels of GSH, GSSG, total glutathione, or the GSH ratio, compared to controls. Prior

studies using an exogenous NAC treatment of cardiomyocytes show increased levels of GSH. This study reports that *in vivo* NAC administration in rodents does not increase GSH levels. Thus, NAC did not alter the total glutathione pool. This is consistent with a study in patients where NAC had no impact on GSH levels that are not depleted in total glutathione. Furthermore, NAC serum levels were not detected in 50% of those patients within 2 hours of administration (Treweeke, Winterburn et al. 2012).

Figure 21

	NTG	NTG +NAC	$\alpha$ TmE180G	$\alpha$ TmE180G +NAC	* p<0.05
sample size	3	5	3	4	
<b>GSH,</b> $\mu\text{mol/g}$ protein	6.32 $\pm$ 0.03	5.95 $\pm$ 0.14	5.97 $\pm$ 0.11	6.06 $\pm$ 0.08	ns
<b>GSSG,</b> $\mu\text{mol/g}$ protein	0.18 $\pm$ 0.003	0.18 $\pm$ 0.01 †	0.22 $\pm$ 0.02 *	0.17 $\pm$ 0.01 †	* vs. NTG † vs. $\alpha$ -TmE180G
<b>Ratio</b>	36.17 $\pm$ 0.44	38.3 $\pm$ 3.04 †	28.77 $\pm$ 2.30 *	37.15 $\pm$ 2.02 †	* vs. NTG † vs. $\alpha$ -TmE180G

**Fig. 21 Graph of intracellular glutathione from 10mg of LV tissue**

Graphical representation of the levels of intracellular glutathione taken from 10 mg of left ventricular tissue from each group. The concentration of reduced glutathione, oxidized glutathione (GSSG), and the glutathione ratio (GSH/GSSG) in heart homogenate are tabulated.

\* p< 0.05 from One-way ANOVA

## **2. NAC administration improves cardiac morphology and function in HCM.**

We conducted *in vivo* cardiac assessment of morphology of the TG- $\alpha$ Tm-E180G and NTG mouse hearts at baseline, and both with or without NAC. M-mode echocardiography demonstrated that Tm-E180G mice have larger left atrial size starting at 1 month of age and was reduced to NTG levels when administered NAC for one month (Fig. 22B). NAC treatment for one month reduced atrial size to NTG levels (Fig. 22B). As previously reported (Prabhakar, Boivin et al. 2001), hearts of  $\alpha$ -Tm-E180G mice demonstrate an increase in left ventricular mass with no change in internal diameter during diastole (LVIDd) (Table 3). Compared to controls, there was also an increase in ERK1/2 phosphorylation in the hearts (Fig. 23). Treatment with NAC reduced this increased LV mass to NTG levels, but did not change LVIDd. There was also a decrease in ERK1/2 phosphorylation in NAC treated TG- $\alpha$ Tm-E180G hearts. Pulse-wave and tissue Doppler, revealed that hearts have increased E/A and E/E<sub>m</sub> ratios, indicating diastolic dysfunction. This dysfunction was reversed to NTG levels when NAC was administered (Table 3). Systolic function was unchanged in Tm-E180G animals, as expected. However, we observed a small decrease in ejection fraction and fractional shortening in NTG mice treated with NAC.

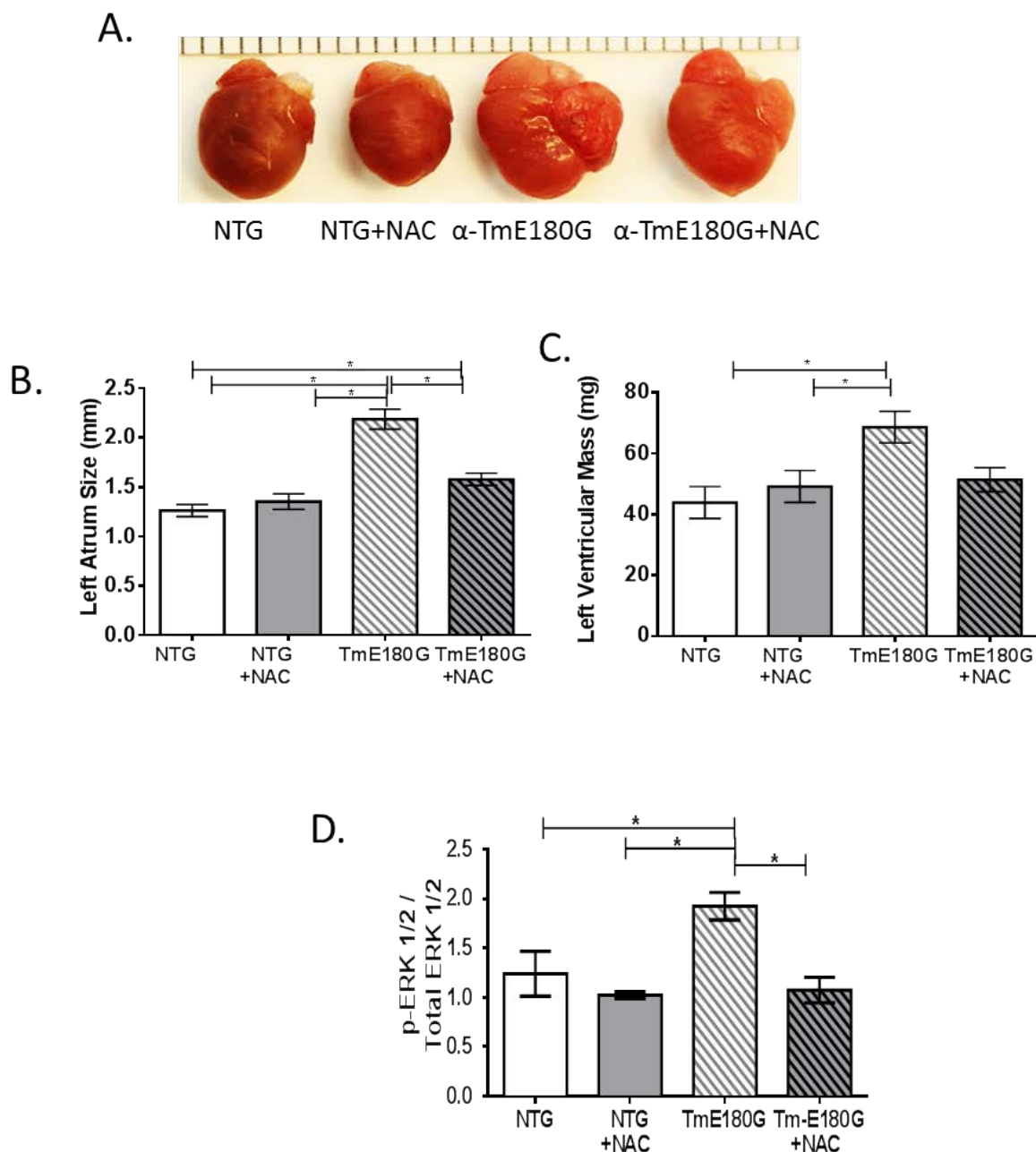
## **3. NAC affects SERCA2a expression and phosphorylation of phospholamban.**

We have previously reported no differences in Ca<sup>2+</sup> transients in ventricular myocytes isolated from NTG controls and the  $\alpha$ Tm-E180G hearts (Sheehan, Arteaga et al. 2011). However, in view of evidence that the expression and activity of SERCA2a and phospholamban are diminished in cardiomyopathies and under oxidative stress conditions (Dillmann 1999, Luckey, Mansoori et al. 2007, Peña, Szkudlarek et al. 2010, Balderas-Villalobos, Molina-Muñoz et al. 2013, Qin, Siwik et al. 2014), we tested for NAC induced alterations in these mechanisms of control of Ca<sup>2+</sup> fluxes. NAC

treatment increased the basal levels of total cardiac SERCA2a protein expression in both NTG and TG- $\alpha$ Tm-E180G hearts, but not in the controls (Fig. 26B). Phosphorylation of TG- $\alpha$ Tm-E180G PLN at the Ser-16 PKA site, tended to approach NTG levels with NAC treatment, but the values failed to reach statistical significance (Fig. 26). However, PLN phosphorylation at the  $\text{Ca}^{2+}$ -calmodulin kinase site Thr-17 was elevated in the TG- $\alpha$ Tm-E180G hearts and returned to control levels following NAC treatment.



Figure 22

**Fig. 22 NAC's effect on morphology in HCM.**

NAC reduces heart size dimensions. A) Gross morphology of HCM hearts with and without NAC administration compared to NTG controls. B) Histogram representing LA and LV size as determined by echocardiography. C) ERK 1/2 phosphorylation (n=6-9 per group) LA= Left Atrium LV = Left Ventricular NTG = non-transgenic

Table 3

Table 3 Echocardiographic phenotype following NAC treatment for one month.				
	NTG	NTG+NAC	$\alpha$ -TmE180G	$\alpha$ -TmE180G +NAC
n (sample size)	6	9	6	9
Age (months)	2	2	2	2
<b>MORPHOLOGY</b>				
LA (mm)	1.26 $\pm$ 0.06	1.36 $\pm$ 0.08 <sup>b</sup>	2.19 $\pm$ 0.10 <sup>a</sup>	1.58 $\pm$ 0.06 <sup>a,b</sup>
LV Mass (g)	43.90 $\pm$ 5.27	49.17 $\pm$ 5.27	65.69 $\pm$ 5.21 <sup>a</sup>	51.39 $\pm$ 3.95
LVIDd (mm)	3.73 $\pm$ 0.09	3.69 $\pm$ 0.11	3.75 $\pm$ 0.14	3.47 $\pm$ 0.10
RWT (mm)	0.34 $\pm$ 0.03	0.29 $\pm$ 0.03	0.37 $\pm$ 0.03	0.38 $\pm$ 0.04
<b>DIASTOLIC FUNCTION</b>				
E/A	1.54 $\pm$ 0.14	1.63 $\pm$ 0.09 <sup>b</sup>	3.03 $\pm$ 0.32 <sup>a</sup>	1.64 $\pm$ 0.15 <sup>b</sup>
E/E <sub>m</sub>	30.94 $\pm$ 3.10	30.40 $\pm$ 2.20 <sup>b</sup>	41.44 $\pm$ 2.49 <sup>a</sup>	28.05 $\pm$ 3.30 <sup>b</sup>
IVRT (ms)	12.14 $\pm$ 0.47	13.72 $\pm$ 0.86	12.34 $\pm$ 0.56	12.85 $\pm$ 0.42
<b>SYSTOLIC FUNCTION</b>				
EF (%)	69.95 $\pm$ 1.44	63.77 $\pm$ 2.61	70.98 $\pm$ 0.56	71.01 $\pm$ 1.47
FS (%)	38.89 $\pm$ 1.12	34.33 $\pm$ 1.94	39.65 $\pm$ 0.45	39.72 $\pm$ 1.18
LA indicates Left Atrium size; LV Left ventricular; LVIDd Left Ventricular Internal Diameter during diastole; RWT Relative Wall Thickness; E/A mitral inflow early to late velocities; E/E <sub>m</sub> ; IVRT Isovolumic Relaxation Time; EF Ejection Fraction; FS Fractional Shortening				
Median values were compared by One-Way ANOVA followed by Tukey's post-hoc test. p < 0.05, <sup>a</sup> vs. NTG; <sup>b</sup> vs. TmE180G				

Figure 23

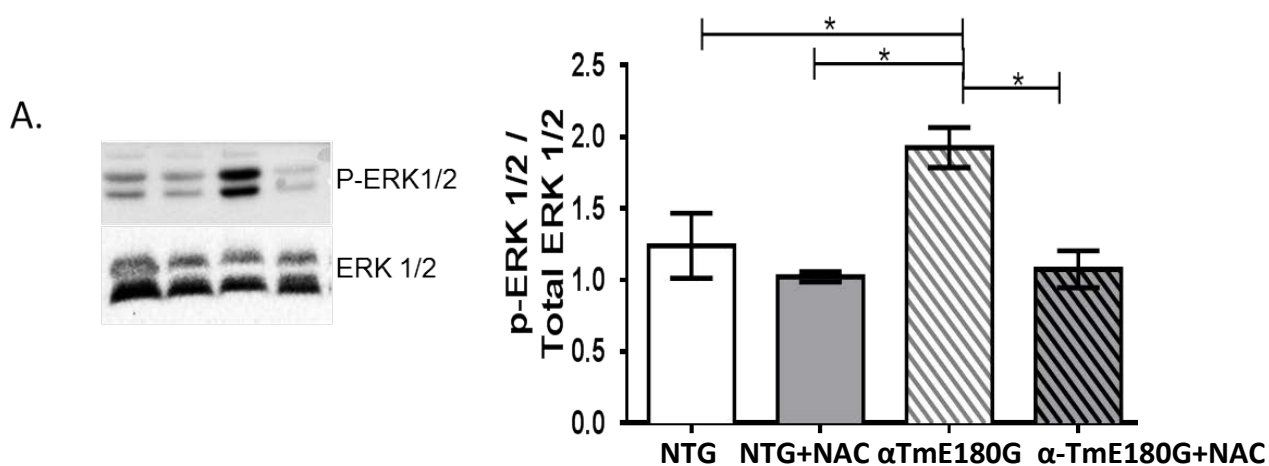


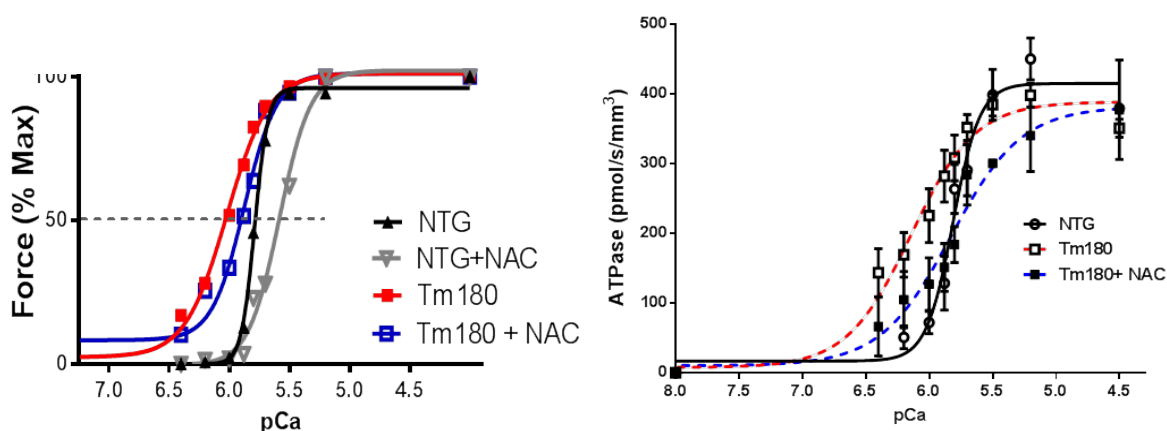
**Figure 23 NAC effect on hypertrophic signal.**

NAC reduces ERK1/2 activity. (A) Western Blot images from pERK1/2 and total ERK1/2  
 (B) Graphical representation of ERK phosphorylation related to total. \* Data are expressed as means  $\pm$  SEM n=6 per group \* p<0.05 Using one-way ANOVA.

**4. NAC decreases isometric tension and improves cross-bridge dynamic measurements in skinned fiber bundles, facilitating relaxation.**

We employed detergent extracted (skinned) fiber bundles to determine the effect of antioxidant treatment on  $\text{Ca}^{2+}$  dependence of isometric tension, acto-myosin ATPase rate, and the kinetics of tension redevelopment of both NTG and TG- $\alpha\text{MyBP-C}$  myofilaments. As expected from previous results (Prabhakar, Boivin et al. 2001), there was a significant increase in  $\text{Ca}^{2+}$  sensitivity, as determined from the  $\text{pCa}_{50}$  values, in the TG- $\alpha\text{cMyBP-C}$  myofilament compared to controls (Fig. 24). After one month of NAC treatment fiber bundles from both NTG and TG- $\alpha\text{cMyBP-C}$  hearts demonstrated a decrease in  $\text{Ca}^{2+}$  sensitivity (Fig. 24). These data support prior studies that showed decreased  $\text{Ca}^{2+}$  sensitivity and maximum tension generation in single skinned cardiomyocytes from male rats treated with NAC for one hour prior to permeabilization (Andre, Fauconnier et al. 2013). We also report that the maximum tension is reduced in myofilaments from both NTG and TG hearts treated with NAC (Fig. 24 ). Compared to NTG controls, the  $\text{Ca}^{2+}$  sensitivity of the rate of ATP hydrolysis, measured simultaneously with the force was significantly increased in the TG fibers. However, NAC treatment significantly reduced the  $\text{Ca}^{2+}$  sensitivity of the rate of ATP hydrolysis in both groups (Fig. 24). NAC treatment was also associated with a significant increase in the kinetics of tension redevelopment ( $k_{tr}$ ), a measure of the rate of entry of cross-bridges into the force generating state (Fig. 27). The slope of the relation between tension and ATPase rate (tension cost) was the same in the fiber bundles in all groups. Thus, NAC administration reduces the amount of contractile force and energy required to maintain cardiac output, as the systolic parameters were not altered in any of the groups (Table 3).

Figure 24



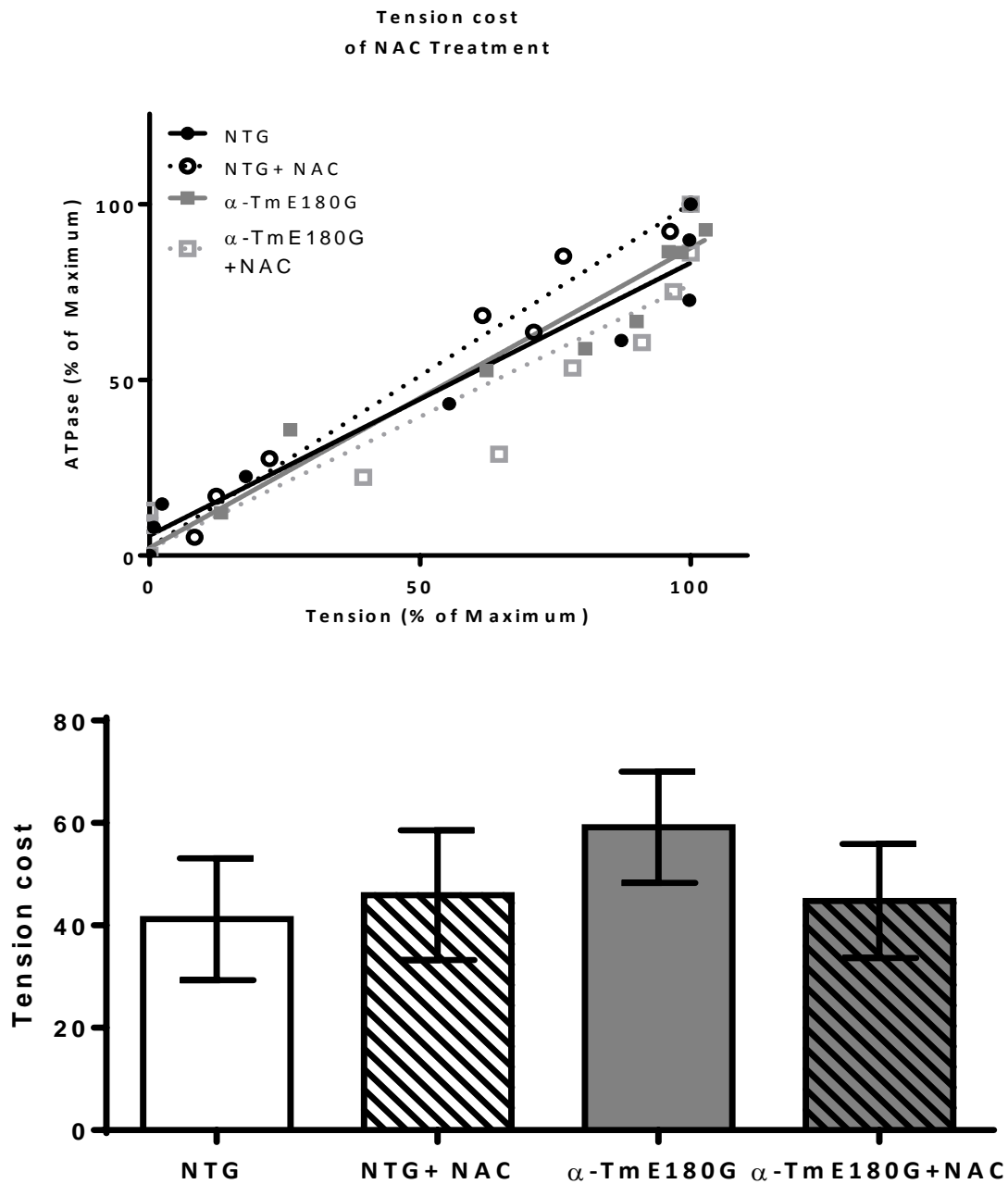
	NTG	NTG +NAC	$\alpha$ -TmE180G	$\alpha$ -TmE180G+NAC
Sample size (n)	6	5	4	4
(# papillary fibers)	7	6	7	6
Max Tension (mN/mm <sup>2</sup> )	38.01 $\pm$ 1.84	25.55 $\pm$ 5.48	33.52 $\pm$ 3.40	27.93 $\pm$ 4.55
Tension pCa <sub>50</sub>	5.78 $\pm$ 0.01	5.58 $\pm$ 0.06 <sup>a</sup>	5.94 $\pm$ 0.05 <sup>a</sup>	5.86 $\pm$ 0.04, ns
Max. ATPase (pmol/s/mm <sup>3</sup> )	379.12 $\pm$ 0.07	363.57 $\pm$ 14.02	350.53 $\pm$ 12.91 <sup>a</sup>	377.09 $\pm$ 0.71 <sup>b</sup>
ATPase rate pCa <sub>50</sub>	5.81 $\pm$ 0.03	5.68 $\pm$ 0.03	6.14 $\pm$ 0.06	5.83 $\pm$ 0.11
Hill Slope	4.09 $\pm$ 0.99	4.76 $\pm$ 1.45	1.72 $\pm$ 0.38	1.56 $\pm$ 0.59
Rate constant of Tension redevelopment, s <sup>-1</sup> (k <sub>tr</sub> )	14.75 $\pm$ 0.81	22.98 $\pm$ 2.54 <sup>a</sup>	14.15 $\pm$ 0.91 <sup>a</sup>	23.47 $\pm$ 1.21 <sup>a,b</sup>

Values are sample means  $\pm$  SEM. Papillary fibers from mouse hearts were extracted and skinned in 1% Triton X-100 for one hour at 4°C and subjected to varying calcium concentrations to simultaneously measure isometric force, ATPase, stiffness and k<sub>tr</sub>. Maximum tension, ATPase, and tension redevelopment rate, as well as pCa<sub>50</sub> (a measure of calcium sensitivity) are shown. Median values were compared by One-Way ANOVA followed by Tukey's post-hoc test. Statistically significant where p < 0.05; <sup>a</sup> vs. NTG, <sup>b</sup> vs.  $\alpha$ -TmE180G.

**Figure 24 Skinned papillary fiber function from mice treated with or without NAC.**

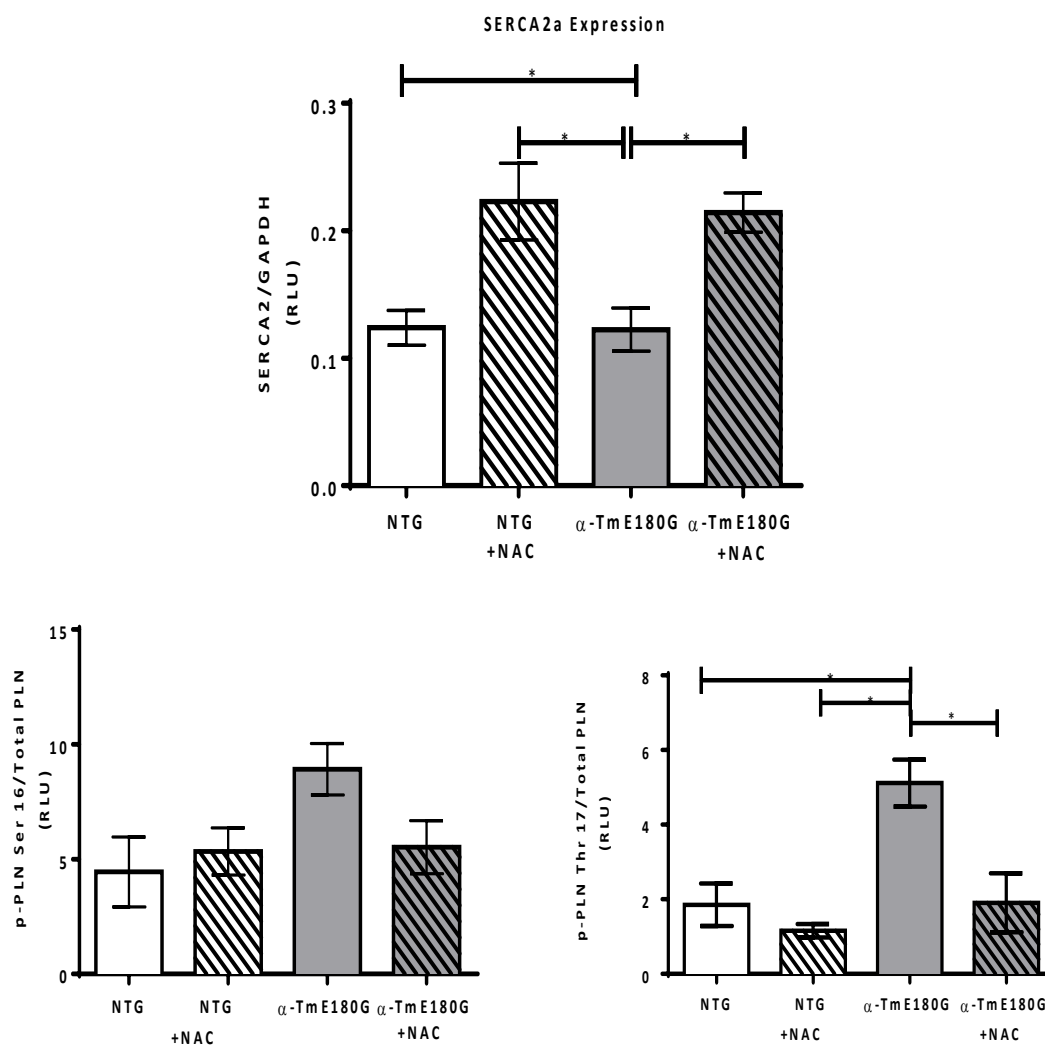
In HCM, NAC reduces Ca<sup>2+</sup> sensitivity and normalizes the ATPase rate without affecting the Hill coefficient.

Figure 25

Figure 25 Tension cost in  $\alpha$ -TmE180G treated with NAC.

The tension cost did not change due to the slope of the relation between both the tension and ATPase rate was the same in the fiber bundles in all groups. (Top) The relationship of ATPase and Tension. (Bottom) histogram of the tension cost among the groups. Not statistically significant.

Figure 26



**Figure 26 Immunoblot analysis of SERCA2a and PLN protein expression.**

(A) Quantified protein expression of SERCA2 (B) Quantified PLN phosphorylation of Ser16 (PKA) And (C) Thr 17 (CaMKII). Data are expressed as means  $\pm$  SEM n= 6 per group. \*  $p < 0.05$  Using one-way ANOVA. followed by Tukey's post-hoc test.

Figure 27 Kinetics of tension redevelopment ( $k_{tr}$ ).

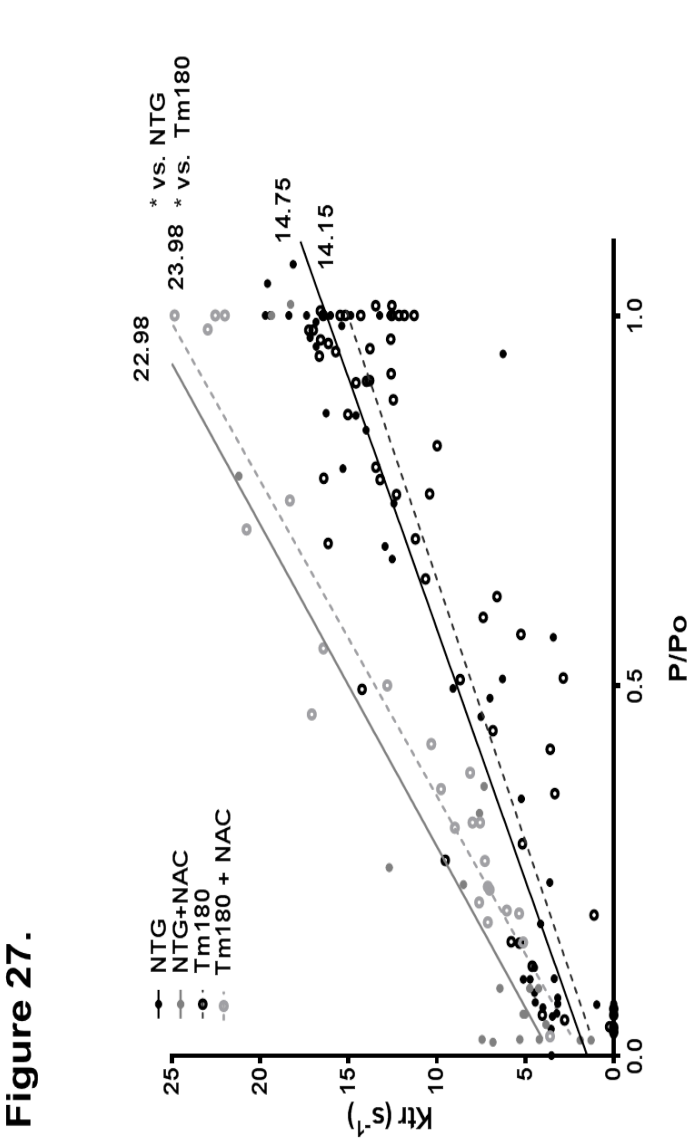
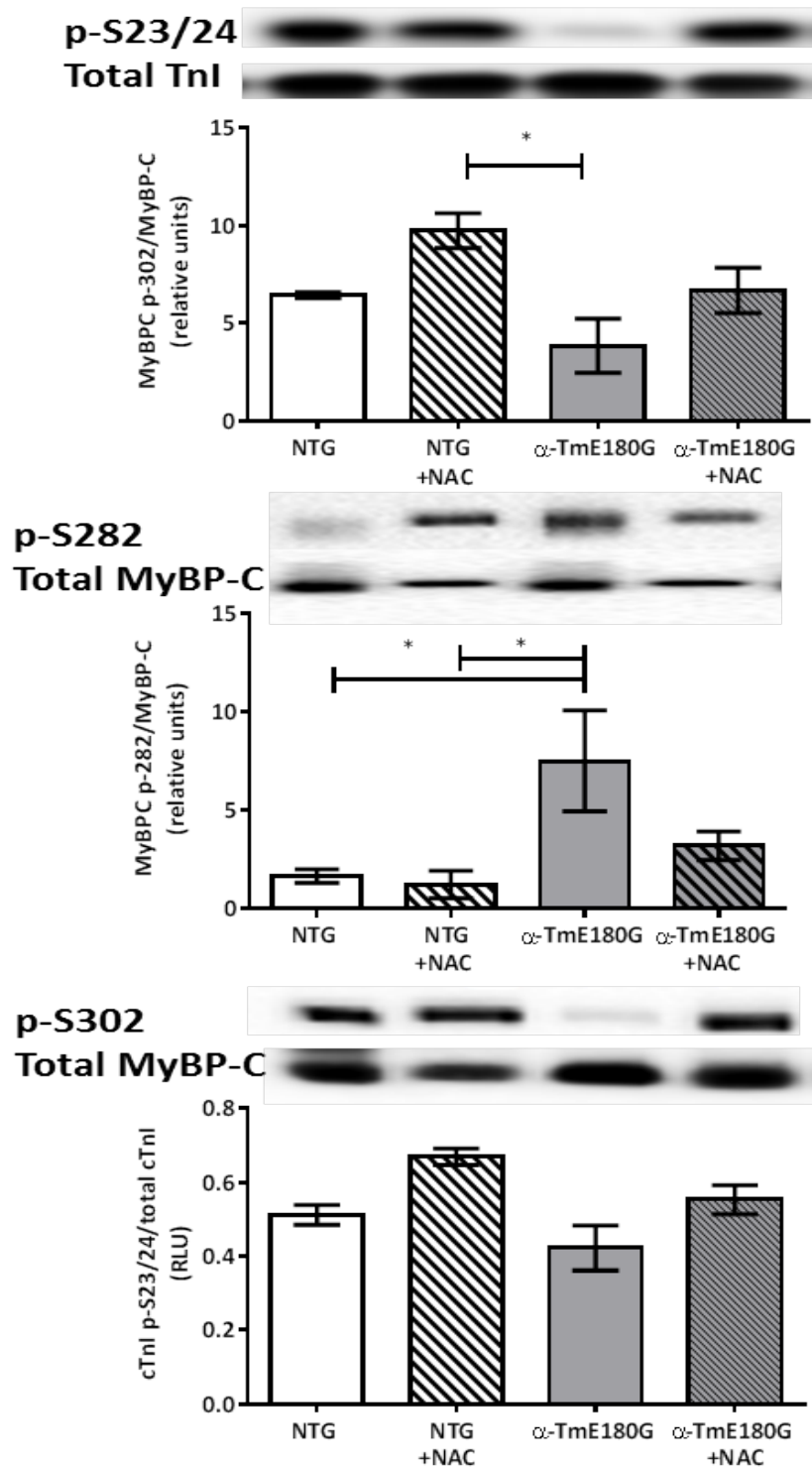


Figure 27. Kinetics of Tension redevelopment ( $K_{tr}$ ).  $K_{tr}$ -relative tension relationship in skinned fiber bundles from mice treated with or without NAC for one month. Showing the slope of the  $k_{tr}$ -relative tension between (black – NTG), (Black dotted – TmE180G), (Gray solid – NTG+NAC) and (Gray dotted – TmE180G+NAC). Relationships are represented as a means  $\pm$  SEM.  $n = 4$  animals, 12 fibers from each group. \* $p < 0.05$  TmE180G+NAC vs. NTG and TmE180G, and NTG+NAC vs. NTG and TmE180G.



Regulatory redox mechanisms that involve post-translational modifications may account for the alterations in the cross-bridge cycling dynamics noted in the TG- $\alpha$ MyBP-C hearts. To explore the oxidative modifications of myofilament proteins elicited by sarcomeric genetic mutation, we assessed the phosphorylation and protein S-glutathionylation status of key regulatory sarcomeric proteins. At two months of age, cTnI Ser23/24 and cMyBP-C Ser302 phosphorylation are reduced (Fig. 28). Previous reports demonstrate that reduction of these two sites results in an increase in the myofilament  $\text{Ca}^{2+}$  sensitivity (Alves, Dias et al. 2014, Sadayappan and de Tombe 2014). Cardiac MyBP-C phosphorylation at Ser 282, on the other hand was increased in TG- $\alpha$ MyBP-C compared to controls. Phosphorylation at this site has been shown to be increased under oxidative stress and by CaMKII, also induced under redox strain (Erickson, Joiner et al. 2008, Gupta and Robbins 2014, Luczak and Anderson 2014). There were no other phospho-protein modifications of any of the other myofilament proteins when assessed by Pro-q Diamond phosphor-stain (data not shown). The results reported here demonstrate that NAC restored the altered redox targeted phosphorylation of all aforementioned myofilament proteins back to NTG control levels (Fig. 28 ).

Figure 27



**Figure 28 Phosphorylation status of myofilament proteins after NAC treatment.**

Representative Western Blots and graphical analysis depicting the phosphorylation status after NAC treatment of (A) cTnI Ser23/24 (B) Ser-282 of MyBP-C and (C) Ser-302 of cMyBP-C. Data are

In a recent report, the oxidative stress marker S-glutathionylation of MyBP-C was the only modification identified in the DOCA-Salt hypertensive mouse compared to controls (Lovelock, Monasky et al. 2012). Functionally, this modification resulted in increased  $\text{Ca}^{+2}$  sensitivity with depressed cross-bridge turn-over kinetics (Lovelock, Monasky et al. 2012). Using mass spectrometry, we have recently identified this same functional effect through GS-SG mediated site-specific MyBP-C glutathionylation (Patel, Wilder et al. 2013). We wanted to determine the implication of S-glutathionylation on the post-translational status of the myofilament in HCM. Basally, TG- $\alpha$ Tm-E180G exhibits a significant increase in protein glutathionylation of MyBP-C (Fig. 29). NAC prevented the increases in the levels of S-glutathionylation of MyBP-C and another higher molecular weight protein.

Figure 29

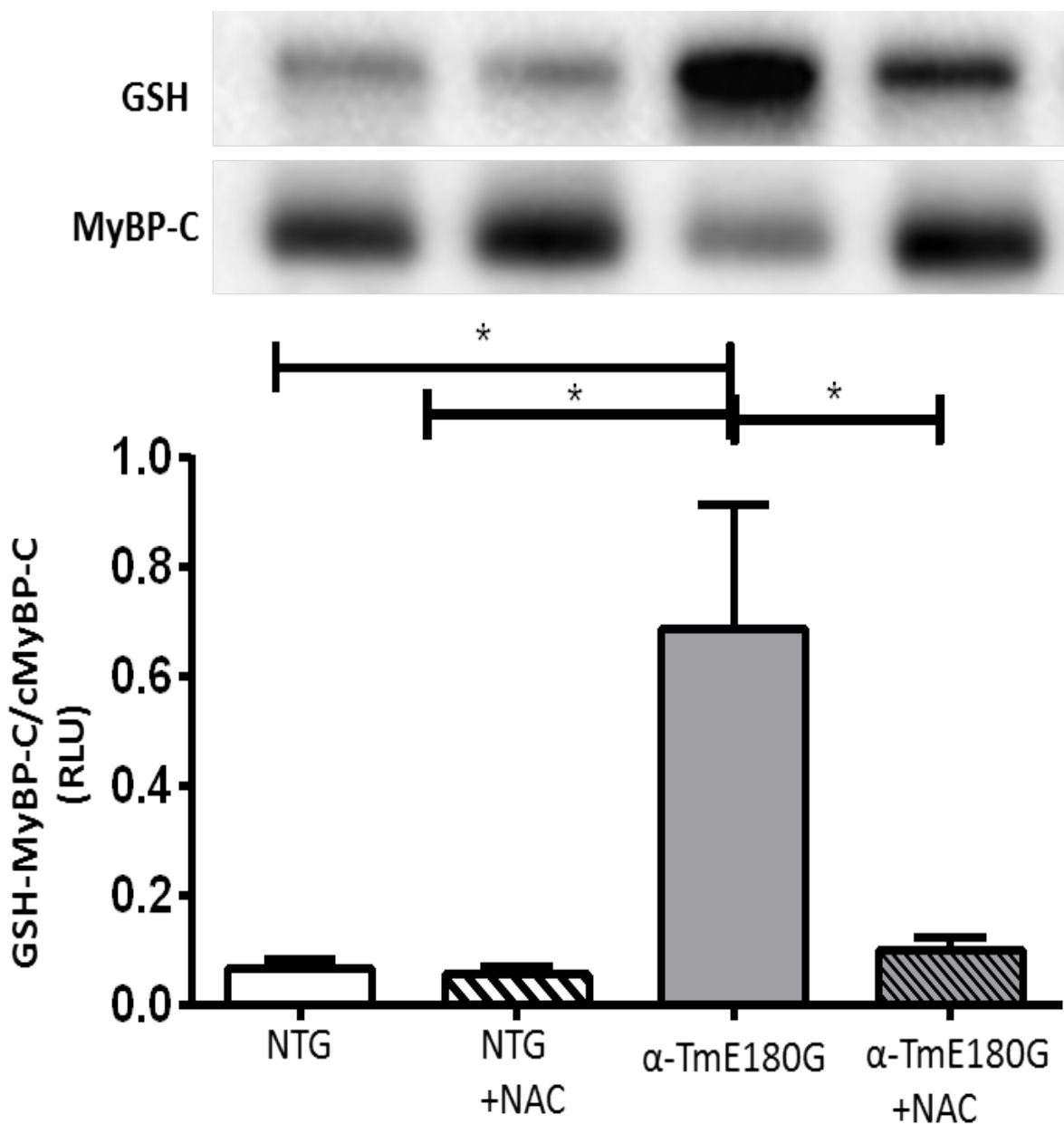


**Figure 29 GSH blot of myofibrillar cMyBP-C protein.**

(A) Western blot image of anti-GSH and total cMyBP-C of NTG and  $\alpha$ -TmE180G both with and without NAC (B) graphical representation of quantified glutathione to cMyBP-C. Data are expressed as means  $\pm$  SEM n=6 per group. \*  $p < 0.05$  Using one-way ANOVA.

#### ***D. Discussion***

Our data are the first to report that NAC administration is able to reverse the established functional and biochemical changes hearts and in sarcomeric proteins with a mutation linked to HCM. Moreover, we report novel evidence that administration of NAC alters expression of SERCA2a as well as phosphorylation of PLN at Thr17, the Ca-CaM site. Previous studies reported that exogenous NAC treatment of models with HCM linked to cTnT (Marian, Senthil et al. 2006) and myosin heavy chain mutations (Lombardi, Rodriguez et al. 2009) is able to decrease fibrosis and hypertrophy. Our studies extend these findings in that in addition to reversing the hypertrophy, we report evidence for a mechanistic basis for the reversal of diastolic abnormalities in HCM. The improvement of the diastolic abnormality was associated with effects of NAC treatment on reducing the elevated  $\text{Ca}^{2+}$  sensitivity of TmE180G myofilaments and increasing cross-bridge kinetics. We have previously presented arguments (Hinken and Solaro 2007) and data (Lovelock, Monasky et al. 2012, Jeong, Monasky et al. 2013) for the significance of cross-bridge kinetics as a determinant of diastolic state.

Our data are the first to demonstrate glutathionylation of MyBP-C in association with the altered GS-SG ratio in hearts of an HCM model, and a reversal of this post-translational modification with NAC treatment. We also found an effect of NAC treatment on S-glutathionylation of a high molecular weight protein, most likely titin (Avner, Shioura et al. 2012, Alegre-Cebollada, Kosuri et al. 2014). Although more experiments are necessary to define the potential role of titin glutathionylation, Alegre-Cebollada et al demonstrated that titin S-glutathionylation reduces stiffness and renders the molecule more extensible in human cardiomyocytes (Alegre-Cebollada, Kosuri et al. 2014). Our previous studies have reported a strong correlation of increased MyBP-C glutathionylation with slowing of cross-bridge kinetics and an increase in myofilament response to

$\text{Ca}^{2+}$  in a model of heart failure with preserved ejection fraction (Lovelock, Monasky et al. 2012, Patel, Wilder et al. 2013). In the present study, we also report slowing of cross-bridge kinetics and modified myofilament response to  $\text{Ca}^{2+}$  in association with increases in MyBP-C glutathionylation in the TG-Tm-E180G myofilaments.

A likely beneficial effect of NAC treatment is its effect to reduce the increased myofilament response to  $\text{Ca}^{2+}$  in the Tm-E180G myofilaments. One plausible mechanism contributing to the reduction in myofilament response to  $\text{Ca}^{2+}$  with NAC treatment is an effect on myofilament protein phosphorylation [27-29](#). We have reported that crossing Tm-E180G mice with a mouse model (Tnl-S23D,S24D) with constitutive myofilament desensitization to  $\text{Ca}^{2+}$  is able to prevent development of the FHC phenotype (Alves, Dias et al. 2014). We have shown previously that the intracellular  $\text{Ca}^{2+}$ -transients in ventricular myocytes of TG-Tm-E180G are not different from controls (Sheehan, Arteaga et al. 2011). Our data revealed that treatment of Tm-E180G mice with NAC is associated with and increase alterations in myofilament Tnl phosphorylation at S23 and S24 that induce desensitization to  $\text{Ca}^{2+}$ . Tm-E180G hearts display differential phosphorylation of cMyBP-C S282 and S302, where S282 is increased and S302 decreases. Previously documented are the effects of oxidative stress on kinase and phosphatase activity (Rybin, Guo et al. 2004, Sumandea, Rybin et al. 2008, Steinberg 2013). In a comprehensive review, Gupta and Robbins discuss that these cMyBP-C sites are alternatively targeted under various pathological conditions to facilitate the fine tuning of the interactions regulating contraction (Gupta and Robbins 2014). The other mechanism involved with altering the responsiveness of  $\text{Ca}^{2+}$  may relate to the aforementioned S-glutathionylation of cMyBPC and titin. The specific post-translational modifiers involved in our model and other FHC models remain to be determined. Taken together, our data showing that NAC treatment is able to improve these myofilament modifications, which are likely to contribute to diastolic dysfunction in

the Tm-E180G hearts, indicate a significant role for oxidative stress in the induction of HCM in addition to the direct functional effects of the sarcomere mutations.

Our data reveal a redox related induction of altered expression of SERCA2a, a key protein regulating Ca-fluxes. It is widely accepted that oxidative stress negatively affects calcium handling in heart failure (Koitabashi, Arai et al. 2005, Kang, Lim et al. 2006, Luo, Xuan et al. 2006, Liu, Huang et al. 2010, Vacek, Vacek et al. 2012). The characteristic increase in the E/A ratio in HCM reverses to NTG levels in Tm-E180G treated with NAC. This reduction correlates with a significant increase in SERCA2 protein expression as noted in both groups treated with NAC. The importance of SERCA2a expression was noted in a three year clinical trial treating severe heart failure patients with adenovirus (AAV1/SERCA), delayed progressive heart failure, hospitalization, and death for years (Zsebo, Yaroshinsky et al. 2014). Moreover, Peña et. al. showed that early adenoviral overexpression of SERCA2 is able to rescue the hypertrophic state of the Tm-E180G and correct diastolic dysfunction (Peña, Szkudlarek et al. 2010).

Although we found that NAC treatment increased the expression of SERCA2a in the Tm180G hearts, there was also significant decrease in PLN phosphorylation at T-17 (with no change at Ser-16), which may counter-act the positive effect on increased Ca-transport. We think this finding reveals the complexity of the responses of the heart to a sarcomeric protein mutation leading to HCM. However, we also think that this is an expected finding in view of the Ca-CaM dependence of PLN phosphorylation at the T-17 site. In various disease states including arrhythmia and sudden cardiac death,  $\text{Ca}^{2+}$ -calmodulin dependent kinase II (CaMKII) is activated (Anderson 2005). Recently, it has been reported that angiotensin II induced oxidation of the regulatory domain of CaMKII at Methionine 281/282 increased the kinase activity independent of  $\text{Ca}^{2+}$ /CaM (Erickson, Joiner et al. 2008). In TmE180G animal hearts, we found that the CaMKII site, T17 increases with no change in

the PKA site further implicating oxidative stress as a regulator of  $\text{Ca}^{2+}$  re-sequestration in HCM.

NAC Overall, despite the decrease in T17 phosphorylation with NAC treatment, diastolic dysfunction was improved in the Tm-E180G hearts. We found no evidence for an increase in PLN expression. Thus, the increase in SERCA2a expression may induce Ca-transporters not regulated by PLN. In addition, the effect of NAC treatment on cross-bridge kinetics and myofilament Ca-sensitivity may be dominant in controlling diastolic state.

Our finding that the GSH/GS-SG ratio, which is a major indicator of redox state, is diminished as early as one month of age in the presence of established dysfunction in the Tm-E180G hearts, agrees with evidence suggesting that induction of reactive oxygen species is a maladaptive effect of HCM. Patients with diastolic dysfunction with preserved systolic function have also been shown to have lower antioxidant protection including decreased glutathione (Dekleva, Celic et al. 2007). One possible explanation relates to a diminished proteosomal degradation pathway that may result in retention of oxidized proteins such as GS-SG. It is important to note that the glutathione induced by NAC treatment occurs only in the presence of B6, B12, and folate (Rimm, Willett et al. 1998, He, Merchant et al. 2004, Pfeiffer, Caudill et al. 2005, Ishihara, Iso et al. 2008, Larsson, Männistö et al. 2008). These vitamins facilitate the breakdown of homocysteine and N-Acetylcysteine into cysteine, the necessary precursors for glutathione production. We did not determine whether the serum levels of homocysteine were increased, as seen in patients with atherosclerosis and coronary heart disease (Waskiewicz 2009). However, standard laboratory animal chow is enriched with these vitamins, which would ensure NAC metabolism. It is interesting that approximately 50% of the worldwide population is deficient in consuming recommended intake values of these vitamins (He, Merchant et al. 2004, Pfeiffer, Caudill et al. 2005, Ishihara, Iso et al. 2008). Since there is no effective



treatment for FHC, the addition of a vitamin supplement could contribute to positive outcomes in clinical trials that investigate potential antioxidant therapies for HCM.

Our data support the evidence that even in the presence of developed cardiomyopathy and redox imbalance; antioxidants are able to offset the deleterious redox signaling cascades that affect cellular  $\text{Ca}^{2+}$  fluxes and, thus the rates of relaxation and contraction. We did find a significant increase in the ejection fraction and fractional shortening in both NTG and TG NAC treated groups, further implicating redox state as a controller of contractile function. This raises questions as to whether NAC could impose a further strain on the heart and elicit pathological pathways that lead to dilated cardiomyopathy; or could NAC be engendering a heart that resembles an exercised heart? We hypothesize that the latter speculation is correct. A long-term study demonstrated that NAC resolved systolic dysfunction in the  $\beta$ -MyHC Q403 HCM model, however they failed to include a NTG control treated with NAC (Lombardi, Rodriguez et al. 2009). Also, in the absence of heart defects, athletes display an increase in their resting fractional shortening with improvements in their  $\text{VO}_2$  max (Hedman, Tamás et al. 2014). Thus, further investigation must be carried out on a long-term basis to determine the effect of NAC on systolic function.

To conclude, our findings advance understanding of the functional importance of oxidative stress in HCM. *Our results reinforce the idea that oxidative stress is implicated in the pathology and progression of FHC. We have shown that our FHC mouse hearts are deficient in their antioxidant capacity and* antioxidant treatment, improves the cellular oxidant capacity, hypertrophy,  $\text{Ca}^{2+}$  handling protein expression, cross-bridge cycling dynamics, and post-translational modification of myofilament proteins to correct function. Moreover, the idea that the inclusion of a genetic mutation in sarcomeric proteins can set the stage/ create an environment that is conducive to offsetting the redox balance to produce a more oxidized than reduced myocyte is fascinating.

Understanding how these mutations induce these redox alterations will require further investigation. NAC treatment elicits many beneficial alterations and it is intriguing to suggest NAC as a therapeutic that could treat FHC, where currently there is no cure. We look forward to the results of the clinical trial that is underway (clinical trial identifier NCT01537926), and its' effects in human populations.

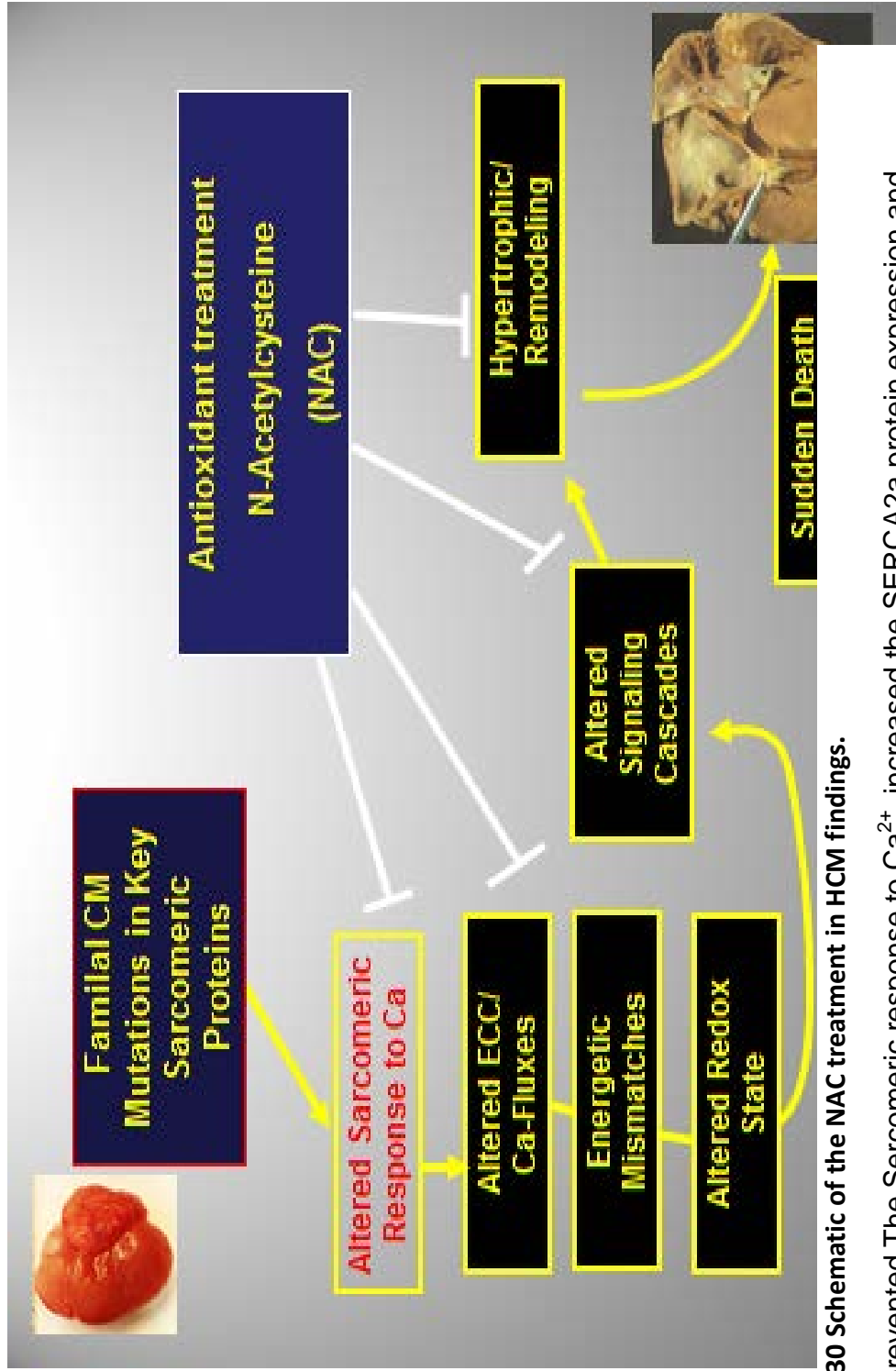


**Figure 30 Schematic of the NAC treatment in HCM findings.**

NAC prevented The Sercomeric response to  $\text{Ca}^{2+}$ , increased the SERCA2a protein expression and improved the PLN regulation, NAC prevented the development of oxidative stress mediated hypertrophy and cardiac dysfunction.

## V. GENERAL CONCLUSIONS AND SPECULATIONS

Our results demonstrate that hypertrophy induced by mutation leads to alternative pathological oxidative signals that result in post-translational modifications of the sarcomere that can be prevented/reversed by antioxidant treatment. This thesis work contributes to the scientific body of knowledge surrounding hypertrophic cardiomyopathy by showing:

1. That dephosphorylation of  $\alpha$ -TmE180G rescues disease and prevents oxidative stress through a mechanism that increases  $\text{Ca}^{2+}$  handling protein expression and the antioxidant capacity of the myocyte. This process facilitates a reduced environment that supports proper pump function.
2. In the presence of oxidants, cMyBP-C is glutathionylated at Cys 655, 627, and 479 and increases calcium sensitivity of the myofilaments, that is reversed by exogenously applied reductants. We have also observed that other myofilament proteins are modified basally by glutathionylation. Further work must be carried out to determine the specific proteins affected as well as the functional implications incurred by these modifications.
3. Antioxidant treatment, specifically N-acetylcysteine (NAC), reverses hypertrophy, prevents diastolic dysfunction and inhibits the oxidative modifications of myofilament proteins that is multifactorial. This report demonstrates that NAC increases the intracellular glutathione concentration. It also prevents hypertrophic signaling cascades that contribute to remodeling. NAC positively influences the  $\text{Ca}^{2+}$  re-uptake process by increasing SERCA2 expression and mediating the phosphorylation of phospholamban, thereby preventing diastolic dysfunction. Finally, NAC modulated cross-bridge cycling, reduced the  $\text{Ca}^{2+}$  sensitivity, and increased the ATPase rate.

The knowledge gained through this body of work leaves me to beg the question as to which comes first in the progression of disease – the increased phosphorylation in the presence of the mutation or oxidative stress? I speculate that the mutation in  $\alpha$ -Tm at position 180 alters the shape, structure, and stability of the  $\alpha$ -helix. Since Tm is connected end to end to another Tm, the alteration affects function over a wide range. If you mutate approximately 60% of the Tm molecules in the heart, the sole phosphorylation site, S283, is exposed to increased kinase activity and the functional inhibitory ability of Tm is diminished. We see that myosin heads bind actin prematurely. This binding increases the  $\text{Ca}^{2+}$  affinity to cTnC, that in turns increases the affinity of myosin to actin that increases the  $\text{Ca}^{2+}$  affinity to cTnC establishing a cyclic feedback mechanism that explains the increased  $\text{Ca}^{2+}$  sensitivity we see in  $\alpha$ -TmE180G (Fig. 24). Perhaps this occurs because of the destabilizing modifications (i.e. phosphorylation and glutathionylation) of the proteins reported here (Fig. 28,29 ). We now know that phosphorylation of Tm definitely plays a role in assisting in the acto-myosin regulation because dephosphorylating  $\alpha$ -Tm rescued the heart and improved function. I further speculate that the altered flexibility propagates as a mechanical strain that translates to the ends of the sarcomere at the Z-discs by way of titin. This strain, so to speak, pulls the folded and unfolded Ig domains of titin and exposes cryptic cysteines to oxidative modification (Alegre-Cebollada, Kosuri et al. 2014). Under constant stress/strain, regulatory proteins docked at the Z-disc are activated and target myofilaments, the nucleus, and possibly the mitochondria inappropriately. Once these proteins are activated, they target what they are in close proximity to and have access to (which are the sarcomeric sequences that are now exposed due to conformational/ structural/ allosteric modifications).

Additionally, factors that regulate expression are elicited. These transcriptional factor activations are translated to the changes we have noted, where SERCA2a and phospholamban

protein expression is increased (Fig. 11 and 26). Generally, the antioxidant capacity of the cell can normalize these insults on an acute and/or intermittent basis. However, when these events occur chronically, the defense mechanism is overrun and loses its capacity to maintain a reduced environment. This establishes what I think of as a perfect devastating storm. That in the aftermath leaves the heart no choice but to attempt to compensate. In this case, the hypertrophy is the initial response. This response may be effective in the short term, but the strain incurred by this compensation chronically leads to a more exacerbated phenotype with age. I believe that the energetic state of the heart plays an important role here, because in the setting of the increased  $\text{Ca}^{2+}$  sensitivity of myofilaments, the cross-bridge turn over and ATPase activity increases. This results in a gain of function of the acto-myosin reaction that leads to a higher energetic cost of force generation (fig. 25) that is observed in hypertrophy. Although our results did not reach statistical significance, which may be due to experimentation, there is a trend toward an increase in tension cost. The hypertrophy leads to an increase in the pressure of ventricles, which displaces onto the atria. Hence, we see drastically enlarged atrial chamber (fig. 22). The implications on atrial cells, which inherently contain the conduction nodes (SA and AV nodes) begin to be affected. These bundles of cells are critical in depolarizing the entire myocardium. When the electrical conduction system shuts down, inevitably the entire heart is suddenly silenced. Contraction and relaxation cease and the patient experiences sudden cardiac death. Today, there is no cure for this tragic set of events. However, the results reported here strongly imply that increasing the hearts ability to maintain a reduced environment on a consistent basis, even in the presence of diminished function of the sarcomere, can prevent and more importantly reverse hypertrophic cardiomyopathies (Fig. 31).

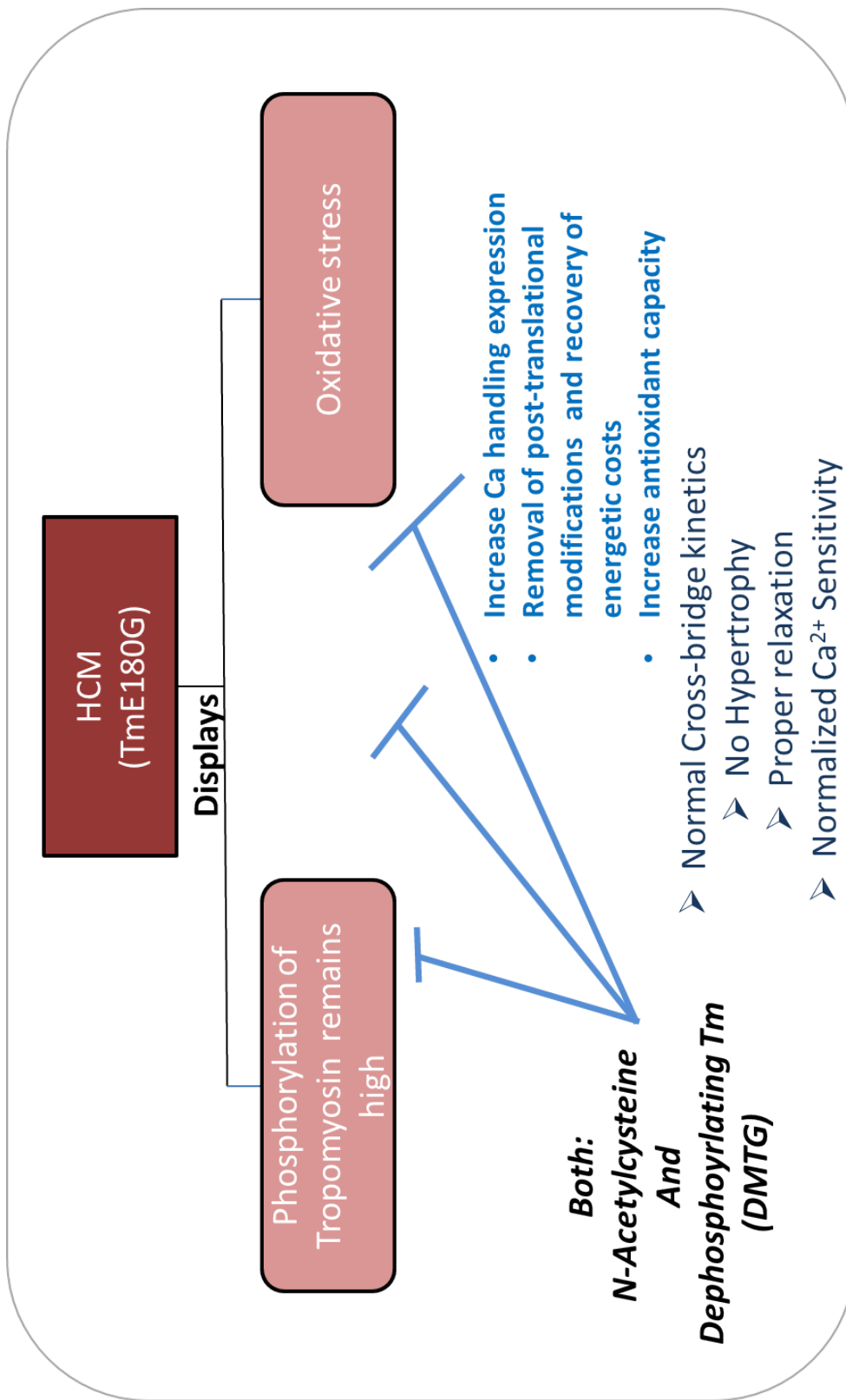


Figure 31 Schematic diagram explaining the findings of collective data.

Extra info

## VI. CITED LITERATURE

- Alegre-Cebollada, J., P. Kosuri, D. Giganti, E. Eckels, Jaime A. Rivas-Pardo, N. Hamdani, Chad M. Warren, R. J. Solaro, Wolfgang A. Linke and Julio M. Fernández (2014). "S-Glutathionylation of Cryptic Cysteines Enhances Titin Elasticity by Blocking Protein Folding." Cell **156**(6): 1235-1246.
- Alves, M. L., F. A. L. Dias, R. D. Gaffin, J. N. Simon, E. M. Montminy, B. J. Biesiadecki, A. C. Hinken, C. M. Warren, M. S. Utter, R. T. Davis, S. Sadayappan, J. Robbins, D. F. Wieczorek, R. J. Solaro and B. M. Wolska (2014). "Desensitization of Myofilaments to Ca<sup>2+</sup> as a Therapeutic Target for Hypertrophic Cardiomyopathy With Mutations in Thin Filament Proteins." Circulation: Cardiovascular Genetics **7**(2): 132-143.
- Alves, M. L., R. D. Gaffin and B. M. Wolska (2010). "Rescue of familial cardiomyopathies by modifications at the level of sarcomere and Ca<sup>2+</sup> fluxes." Journal of Molecular and Cellular Cardiology **48**(5): 834-842.
- Anderson, M. E. (2005). "Calmodulin kinase signaling in heart: an intriguing candidate target for therapy of myocardial dysfunction and arrhythmias." Pharmacology & Therapeutics **106**(1): 39-55.
- Andre, L., J. Fauconnier, C. Reboul, C. Feillet-Coudray, P. Meschin, C. Farah, G. Fouret, S. Richard, A. Lacampagne and O. Cazorla (2013). "Subendocardial increase in reactive oxygen species production affects regional contractile function in ischemic heart failure." Antioxid Redox Signal **18**(9): 1009-1020.
- Anwar, A., K. D. Schlüter, J. Heger, H. M. Piper and G. Euler (2008). "Enhanced SERCA2A expression improves contractile performance of ventricular cardiomyocytes of rat under adrenergic stimulation." Pflügers Archiv - European Journal of Physiology **457**(2): 485-491.
- Asensi, M., J. Sastre, F. V. Pallardo, J. M. Estrela and J. Viña [35] Determination of oxidized glutathione in blood: High-performance liquid chromatography. Methods in Enzymology, Academic Press. **Volume 234**: 367-371.
- Ashrafian, H., C. Redwood, E. Blair and H. Watkins (2003). "Hypertrophic cardiomyopathy: a paradigm for myocardial energy depletion." Trends in Genetics **19**(5): 263-268.
- Avner, B. S., K. M. Shioura, S. B. Scruggs, M. Grachoff, D. L. Geenen, D. L. Helseth, Jr., M. Farjah, P. H. Goldspink and R. John Solaro (2012). "Myocardial infarction in mice alters sarcomeric function via post-translational protein modification." Molecular and cellular biochemistry **363**(1-2): 203-215.
- Baker, D. L., K. Hashimoto, I. L. Grupp, Y. Ji, T. Reed, E. Loukianov, G. Grupp, A. Bhagwat, B. Hoit, R. Walsh, E. Marban and M. Periasamy (1998). "Targeted overexpression of the sarcoplasmic reticulum Ca<sup>2+</sup>-ATPase increases cardiac contractility in transgenic mouse hearts." Circ Res **83**(12): 1205-1214.
- Balderas-Villalobos, J., T. Molina-Muñoz, P. Mailloux-Salinas, G. Bravo, K. Carvajal and N. L. Gómez-Viquez (2013). "Oxidative stress in cardiomyocytes contributes to decreased SERCA2a activity in rats with metabolic syndrome." American Journal of Physiology - Heart and Circulatory Physiology **305**(9): H1344-H1353.
- Beyar, R., E. P. Shapiro, W. L. Graves, W. J. Rogers, W. H. Guier, G. A. Carey, R. L. Soulen, E. A. Zerhouni, M. L. Weisfeldt and J. L. Weiss (1990). "Quantification and validation of left ventricular wall thickening by a three-dimensional volume element magnetic resonance imaging approach." Circulation **81**(1): 297-307.
- Bottinelli, R., D. A. Coviello, C. S. Redwood, M. A. Pellegrino, B. J. Maron, P. Spirito, H. Watkins and C. Reggiani (1998). "A mutant tropomyosin that causes hypertrophic cardiomyopathy is expressed in vivo and associated with an increased calcium sensitivity." Circ Res **82**(1): 106-115.
- Brennan, J. P., J. I. Miller, W. Fuller, R. Wait, S. Begum, M. J. Dunn and P. Eaton (2006). "The utility of N,N-biotinyl glutathione disulfide in the study of protein S-glutathiolation." Molecular & cellular proteomics : MCP **5**(2): 215-225.
- Brenner, B. and E. Eisenberg (1986). "Rate of force generation in muscle: Correlation with actomyosin ATPase activity in solution." Proceedings of the National Academy of Sciences of the United States of America **83**(10): 3542-3546.
- Cazorla, O., S. Szilagyi, N. Vignier, G. Salazar, E. Kramer, G. Vassort, L. Carrier and A. Lacampagne (2006). "Length and protein kinase A modulations of myocytes in cardiac myosin binding protein C-deficient mice." Cardiovascular research **69**(2): 370-380.



- Chalovich, J. M., P. B. Chock and E. Eisenberg (1981). "Mechanism of action of troponin . tropomyosin. Inhibition of actomyosin ATPase activity without inhibition of myosin binding to actin." J Biol Chem **256**(2): 575-578.
- Chen, C. L., L. Zhang, A. Yeh, C. A. Chen, K. B. Green-Church, J. L. Zweier and Y. R. Chen (2007). "Site-specific S-glutathiolation of mitochondrial NADH ubiquinone reductase." Biochemistry **46**(19): 5754-5765.
- Conway, J. F. and D. A. D. Parry (1990). "Structural features in the heptad substructure and longer range repeats of two-stranded  $\alpha$ -fibrous proteins." International Journal of Biological Macromolecules **12**(5): 328-334.
- Coviello, D. A., B. J. Maron, P. Spirito, H. Watkins, H. P. Vosberg, L. Thierfelder, F. J. Schoen, J. G. Seidman and C. E. Seidman (1997). "Clinical features of hypertrophic cardiomyopathy caused by mutation of a "hot spot" in the alpha-tropomyosin gene." J Am Coll Cardiol **29**(3): 635-640.
- Crilly, J. G., E. A. Boehm, E. Blair, B. Rajagopalan, A. M. Blamire, P. Styles, W. J. McKenna, I. Östman-Smith, K. Clarke and H. Watkins (2003). "Hypertrophic cardiomyopathy due to sarcomeric gene mutations is characterized by impaired energy metabolism irrespective of the degree of hypertrophy." Journal of the American College of Cardiology **41**(10): 1776-1782.
- D, S. H. a. J. (2007). Oxidative Stress. Encyclopedia of Stress. A. P. Fink G. Elsevier, Academic Press. **3**: 45-48.
- Dalle-Donne, I., D. Giustarini, R. Rossi, R. Colombo and A. Milzani (2003). "Reversible S-glutathionylation of Cys 374 regulates actin filament formation by inducing structural changes in the actin molecule." Free Radic Biol Med **34**(1): 23-32.
- Dalle-Donne, I., A. Milzani, N. Gagliano, R. Colombo, D. Giustarini and R. Rossi (2008). "Molecular mechanisms and potential clinical significance of S-glutathionylation." Antioxid Redox Signal **10**(3): 445-473.
- De Tombe, P. P. and H. E. D. J. Ter Keurs (1990). "Force and velocity of sarcomere shortening in trabeculae from rat heart. Effects of temperature." Circulation Research **66**(5): 1239-1254.
- Dekleva, M., V. Celic, N. Kostic, B. Pencic, A. M. Ivanovic and Z. Caparevic (2007). "Left Ventricular Diastolic Dysfunction Is Related to Oxidative Stress and Exercise Capacity in Hypertensive Patients with Preserved Systolic Function." Cardiology **108**(1): 62-70.
- Dillmann, W. H. (1999). "Calcium regulatory proteins and their alteration by transgenic approaches." Am J Cardiol **83**(12a): 89h-91h.
- Erickson, J. R., M.-I. A. Joiner, X. Guan, W. Kutschke, J. Yang, C. V. Oddis, R. K. Bartlett, J. S. Lowe, S. E. O'Donnell, N. Aykin-Burns, M. C. Zimmerman, K. Zimmerman, A.-J. L. Ham, R. M. Weiss, D. R. Spitz, M. A. Shea, R. J. Colbran, P. J. Mohler and M. E. Anderson (2008). "A Dynamic Pathway for Calcium-Independent Activation of CaMKII by Methionine Oxidation." Cell **133**(3): 462-474.
- Evans, C. C., J. R. Pena, R. M. Phillips, M. Muthuchamy, D. F. Wieczorek, R. J. Solaro and B. M. Wolska (2000). "Altered hemodynamics in transgenic mice harboring mutant tropomyosin linked to hypertrophic cardiomyopathy." American journal of physiology. Heart and circulatory physiology **279**(5): H2414-2423.
- Evans, C. C., J. R. Pena, R. M. Phillips, M. Muthuchamy, D. F. Wieczorek, R. J. Solaro and B. M. Wolska (2000). "Altered hemodynamics in transgenic mice harboring mutant tropomyosin linked to hypertrophic cardiomyopathy." American Journal of Physiology - Heart and Circulatory Physiology **279**(5): H2414-H2423.
- Farah, C. S. and F. C. Reinach (1999). "Regulatory Properties of Recombinant Tropomyosins Containing 5-Hydroxytryptophan: Ca<sup>2+</sup>-Binding to Troponin Results in a Conformational Change in a Region of Tropomyosin outside the Troponin Binding Site<sup>†</sup>." Biochemistry **38**(32): 10543-10551.
- Flashman, E., C. Redwood, J. Moolman-Smook and H. Watkins (2004). "Cardiac myosin binding protein C: its role in physiology and disease." Circulation research **94**(10): 1279-1289.
- Fritz, J. D., D. R. Swartz and M. L. Greaser (1989). "Factors affecting polyacrylamide gel electrophoresis and electroblotting of high-molecular-weight myofibrillar proteins." Anal Biochem **180**(2): 205-210.
- Gaffin, R. D., J. R. Peña, M. S. L. Alves, F. A. L. Dias, S. A. K. Chowdhury, L. S. Heinrich, P. H. Goldspink, E. G. Kranias, D. F. Wieczorek and B. M. Wolska (2011). "Long-term rescue of a familial hypertrophic cardiomyopathy caused by a mutation in the thin filament protein, tropomyosin, via modulation of a calcium cycling protein." Journal of Molecular and Cellular Cardiology **51**(5): 812-820.

- Geisterfer-Lowrance, A. A., S. Kass, G. Tanigawa, H. P. Vosberg, W. McKenna, C. E. Seidman and J. G. Seidman (1990). "A molecular basis for familial hypertrophic cardiomyopathy: a beta cardiac myosin heavy chain gene missense mutation." Cell **62**(5): 999-1006.
- Golitsina, N., Y. An, N. J. Greenfield, L. Thierfelder, K. Iizuka, J. G. Seidman, C. E. Seidman, S. S. Lehrer and S. E. Hitchcock-DeGregori (1997). "Effects of two familial hypertrophic cardiomyopathy-causing mutations on alpha-tropomyosin structure and function." Biochemistry **36**(15): 4637-4642.
- Gupta, M. and J. Robbins (2014). "Post-translational control of cardiac hemodynamics through myosin binding protein C." Pflügers Archiv - European Journal of Physiology **466**(2): 231-236.
- Harris, S. P., R. G. Lyons and K. L. Bezold (2011). "In the thick of it: HCM-causing mutations in myosin binding proteins of the thick filament." Circulation research **108**(6): 751-764.
- He, K., A. Merchant, E. B. Rimm, B. A. Rosner, M. J. Stampfer, W. C. Willett and A. Ascherio (2004). "Folate, Vitamin B6, and B12 Intakes in Relation to Risk of Stroke Among Men." Stroke **35**(1): 169-174.
- Hedman, K., É. Tamás, J. Henriksson, N. Bjarnegård, L. Brudin and E. Nylander (2014). "Female athlete's heart: Systolic and diastolic function related to circulatory dimensions." Scandinavian Journal of Medicine & Science in Sports: n/a-n/a.
- Heeley, D. A., A. J. G. Moir and S. V. Perry (1982). "Phosphorylation of tropomyosin during development in mammalian striated muscle." FEBS Letters **146**(1): 115-118.
- Heeley, D. H., M. H. Watson, A. S. Mak, P. Dubord and L. B. Smillie (1989). "Effect of phosphorylation on the interaction and functional properties of rabbit striated muscle alpha alpha-tropomyosin." Journal of Biological Chemistry **264**(5): 2424-2430.
- Henze, M., S. E. Patrick, A. Hinken, S. B. Scruggs, P. Goldspink, P. P. de Tombe, M. Kobayashi, P. Ping, T. Kobayashi and R. J. Solaro (2013). "New insights into the functional significance of the acidic region of the unique N-terminal extension of cardiac troponin I." Biochim Biophys Acta **1833**(4): 823-832.
- Hill, B. G., K. V. Ramana, J. Cai, A. Bhatnagar and S. K. Srivastava (2010). "Measurement and identification of S-glutathiolated proteins." Methods Enzymol **473**: 179-197.
- Hill, B. G., K. V. Ramana, J. Cai, A. Bhatnagar and S. K. Srivastava (2010). "Measurement and identification of S-glutathiolated proteins." Methods in enzymology **473**: 179-197.
- Himes, R. H. and T. Wilder (1965). "Formyltetrahydrofolate synthetase: mechanism of cation activation." Biochimica et biophysica acta **99**(3): 464-475.
- Hinken, A. C. and R. J. Solaro (2007). "A Dominant Role of Cardiac Molecular Motors in the Intrinsic Regulation of Ventricular Ejection and Relaxation." Physiology **22**(2): 73-80.
- Ishihara, J., H. Iso, M. Inoue, M. Iwasaki, K. Okada, Y. Kita, Y. Kokubo, A. Okayama and S. Tsugane (2008). "Intake of Folate, Vitamin B6 and Vitamin B12 and the Risk of CHD: The Japan Public Health Center-Based Prospective Study Cohort I." Journal of the American College of Nutrition **27**(1): 127-136.
- Ishikawa, T. and H. Sies (1984). "Cardiac transport of glutathione disulfide and S-conjugate. Studies with isolated perfused rat heart during hydroperoxide metabolism." J Biol Chem **259**(6): 3838-3843.
- Jagatheesan, G., S. Rajan, N. Petrashevskaya, A. Schwartz, G. Boivin, S. Vahebi, P. DeTombe, R. J. Solaro, E. Labitzke, G. Hilliard and D. F. Wieczorek (2003). "Functional importance of the carboxyl-terminal region of striated muscle tropomyosin." J Biol Chem **278**(25): 23204-23211.
- Jeong, E. M., M. M. Monasky, L. Gu, D. M. Taglieri, B. G. Patel, H. Liu, Q. Wang, I. Greener, S. C. Dudley, Jr. and R. J. Solaro (2013). "Tetrahydrobiopterin improves diastolic dysfunction by reversing changes in myofilament properties." Journal of molecular and cellular cardiology **56**: 44-54.
- Jeong, E. M., M. M. Monasky, L. Gu, D. M. Taglieri, B. G. Patel, H. Liu, Q. Wang, I. Greener, S. C. Dudley, Jr. and R. J. Solaro (2013). "Tetrahydrobiopterin improves diastolic dysfunction by reversing changes in myofilament properties." J Mol Cell Cardiol **56**: 44-54.
- Jin, J. P. and S. M. Chong (2010). "Localization of the two tropomyosin-binding sites of troponin T." Archives of Biochemistry and Biophysics **500**(2): 144-150.
- Kang, S. M., S. Lim, H. Song, W. Chang, S. Lee, S. M. Bae, J. H. Chung, H. Lee, H. G. Kim, D. H. Yoon, T. W. Kim, Y. Jang, J. M. Sung, N. S. Chung and K. C. Hwang (2006). "Allopurinol modulates reactive oxygen species

- generation and Ca<sup>2+</sup> overload in ischemia-reperfused heart and hypoxia-reoxygenated cardiomyocytes." *Eur J Pharmacol* **535**(1-3): 212-219.
- Kentish, J. C., D. T. McCloskey, J. Layland, S. Palmer, J. M. Leiden, A. F. Martin and R. J. Solaro (2001). "Phosphorylation of Troponin I by Protein Kinase A Accelerates Relaxation and Crossbridge Cycle Kinetics in Mouse Ventricular Muscle." *Circulation Research* **88**(10): 1059-1065.
- Kobayashi, T. and R. J. Solaro (2006). "Increased Ca<sup>2+</sup> affinity of cardiac thin filaments reconstituted with cardiomyopathy-related mutant cardiac troponin I." *J Biol Chem* **281**(19): 13471-13477.
- Kobayashi, T. and R. J. Solaro (2006). "Increased Ca<sup>2+</sup> affinity of cardiac thin filaments reconstituted with cardiomyopathy-related mutant cardiac troponin I." *Journal of Biological Chemistry* **281**(19): 13471-13477.
- Kodama, T., K. Fukui and K. Kometani (1986). "The initial phosphate burst in ATP hydrolysis by myosin and subfragment-1 as studied by a modified malachite green method for determination of inorganic phosphate." *Journal of biochemistry* **99**(5): 1465-1472.
- Koitaishi, N., M. Arai, K. Tomaru, T. Takizawa, A. Watanabe, K. Niwano, T. Yokoyama, F. Wuytack, M. Periasamy, R. Nagai and M. Kurabayashi (2005). "Carvedilol effectively blocks oxidative stress-mediated downregulation of sarcoplasmic reticulum Ca<sup>2+</sup>-ATPase 2 gene transcription through modification of Sp1 binding." *Biochem Biophys Res Commun* **328**(1): 116-124.
- Labeit, S. and B. Kolmerer (1995). "Titins: Giant Proteins in Charge of Muscle Ultrastructure and Elasticity." *Science* **270**(5234): 293-296.
- Laemmli, U. K. (1970). "Cleavage of structural proteins during the assembly of the head of bacteriophage T4." *Nature* **227**(5259): 680-685.
- Lang, D. (2002). "Cardiac hypertrophy and oxidative stress: a leap of faith or stark reality?" *Heart* **87**(4): 316-317.
- Lang, R. M., M. Bierig, R. B. Devereux, F. A. Flachskampf, E. Foster, P. A. Pellikka, M. H. Picard, M. J. Roman, J. Seward, J. S. Shanewise, S. D. Solomon, K. T. Spencer, M. S. Sutton and W. J. Stewart (2005). "Recommendations for chamber quantification: a report from the American Society of Echocardiography's Guidelines and Standards Committee and the Chamber Quantification Writing Group, developed in conjunction with the European Association of Echocardiography, a branch of the European Society of Cardiology." *J Am Soc Echocardiogr* **18**(12): 1440-1463.
- Larsson, S. C., S. Männistö, M. J. Virtanen, J. Kontto, D. Albanes and J. Virtamo (2008). "Folate, Vitamin B6, Vitamin B12, and Methionine Intakes and Risk of Stroke Subtypes in Male Smokers." *American Journal of Epidemiology* **167**(8): 954-961.
- Layland, J., A. C. Cave, C. Warren, D. J. Grieve, E. Sparks, J. C. Kentish, R. J. Solaro and A. M. Shah (2005). "Protection against endotoxemia-induced contractile dysfunction in mice with cardiac-specific expression of slow skeletal troponin I." *FASEB J* **19**(9): 1137-1139.
- Lehrer, S. S. and M. A. Geeves (2014). "The myosin-activated thin filament regulatory state, M (-) -open: a link to hypertrophic cardiomyopathy (HCM)." *J Muscle Res Cell Motil* **35**(2): 153-160.
- Li, M. X., S. M. Gagne, L. Spyropoulos, C. P. Klocks, G. Audette, M. Chandra, R. J. Solaro, L. B. Smillie and B. D. Sykes (1997). "NMR studies of Ca<sup>2+</sup> binding to the regulatory domains of cardiac and E41A skeletal muscle troponin C reveal the importance of site I to energetics of the induced structural changes." *Biochemistry* **36**(41): 12519-12525.
- Li, Y., S. Mui, J. H. Brown, J. Strand, L. Reshetnikova, L. S. Tobacman and C. Cohen (2002). "The crystal structure of the C-terminal fragment of striated-muscle alpha-tropomyosin reveals a key troponin T recognition site." *Proc Natl Acad Sci U S A* **99**(11): 7378-7383.
- Linke, W. A. and M. Krüger (2010). "The Giant Protein Titin as an Integrator of Myocyte Signaling Pathways." *Physiology* **25**(3): 186-198.
- Liu, Y., H. Huang, W. Xia, Y. Tang, H. Li and C. Huang (2010). "NADPH oxidase inhibition ameliorates cardiac dysfunction in rabbits with heart failure." *Mol Cell Biochem* **343**(1-2): 143-153.
- Lombardi, R., G. Rodriguez, S. N. Chen, C. M. Ripplinger, W. Li, J. Chen, J. T. Willerson, S. Betocchi, S. A. Wickline, I. R. Efimov and A. J. Marian (2009). "Resolution of Established Cardiac Hypertrophy and Fibrosis

- and Prevention of Systolic Dysfunction in a Transgenic Rabbit Model of Human Cardiomyopathy Through Thiol-Sensitive Mechanisms." Circulation **119**(10): 1398-1407.
- Loong, C. K., H. X. Zhou and P. B. Chase (2012). "Familial hypertrophic cardiomyopathy related E180G mutation increases flexibility of human cardiac alpha-tropomyosin." FEBS Lett **586**(19): 3503-3507.
- Lovelock, J. D., M. M. Monasky, E.-M. Jeong, H. A. Lardin, H. Liu, B. G. Patel, D. M. Taglieri, L. Gu, P. Kumar, N. Pokhrel, D. Zeng, L. Belardinelli, D. Sorescu, R. J. Solaro and S. C. Dudley (2012). "Ranolazine Improves Cardiac Diastolic Dysfunction Through Modulation of Myofilament Calcium Sensitivity / Novelty and Significance." Circulation research **110**(6): 841-850.
- Lovelock, J. D., M. M. Monasky, E. M. Jeong, H. A. Lardin, H. Liu, B. G. Patel, D. M. Taglieri, L. Gu, P. Kumar, N. Pokhrel, D. Zeng, L. Belardinelli, D. Sorescu, R. J. Solaro and S. C. Dudley, Jr. (2012). "Ranolazine improves cardiac diastolic dysfunction through modulation of myofilament calcium sensitivity." Circulation research **110**(6): 841-850.
- Lovelock, J. D., M. M. Monasky, E. M. Jeong, H. A. Lardin, H. Liu, B. G. Patel, D. M. Taglieri, L. Gu, P. Kumar, N. Pokhrel, D. Zeng, L. Belardinelli, D. Sorescu, R. J. Solaro and S. C. Dudley, Jr. (2012). "Ranolazine Improves Cardiac Diastolic Dysfunction Through Modulation of Myofilament Calcium Sensitivity." Circ Res.
- Luckey, S. W., J. Mansoori, K. Fair, C. L. Antos, E. N. Olson and L. A. Leinwand (2007). "Blocking cardiac growth in hypertrophic cardiomyopathy induces cardiac dysfunction and decreased survival only in males." Am J Physiol Heart Circ Physiol **292**(2): H838-845.
- Luczak, E. D. and M. E. Anderson (2014). "CaMKII oxidative activation and the pathogenesis of cardiac disease." Journal of Molecular and Cellular Cardiology **73**(0): 112-116.
- Luo, J., Y. T. Xuan, Y. Gu and S. D. Prabhu (2006). "Prolonged oxidative stress inverts the cardiac force-frequency relation: role of altered calcium handling and myofilament calcium responsiveness." J Mol Cell Cardiol **40**(1): 64-75.
- Maddika, S., V. Elimban, D. Chapman and N. S. Dhalla (2009). "Role of oxidative stress in ischemia-reperfusion-induced alterations in myofibrillar ATPase activities and gene expression in the heart." Can J Physiol Pharmacol **87**(2): 120-129.
- Mak, A., L. B. Smillie and M. Barany (1978). "Specific phosphorylation at serine-283 of alpha tropomyosin from frog skeletal and rabbit skeletal and cardiac muscle." Proc Natl Acad Sci U S A **75**(8): 3588-3592.
- Marian, A. J., V. Senthil, S. N. Chen and R. Lombardi (2006). "Antifibrotic Effects of Antioxidant N-Acetylcysteine in a Mouse Model of Human Hypertrophic Cardiomyopathy Mutation." Journal of the American College of Cardiology **47**(4): 827-834.
- Maron, B. J. (2002). "Hypertrophic cardiomyopathy: a systematic review." Jama **287**(10): 1308-1320.
- Matsudaira, P. (1987). "Sequence from picomole quantities of proteins electroblotted onto polyvinylidene difluoride membranes." J Biol Chem **262**(21): 10035-10038.
- Maulik, S. K. and S. Kumar (2012). "Oxidative stress and cardiac hypertrophy: a review." Toxicology Mechanisms and Methods **22**(5): 359-366.
- Muthuchamy, M., I. L. Grupp, G. Grupp, B. A. O'Toole, A. B. Kier, G. P. Boivin, J. Neumann and D. F. Wieczorek (1995). "Molecular and physiological effects of overexpressing striated muscle beta-tropomyosin in the adult murine heart." The Journal of biological chemistry **270**(51): 30593-30603.
- Muthuchamy, M., K. Pieples, P. Rethinasamy, B. Hoit, I. L. Grupp, G. P. Boivin, B. Wolska, C. Evans, R. J. Solaro and D. F. Wieczorek (1999). "Mouse model of a familial hypertrophic cardiomyopathy mutation in alpha-tropomyosin manifests cardiac dysfunction." Circulation research **85**(1): 47-56.
- Nagueh, S. F., C. P. Appleton, T. C. Gillebert, P. N. Marino, J. K. Oh, O. A. Smiseth, A. D. Waggoner, F. A. Flachskampf, P. A. Pellikka and A. Evangelisa (2009). "Recommendations for the evaluation of left ventricular diastolic function by echocardiography." Eur J Echocardiogr **10**(2): 165-193.
- Nakajima-Taniguchi, C., H. Matsui, S. Nagata, T. Kishimoto and K. Yamauchi-Takahara (1995). "Novel missense mutation in alpha-tropomyosin gene found in Japanese patients with hypertrophic cardiomyopathy." J Mol Cell Cardiol **27**(9): 2053-2058.

- Nixon, B., B. Liu, B. Scellini, C. Tesi, O. Ogut, R. Fishel, M. Ziolo, P. Janssen, R. J. Solaro, J. P. Davis, C. Poggesi and B. J. Biesiadecki (2012). "Tropomyosin Ser-283 pseudo-phosphorylation slows myofibril relaxation." Arch Biochemical Biophysics In Press In Press(Journal Article).
- Palmer, B. M., S. Sadayappan, Y. Wang, A. E. Weith, M. J. Previs, T. Bekyarova, T. C. Irving, J. Robbins and D. W. Maughan (2011). "Roles for cardiac MyBP-C in maintaining myofilament lattice rigidity and prolonging myosin cross-bridge lifetime." Biophysical journal **101**(7): 1661-1669.
- Pastore, A. and F. Piemonte (2012). "S-Glutathionylation signaling in cell biology: progress and prospects." European journal of pharmaceutical sciences : official journal of the European Federation for Pharmaceutical Sciences **46**(5): 279-292.
- Patel, B. G., T. Wilder and R. J. Solaro (2013). "Novel control of cardiac myofilament response to calcium by S-glutathionylation at specific sites of myosin binding protein C." Frontiers in Physiology **4**.
- Peña, J. R., A. C. Szkudlarek, C. M. Warren, L. S. Heinrich, R. D. Gaffin, G. Jagatheesan, F. del Monte, R. J. Hajjar, P. H. Goldspink, R. J. Solaro, D. F. Wieczorek and B. M. Wolska (2010). "Neonatal gene transfer of Serca2a delays onset of hypertrophic remodeling and improves function in familial hypertrophic cardiomyopathy." Journal of Molecular and Cellular Cardiology **49**(6): 993-1002.
- Perkins, D. N., D. J. Pappin, D. M. Creasy and J. S. Cottrell (1999). "Probability-based protein identification by searching sequence databases using mass spectrometry data." Electrophoresis **20**(18): 3551-3567.
- Pfaffl, M. W. (2001). "A new mathematical model for relative quantification in real-time RT-PCR." Nucleic acids research **29**(9): e45.
- Pfeiffer, C. M., S. P. Caudill, E. W. Gunter, J. Osterloh and E. J. Sampson (2005). "Biochemical indicators of B vitamin status in the US population after folic acid fortification: results from the National Health and Nutrition Examination Survey 1999–2000." The American Journal of Clinical Nutrition **82**(2): 442-450.
- Pizarro, G. O. and O. Ogut (2009). "Impact of actin glutathionylation on the actomyosin-S1 ATPase." Biochemistry **48**(31): 7533-7538.
- Prabhakar, R., G. P. Boivin, I. L. Grupp, B. Hoit, G. Arteaga, J. R. Solaro and D. F. Wieczorek (2001). "A familial hypertrophic cardiomyopathy alpha-tropomyosin mutation causes severe cardiac hypertrophy and death in mice." Journal of Molecular and Cellular Cardiology **33**(10): 1815-1828.
- Prabhakar, R., N. Petrashevskaya, A. Schwartz, B. Aronow, G. P. Boivin, J. D. Molkentin and D. F. Wieczorek (2003). "A mouse model of familial hypertrophic cardiomyopathy caused by a alpha-tropomyosin mutation." Molecular and cellular biochemistry **251**(1-2): 33-42.
- Prochniewicz, E., D. A. Lowe, D. J. Spakowicz, L. Higgins, K. O'Connor, L. V. Thompson, D. A. Ferrington and D. D. Thomas (2008). "Functional, structural, and chemical changes in myosin associated with hydrogen peroxide treatment of skeletal muscle fibers." Am J Physiol Cell Physiol **294**(2): C613-626.
- Qin, F., D. A. Siwik, D. R. Pimentel, R. J. Morgan, A. Biolo, V. H. Tu, Y. J. Kang, R. A. Cohen and W. S. Colucci (2014). "Cytosolic H2O2 mediates hypertrophy, apoptosis, and decreased SERCA activity in mice with chronic hemodynamic overload." Am J Physiol Heart Circ Physiol **306**(10): H1453-1463.
- Rajan, S., G. Jagatheesan, C. N. Karam, M. L. Alves, I. Bodi, A. Schwartz, C. F. Bulcao, K. M. D'Souza, S. A. Akhter, G. P. Boivin, D. K. Dube, N. Petrashevskaya, A. B. Herr, R. Hullin, S. B. Liggett, B. M. Wolska, R. J. Solaro and D. F. Wieczorek (2010). "Molecular and functional characterization of a novel cardiac-specific human tropomyosin isoform." Circulation **121**(3): 410-418.
- Rajan, S., J. R. Pena, A. G. Jegga, B. J. Aronow, B. M. Wolska and D. F. Wieczorek (2013). "Microarray analysis of active cardiac remodeling genes in a familial hypertrophic cardiomyopathy mouse model rescued by a phospholamban knockout." Physiological Genomics **45**(17): 764-773.
- Razumova, M. V., A. E. Bukatina and K. B. Campbell (2000). "Different Myofilament Nearest-Neighbor Interactions Have Distinctive Effects on Contractile Behavior." Biophysical Journal **78**(6): 3120-3137.
- Rimm, E. B., W. C. Willett, F. B. Hu and et al. (1998). "Folate and vitamin b6 from diet and supplements in relation to risk of coronary heart disease among women." JAMA **279**(5): 359-364.
- Rutledge, C. and S. Dudley (2013). "Mitochondria and arrhythmias." Expert Review of Cardiovascular Therapy **11**(7): 799-801.

- Rybakova, I. N., M. L. Greaser and R. L. Moss (2011). "Myosin binding protein C interaction with actin: characterization and mapping of the binding site." The Journal of biological chemistry **286**(3): 2008-2016.
- Rybin, V. O., J. Guo, A. Sabri, H. Elouardighi, E. Schaefer and S. F. Steinberg (2004). "Stimulus-specific Differences in Protein Kinase C $\delta$  Localization and Activation Mechanisms in Cardiomyocytes." Journal of Biological Chemistry **279**(18): 19350-19361.
- Sadayappan, S. and P. P. de Tombe (2012). "Cardiac myosin binding protein-C: redefining its structure and function." Biophysical reviews **4**(2): 93-106.
- Sadayappan, S. and P. P. de Tombe (2014). "Cardiac myosin binding protein-C as a central target of cardiac sarcomere signaling: a special mini review series." Pflugers Arch **466**(2): 195-200.
- Sadayappan, S., J. Gulick, R. Klevitsky, J. N. Lorenz, M. Sargent, J. D. Molkentin and J. Robbins (2009). "Cardiac myosin binding protein-C phosphorylation in a {beta}-myosin heavy chain background." Circulation **119**(9): 1253-1262.
- Sadayappan, S., H. Osinska, R. Klevitsky, J. N. Lorenz, M. Sargent, J. D. Molkentin, C. E. Seidman, J. G. Seidman and J. Robbins (2006). "Cardiac myosin binding protein c phosphorylation is cardioprotective." Proceedings of the National Academy of Sciences **103**(45): 16918-16923.
- Sawyer, D. B., D. A. Siwik, L. Xiao, D. R. Pimentel, K. Singh and W. S. Colucci (2002). "Role of Oxidative Stress in Myocardial Hypertrophy and Failure." Journal of Molecular and Cellular Cardiology **34**(4): 379-388.
- Schultz Jel, J., B. J. Glascock, S. A. Witt, M. L. Nieman, K. J. Nattamai, L. H. Liu, J. N. Lorenz, G. E. Shull, T. R. Kimball and M. Periasamy (2004). "Accelerated onset of heart failure in mice during pressure overload with chronically decreased SERCA2 calcium pump activity." Am J Physiol Heart Circ Physiol **286**(3): H1146-1153.
- Schulz, E. M., R. N. Correll, H. N. Sheikh, M. S. Lofrano-Alves, P. L. Engel, G. Newman, J. E. J. Schultz, J. D. Molkentin, B. M. Wolska, R. J. Solaro and D. F. Wieczorek (2012). "Tropomyosin Dephosphorylation Results in Compensated Cardiac Hypertrophy." Journal of Biological Chemistry(Journal Article).
- Schulz, E. M., R. N. Correll, H. N. Sheikh, M. S. Lofrano-Alves, P. L. Engel, G. Newman, J. Schultz Jel, J. D. Molkentin, B. M. Wolska, R. J. Solaro and D. F. Wieczorek (2012). "Tropomyosin dephosphorylation results in compensated cardiac hypertrophy." The Journal of biological chemistry **287**(53): 44478-44489.
- Schulz, E. M., T. Wilder, S. A. K. Chowdhury, H. N. Sheikh, B. M. Wolska, R. J. Solaro and D. F. Wieczorek (2013). "Decreasing Tropomyosin Phosphorylation Rescues Tropomyosin-induced Familial Hypertrophic Cardiomyopathy." Journal of Biological Chemistry **288**(40): 28925-28935.
- Seidman, J. G. and C. Seidman (2001). "The genetic basis for cardiomyopathy: from mutation identification to mechanistic paradigms." Cell **104**(4): 557-567.
- Sheehan, K. A., G. M. Arteaga, A. C. Hinken, F. A. Dias, C. Ribeiro, D. F. Wieczorek, R. J. Solaro and B. M. Wolska (2011). "Functional effects of a tropomyosin mutation linked to FHC contribute to maladaptation during acidosis." Journal of Molecular and Cellular Cardiology **50**(3): 442-450.
- Sheikh, H. N. (2009). Tropomyosin Phosphorylation in Health and Disease M. Sc Thesis, University of Cincinnati.
- Solaro, R. J. (2011). Modulation of Cardiac Myofilament Activity by Protein Phosphorylation. Comprehensive Physiology, John Wiley & Sons, Inc.
- Solaro, R. J., A. J. Moir and S. V. Perry (1976). "Phosphorylation of troponin I and the inotropic effect of adrenaline in the perfused rabbit heart." Nature **262**(5569): 615-617.
- Solaro, R. J., D. C. Pang and F. N. Briggs (1971). "The purification of cardiac myofibrils with Triton X-100." Biochimica et biophysica acta **245**(1): 259-262.
- Solaro, R. J. and H. M. Rarick (1998). "Troponin and Tropomyosin: Proteins That Switch on and Tune in the Activity of Cardiac Myofilaments." Circulation Research **83**(5): 471-480.
- Solaro, R. J., P. Rosevear and T. Kobayashi (2008). "The unique functions of cardiac troponin I in the control of cardiac muscle contraction and relaxation." Biochemical and Biophysical Research Communications **369**(1): 82-87.
- Solaro, R. J. and J. Van Eyk (1996). "Altered interactions among thin filament proteins modulate cardiac function." Journal of Molecular and Cellular Cardiology **28**(2): 217-230.

- Spyracopoulos, L., M. X. Li, S. K. Sia, S. M. Gagné, M. Chandra, R. J. Solaro and B. D. Sykes (1997). "Calcium-Induced Structural Transition in the Regulatory Domain of Human Cardiac Troponin C†,‡." Biochemistry **36**(40): 12138-12146.
- Stein, L. A., R. P. Schwarz, Jr., P. B. Chock and E. Eisenberg (1979). "Mechanism of actomyosin adenosine triphosphatase. Evidence that adenosine 5'-triphosphate hydrolysis can occur without dissociation of the actomyosin complex." Biochemistry **18**(18): 3895-3909.
- Steinberg, S. F. (2013). "Oxidative stress and sarcomeric proteins." Circ Res **112**(2): 393-405.
- Subramaniam, A., W. K. Jones, J. Gulick, S. Wert, J. Neumann and J. Robbins (1991). "Tissue-specific regulation of the alpha-myosin heavy chain gene promoter in transgenic mice." The Journal of biological chemistry **266**(36): 24613-24620.
- Sumandea, M. P., V. O. Rybin, A. C. Hinken, C. Wang, T. Kobayashi, E. Harleton, G. Sievert, C. W. Balke, S. J. Feinmark, R. J. Solaro and S. F. Steinberg (2008). "Tyrosine Phosphorylation Modifies Protein Kinase C  $\delta$ -dependent Phosphorylation of Cardiac Troponin I." Journal of Biological Chemistry **283**(33): 22680-22689.
- Takeda, S., T. Kobayashi, H. Taniguchi, H. Hayashi and Y. Maeda (1997). "Structural and functional domains of the troponin complex revealed by limited digestion." Eur J Biochem **246**(3): 611-617.
- Takimoto, E. and D. A. Kass (2007). "Role of Oxidative Stress in Cardiac Hypertrophy and Remodeling." Hypertension **49**(2): 241-248.
- Tang, H., H. M. Viola, A. Filipovska and L. C. Hool (2011). "Ca(v)1.2 calcium channel is glutathionylated during oxidative stress in guinea pig and ischemic human heart." Free radical biology & medicine **51**(8): 1501-1511.
- Tong, C. W., J. E. Stelzer, M. L. Greaser, P. A. Powers and R. L. Moss (2008). "Acceleration of crossbridge kinetics by protein kinase A phosphorylation of cardiac myosin binding protein C modulates cardiac function." Circulation research **103**(9): 974-982.
- Treweeke, A. T., T. J. Winterburn, I. Mackenzie, F. Barrett, C. Barr, G. F. Rushworth, I. Dransfield, S. M. MacRury and I. L. Megson (2012). "N-Acetylcysteine inhibits platelet-monocyte conjugation in patients with type 2 diabetes with depleted intraplatelet glutathione: a randomised controlled trial." Diabetologia **55**(11): 2920-2928.
- Vacek, T. P., J. C. Vacek and S. C. Tyagi (2012). "Mitochondrial mitophagic mechanisms of myocardial matrix metabolism and remodelling." Archives Of Physiology And Biochemistry **118**(1): 31-42.
- Vahebi, S., A. Ota, M. Li, C. M. Warren, P. P. de Tombe, Y. Wang and R. J. Solaro (2007). "p38-MAPK Induced Dephosphorylation of  $\alpha$ -Tropomyosin Is Associated With Depression of Myocardial Sarcomeric Tension and ATPase Activity." Circulation research **100**(3): 408-415.
- Wang, J., E. S. Boja, W. Tan, E. Tekle, H. M. Fales, S. English, J. J. Mieyal and P. B. Chock (2001). "Reversible glutathionylation regulates actin polymerization in A431 cells." J Biol Chem **276**(51): 47763-47766.
- Warren, C. M., G. M. Arteaga, S. Rajan, R. P. Ahmed, D. F. Wieczorek and R. J. Solaro (2008). "Use of 2-D DIGE analysis reveals altered phosphorylation in a tropomyosin mutant (Glu54Lys) linked to dilated cardiomyopathy." Proteomics **8**(1): 100-105.
- Waskiewicz, A. (2009). "Dietary intake of B6, B12, and folate in relation to homocysteine serum concentration in the adult Polish population - WOBASZ Project " Kardiologia Polska **3**(68): 275-282.
- Wieczorek, D. F., G. Jagatheesan and S. Rajan (2008). "The role of tropomyosin in heart disease." Adv Exp Med Biol **644**: 132-142.
- Wolska, B. and D. Wieczorek (2003). "The role of tropomyosin in the regulation of myocardial contraction and relaxation." Pflügers Archiv **446**(1): 1-8.
- Xu, H. and M. A. Freitas (2009). "MassMatrix: a database search program for rapid characterization of proteins and peptides from tandem mass spectrometry data." Proteomics **9**(6): 1548-1555.
- Yang, Q., A. Sanbe, H. Osinska, T. E. Hewett, R. Klevitsky and J. Robbins (1998). "A mouse model of myosin binding protein C human familial hypertrophic cardiomyopathy." The Journal of clinical investigation **102**(7): 1292-1300.
- Zhang, R., J. Zhao and J. D. Potter (1995). "Phosphorylation of both serine residues in cardiac troponin I is required to decrease the Ca<sup>2+</sup> affinity of cardiac troponin C." The Journal of biological chemistry **270**(51): 30773-30780.

Zsebo, K., A. Yaroshinsky, J. J. Rudy, K. Wagner, B. Greenberg, M. Jessup and R. J. Hajjar (2014). "Long-term effects of AAV1/SERCA2a gene transfer in patients with severe heart failure: analysis of recurrent cardiovascular events and mortality." Circ Res **114**(1): 101-108.



## VII. APPENDICES



Office of Animal Care and Institutional  
Biosafety Committee (M/C 672)  
Office of the Vice Chancellor for Research  
206 Administrative Office Building  
1737 West Polk Street  
Chicago, Illinois 60612

July 26, 2013

R. John Solaro  
Physiology & Biophysics  
M/C 901

Dear Dr. Solaro:

The modifications requested in modification indicated below pertaining to your approved protocol indicated below have been reviewed and approved in accordance with the Animal Care Policies of the University of Illinois at Chicago on 7/15/13.

**Title of Application: Modulation of Calcium Control of Cardiac Myofibrils**

**ACC Number: 11-228**

**Modification Number: 9**

**Nature of Modification:** *Request for treatment of 4 week old FVB/N non-transgenic and Tm180 TG mice (20 total) with water or N-Acetylcysteine (an antioxidant, given ad-lib, in drinking water for 4 weeks). Animals will be subjected to Echoc at 4 weeks of age to set the baseline and after 4 weeks of treatment. After 4 weeks of treatment, cardioectomy will be performed and hearts will be harvested.*

**Protocol Approved: 2/13/2012**

**Current Approval Period:** 1/17/2013 to 1/17/2014. *Protocol is eligible for 1 additional year of renewal prior to expiration and resubmission.*

**Current Funding:** *Portions of this protocol are supported by the funding sources indicated in the table below.*

**Number of funding sources: 3**

Funding Agency	Funding Title			Portion of Funding Matched
NIH	Troponin Modulation In Heart Failure			Protocol is linked to form G
				ACC 12-054
Funding Number	Current Status	UIC PAF NO.	Performance Site	Funding PI
RO1 HL64035 (years 11-15)	Funded	200901189	UIC	R. John Solaro
Funding Agency	Funding Title			Portion of Funding Matched
NIH	Modulation of Calcium Control in Cardiac Myofibrils (linked to 11-229)			Portion of Grant is matched
Funding	Current Status	UIC PAF	Performance	Funding PI

Number		NO.	Site	
<i>RO1 HL022231</i> <i>(years 33-37)</i> <i>Original</i>	<i>Funded</i>	<i>201101862</i>	<i>UIC</i>	<i>R. John Solaro</i>
Funding Agency	Funding Title			Portion of Funding Matched
<i>NIH</i>	<i>Integrated Mechanisms Of Cardiac Maladaptation</i> <i>(Tied to ACC Form G 10-098)</i>			<i>Protocol is linked to form G</i> <i>ACC 10-098</i>
Funding Number	Current Status	UIC PAF NO.	Performance Site	Funding PI
<i>PO1 HL062426</i> <i>(years 11-15)</i>	<i>Funded</i>	<i>200906478</i>	<i>UIC</i>	<i>R. John Solaro</i>

This institution has Animal Welfare Assurance Number A3460.01 on file with the Office of Laboratory Animal Welfare, NIH. This letter may only be provided as proof of IACUC approval for those specific funding sources listed above in which all portions of the grant are matched to this ACC protocol.

Thank you for complying with the Animal Care Policies and Procedures of UIC.

Sincerely yours,



Bradley Merrill, PhD  
Chair, Animal Care Committee

BM/mbb

cc: BRL, ACC File, Beata M. Wolska, Madhu Gupta, Catherine Osborn



11200 Rockville Pike  
Suite 302  
Rockville, Maryland 20852

August 19, 2011

American Society for Biochemistry and Molecular Biology

---

To whom it may concern,

It is the policy of the American Society for Biochemistry and Molecular Biology to allow reuse of any material published in its journals (the Journal of Biological Chemistry, Molecular & Cellular Proteomics and the Journal of Lipid Research) in a thesis or dissertation at no cost and with no explicit permission needed. Please see our copyright permissions page on the journal site for more information.

Best wishes,

Sarah Crespi

[American Society for Biochemistry and Molecular Biology](#)

11200 Rockville Pike, Rockville, MD

Suite 302

240-283-6616

[JBC](#) | [MCP](#) | [JLR](#)

## VIII. CURRICULUM VITAE

### TANGANYIKA WILDER

---

#### EDUCATION

**University of Illinois at Chicago**, Chicago, Illinois 2007 – Current  
Ph.D. Department of Physiology and Biophysics  
Anticipated graduation: Summer 2014  
Thesis Advisor: **R. John Solaro**, PhD, Distinguished University Professor and Head

**Florida A & M University**, Tallahassee, Florida 1996-2004  
Bachelor of Science graduated with Honors, Cum Laude

#### SKILLS/TECHNIQUES

- Animal husbandry
- Cardiac cell isolation
- Cell shortening/calcium transient analysis
- Echocardiography
- Force-Calcium relationship measurements
- GSH/Carbonylation Molecular Assays
- Immuno-blotting, immunofluorescence studies
- Myofibril Isolation
- Simultaneous Mg-ATPase, Tension redevelopment, and Stiffness Analysis
- Tissue processing

#### FUNDING AND GRANTS

National Institutes of Health Pre-Doctoral Fellow, 2010-current  
American Physiological Society Porter Fellowship, 2010-2011, Declined continuation  
American Physiological Society Porter Fellowship, 2009 - 2010  
National Science Foundation Bridge to the Doctorate Fellowship, 2007 - 2009  
Florida Georgia-Louis Stokes Alliance for Minority Participation Scholarship, 2002 - 2004  
John G. Calvert Merit Scholarship

#### HONORS AND AWARDS

ISHR URM Travel Award, ISHR World Congress, San Diego, CA 2013  
Mark Lambrecht Award for Scholarship and Commitment, University of Illinois at Chicago, Chicago, IL, 2012 (Offered to one graduate student annually for scholastic achievement and service to the department)  
NSF Graduate Research Fellowship Proposal – Honorable Mention, 2009  
Federation of American Societies for Experimental Biology-MARC Travel Award Recipient for Grant Writing and Leadership Development Seminar, 2009  
Biology in the Office of Naval Research Honorary Scholar (BIONR), 2002 - 2004

## PUBLICATIONS

Schulz, E.M, **Wilder, T**, Chowdhury, S. A, Wolska, B.M, Solaro, R.J, Wieczorek, D.F. Tropomyosin Dephosphorylation Rescues Tropomyosin Induced Familial Hypertrophic Cardiomyopathy. *Journal of Biological Chemistry* 2013 Oct 4;288(40):28925-35.

Patel, B.G, **Wilder, T.**, and Solaro, R.J. Novel Control of Cardiac Myofilament Ca-Responsiveness by S-Glutathionylation of Specific Sites on Myosin Binding Protein C. *Frontiers in Physiology* 2013 Nov 20;4:336.

Pound, K. M., Arteaga, G. M., Fasano, M., **Wilder, T.**, Fischer, S. K., Warren, C. M., Wende, A. R., Farjah, M., Abel, E. D., Solaro, R. J., and Lewandowski, E. D. *Journal of molecular and cellular cardiology* 2011 51, 236-243.

**Wilder, T.**, Hinken, A.C.; Solaro, R. J. Altered Myofilament Targeting with Differential PKC $\delta$  Activation. *Biophysical Journal* 2008 vol. 96, issue 3, pp. 500a-501a.

**Wilder, T.**, Schulz, E., Ryba. D. M., Mungai, P, Wolska, B. M., Wieczorek, D., Solaro, R. J. Oral Antioxidant N-Acetylcysteine (NAC) Reverses the Progression of Cardiac Hypertrophy and Diastolic Dysfunction in a Model that Mimics Human Familial Hypertrophic Cardiomyopathy. *Manuscript in progress*.

## ABSTRACTS

**Wilder T**, Schulz, EM., Chowdhury, S.; Wolska, BM.; Wieczorek, DF.; Solaro, RJ. Altered Phosphorylation of Cardiac  $\alpha$ -Tropomyosin Modified Progression of the Phenotype of Mice Expressing Tropomyosin E180G, a Hypertrophic Cardiomyopathy Linked Mutant. (2012) *ISHR North American Section* Volume 53, Issue 2 supplement Banff, Alberta, Canada

**Wilder, T.**; Schulz, EM.; Chowdhury, S.; Ryba, DM.; Wolska, BM.; Wieczorek, DF.; Solaro, RJ. Tropomyosin Phosphorylation and Oxidative Stress in Familial Hypertrophic Cardiomyopathy. (2013) *World Congress of ISHR*. Volume 65, supplement San Diego, CA.

**Wilder, T.**, Devi, S. Shehu, A., Le, J., Halperin, J., and Gibori, G. Cross-talk between prolactin signaling through the short and long form of its receptors activates the Jak2 pathway in rodent corpus luteal cells. (2008) *National Science Foundation Joint Annual Meeting*, Chicago, IL.

**Wilder, T.**, Garcia-Martinez, J. Elucidating the functional significance of the interplay between  $\alpha$ 2-delta and the voltage gated calcium channel in heart. (2007) *Purdue CIC/SROP Exposition*, Purdue, IN.

**Wilder, T.**, Garcia-Martinez, J. Elucidating the functional significance of the interplay between  $\alpha$ 2-delta and the voltage gated calcium channel in heart. (2008) *Michigan State CIC/SROP*, Ann Arbor, MI.

## **PRESENTATIONS**

### Oral Presentations

Center for Cardiovascular Research Annual Research Day, 2009

### Poster Presentations

International Society for Heart Research World Conference 2013

International Society for Heart Research 2012

Biophysical Society Annual Conference 2009

Annual Biomedical Research Conference for Minority Students 2008

NSF Joint Annual Meeting 2008

Michigan State CIC/SROP Conference 2008

Purdue CIC/SROP Exposition 2007

## **MENTORSHIP -TRAINING EXPERIENCE**

David Ryba – Undergraduate/Graduate, University of Illinois at Chicago

Magdalese Gonzales-Vega, Graduate research rotation

Clara Garcia – Hinsdale High School Summer Research Opportunity

Gisella Newberry – Summer Undergraduate, Kalamazoo College

David Lewandowski – Undergraduate, University of IL at Urbana

## **TEACHING EXPERIENCE**

Urban Health Program, Chicago, IL

July 2010 - July 2013

### Lecturer

Taught ten lectures during the summer in the subject areas of Human Physiology, and Cell Communication and Respiratory Systems. Prepared all sessions, made presentations to students, designed quizzes and reviewed materials.

Florida A & M University, Tallahassee, FL

August 2004 - August 2007

### Lab Instructor

Assisted and facilitated learning molecular biology methods to undergraduate students. Conducted material/subject reviews, assist in homework assignment, organization and time management.

## **PROFESSIONAL ASSOCIATIONS**

American Physiological Society

Biophysical Society Member

ISHR Society Member

## **COMMUNITY LEADERSHIP**

PBGSA - Graduate Student Representative 2009-2012

UIC Special Interest Organization Resident Assistant for Family Housing 2008-2012

Gilchrist Marchman Easter Seals- Volunteer 2008-2009

Washington Irving Elementary - Volunteer 2008-2009

Women in Science and Engineering Mentor 2008

Chicago Public Schools – Science fair judge 2008 and 2009

Central Housing SSR Apartment Council – Community Service Co-Advisor 2008- 2009

Family Housing Children's HIPPY Program Instructor 20